

000-1393-1

**MASTER**

RECEIVED BY DTIC MAR 8 1970

# EVALUATION OF PROTECTION FROM EXPLOSION OVERPRESSURE IN AEC GLOVEBOXES

By

C. Yao, J. deRis

S. N. Bajpai, J. L. Buckley

For

U. S. Atomic Energy Commission  
Chicago Operations Office  
Argonne, Illinois

December 1969



FM RESEARCH CORPORATION

## **DISCLAIMER**

**This report was prepared as an account of work sponsored by an agency of the United States Government. Neither the United States Government nor any agency Thereof, nor any of their employees, makes any warranty, express or implied, or assumes any legal liability or responsibility for the accuracy, completeness, or usefulness of any information, apparatus, product, or process disclosed, or represents that its use would not infringe privately owned rights. Reference herein to any specific commercial product, process, or service by trade name, trademark, manufacturer, or otherwise does not necessarily constitute or imply its endorsement, recommendation, or favoring by the United States Government or any agency thereof. The views and opinions of authors expressed herein do not necessarily state or reflect those of the United States Government or any agency thereof.**

## **DISCLAIMER**

**Portions of this document may be illegible in electronic image products. Images are produced from the best available original document.**

C08-1393-1

**LEGAL NOTICE**

This report was prepared as an account of Government-sponsored work under the United States of the Commission. See any notice being on label of the Commission.  
A. Neither the Commission nor any person acting on behalf of the Commission:  
1. Makes any warranty of representation expressed or implied with respect to the accuracy, completeness, or usefulness of the information recorded in this report or the use of any information, apparatus, method, or process disclosed in this report for any purposes other than those for which it was originally prepared;  
2. Assumes any liability with respect to the use of, or for damages resulting from the use of any information, apparatus, method, or process disclosed in this report.  
As used in the above provisions, the term "the Commission" includes any employee or contractor of the Commission or employee of such contractor, to the extent that such employee or contractor of the Commission, or employee of such contractor, prepares, disseminates, or provides access to any information pursuant to the employment or contract with the Commission, or the employment with such contractor.

**EVALUATION OF PROTECTION FROM EXPLOSION OVERPRESSURE  
IN AEC GLOVEBOXES**

By

C. Yao, J. deRis  
S. N. Bajpai, J. L. Buckley

Prepared For


**U.S. ATOMIC ENERGY COMMISSION  
CHICAGO OPERATIONS OFFICE  
ARGONNE, ILLINOIS**

CONTRACT NO. AT(11-1)-1393

FMRC Serial No. 16215.1  
RC69-T-23

DECEMBER 1969



Approved by:  
  
J. B. Smith  
Vice President

**FACTORY MUTUAL RESEARCH CORPORATION**

1151 BOSTON-PROVIDENCE TURNPIKE, NORWOOD, MASS. 02062

DISTRIBUTION OF THIS DOCUMENT IS UNLIMITED

FACTORY MUTUAL RESEARCH CORPORATION

LEGAL NOTICE

This report was prepared as an account of Government sponsored work. Neither the United States, nor the U. S. Atomic Energy Commission, nor any person acting on behalf of the Commission:

A. Makes any warranty or representation, expressed or implied, with respect to the accuracy, completeness, or usefulness of the information contained in this report, or that the use of any information, apparatus, method, or process disclosed in this report may not infringe privately owned rights; or

B. Assumes any liabilities with respect to the use of, or for damages resulting from the use of any information, apparatus, method, or process disclosed in this report.

As used in the above, "person acting on behalf of the Commission" includes any employee or contractor of the Commission, or employee of such contractor, to the extent that such employee or contractor of the Commission, or employee of such contractor prepares, disseminates, or provides access to, any information pursuant to his employment or contract with the Commission, or his employment with such contractor.

DISCLAIMER NOTICE

Any comparison of the design or performance characteristics of manufacturers' products is not to be construed as an endorsement of one product over another. Stated preferences for a particular design or set of performance characteristics are intended solely to establish minimum acceptable specifications for a particular type of product when used in glovebox applications described herein. Any future procurement of products referred to herein by the AEC or its contractors, will be based upon normal competitive procedures. The procuring organization will in all instances specify the minimum specifications required.

ACKNOWLEDGEMENTS

The authors gratefully appreciate the cooperation, assistance and advice of the United States Atomic Energy Commission, in particular Messrs. L. E. Oldendorf and R. B. Smith, throughout this investigation.

Special acknowledgement is given to E. Stein, and L. A. Post, of FMRC for their contribution in the preparation of this report; and to Messrs. A. L. Bennett, K. Harvey and W. Seale for the performance of the experimental studies.

FOREWORD

Pursuant to a request from the Division of Operational Safety, Headquarters, U. S. Atomic Energy Commission (AEC), the AEC Chicago Operations Office (CH) contracted with the Factory Mutual Research Corporation (FMRC) to study glovebox fire safety problems relating to activities of the AEC and its contractors.

Most of the work under that contract was reported in "Glovebox Fire Safety, A Guide for Safe Practices in Design, Protection and Operation," TID-24236, issued in 1967. Other FMRC glovebox fire safety work in specialized areas is covered in separate reports such as the one given on the following pages.

Technical administration of the contract was handled largely by L. E. Oldendorf, Safety and Fire Protection Engineer, Safety & Technical Services Division, CH.



D. E. Patterson, Chief  
Industrial Safety & Fire  
Protection Branch  
Division of Operational Safety

PREFACE

This publication provides guidelines for improved explosion safety in the design, construction, and operation of gloveboxes. It contains theoretical evaluations and experimental results of studies conducted to investigate the problem of pressure relief venting for explosions. Prior to this work, there were no design criteria available which took into consideration the overpressurization resulting from explosions in gloveboxes.

In July 1968, Factory Mutual Research Corporation began studies and tests for the Atomic Energy Commission to determine the severity of a "maximum credible accident" due to a vented explosion of representative combustible-air mixtures. The information was to be used for evaluating several possible minimum requirements for venting these explosions, without losing containment of radioactive material or affecting the integrity of the glovebox. To avoid duplication of studies and considerations previously made by AEC and its contractors, the AEC, Chicago Operations Office, Safety and Technical Services Division, solicited information on the glovebox venting problem from all AEC glovebox facilities. The information received further substantiated the need to conduct tests and studies on glovebox explosion venting. The methods currently used to control overpressures in gloveboxes at AEC facilities are summarized in Appendix B.

The information produced by this work provides a design procedure which determines the adequacy of explosion protection for enclosures such as gloveboxes. A general mathematical model was developed to describe explosions in gloveboxes which are vented in a variety of different ways.



SUMMARY

Effective protection should be given to gloveboxes where the possibility of accidents may lead to explosions. Since gloveboxes are basically very weak structures, protective measures must be taken at an early stage in the development of an explosion before damage has been done. The type of explosion referred to in this report is commonly known as "deflagration", a subsonic propagating combustion wave accompanied by pressure effects.

A theoretical and experimental research program was designed at FMRC 1) to collect and generate knowledge pertaining to the problem of explosion venting, 2) to apply this information specifically to AEC glovebox safety and protection. The program comprised the following areas of investigation.

A general mathematical model describing the explosion characteristics inside a vented enclosure was derived. The model can be solved numerically to predict the pressure-time history for a wide variety of venting arrangements, such as free-vent, bursting diaphragm relief venting, and filter venting. The model showed that the explosion pressure developed inside a vented enclosure is a function of turbulence level,  $\chi$ , and a dimensionless parameter,  $\alpha$ , which consists of geometrical dimensions as well as physical properties of the combustible mixture. For a given combustible mixture, the parameter,  $\alpha$ , can be simplified to the commonly used vent area factor,  $K$  (cross-sectional area containing the vent/vent area).

Good agreement is obtained between the theoretical and experimental results and published data for cases of localized explosion in a closed vessel and completely filled explosion in an enclosure with free-vent.

The calculated and measured pressure-time record for bursting diaphragm explosion relief venting shows distinct double pressure peaks. The first pressure peak represents the bursting pressure of the diaphragm and the second pressure peak represents the flow resistance of the vent opening on the fast expanding combustion products. For low pressure relief cases, the second-peak pressure can be many times higher than the bursting pressure of the diaphragm (first peak). For the same vent area in a given enclosure (that is, same  $\alpha$  and  $K$  factors) the maximum explosion pressure (second-peak) for bursting diaphragm explosion relief is about four times higher than the free-vent relief. This high second-peak pressure measured from bursting diaphragm experiments can be explained theoretically by using a high turbulence factor of  $\chi > 1$  (increase in the burning velocity after the bursting of the diaphragm).

Information generated from this investigation has been analyzed and reduced into the form of general guidelines for explosion protection in

gloveboxes. Several unique features of AEC gloveboxes, i.e. air ventilation pattern, filters, gloves, etc. have been considered in this study. Gloveboxes designed to be leakage proof up to 4 in. water gauge cannot withstand even a localized explosion resulting from the ignition of a cumulated combustible gas mixture at a volume of more than 0.3 percent of the glovebox volume. With proper design and relocation of components, the glovebox can be upgraded to a higher value of 2 to 5 psi level to cope with a much larger explosive volume ratio of 4 to 9 percent by volume.

In the event that a large portion of the glovebox space can be involved with a combustible mixture, a large size explosion relief device is necessary. The venting requirement is not only a function of the size and location of the pressure relief device but also varies with the manner and condition in which the relief is to be uncovered and where or how the explosion discharge will be exhausted.

A general procedure for designing a bursting diaphragm type of explosion relief and for confining and exhausting the explosion discharge is presented in this report. The effects of various parameters such as gloves, filters, obstacles, mixture strength, and ventilation on design considerations are also discussed. In general, the most serious glovebox explosion condition is the center ignition in a small cubical glovebox which is filled completely with a homogeneous combustible mixture, slightly richer than stoichiometric condition. Multiple sources of ignition and added turbulence would increase the explosion intensity. However, under normal ventilation conditions where velocity of gas movement inside the glovebox is about the same order of magnitude as the burning velocity of the combustible mixture itself, no significant effect on explosion pressure has been experienced. Theoretical and experimental results obtained from this study have been presented graphically, and can be used as a guide to select a suitable method of pressure relief to meet the specific protection requirement. A numerical example is also included to illustrate the uses of these graphs. In view of the wide diversity in design, construction and operation of the AEC glovebox, considerable caution should be exercised so as not to extrapolate the data too much beyond the range of the conditions investigated in this program.

Several possible methods of confining and exhausting the explosion discharge from the glovebox have been recommended. The explosion discharge can be exhausted into a fixed chamber, expandable chamber or through a filter wall into the working area. The possibility of venting an explosion with a filter wall seems to be a very attractive method for AEC glovebox operation. It is anticipated that the filter wall will provide opening area for continuous venting of combustion products, and will produce minimum amounts of turbulence and low explosion pressure. The filter wall can vent the explosion discharge directly into the room without causing radioactive contamination to the operational area.

TABLE OF CONTENTS

<u>Section</u>	<u>Page</u>
PREFACE	v
SUMMARY	vii
I INTRODUCTION	1
II MECHANISM OF EXPLOSION PRESSURE RELIEF	3
2.1 Burning Velocity and Flame Speed	3
2.2 Explosion in a Closed Vessel	4
2.2.1 Previous Work	4
2.2.2 Maximum Explosion Pressure Resulting From A Localized Explosion	9
2.3 Explosion Relief With Free-Vent	13
2.3.1 Previous Work	13
2.3.2 Mathematical Model	14
2.3.3 Discussion	16
2.4 Explosion Relief With Filters	19
2.5 Explosion Relief With Bursting Diaphragm	23
2.5.1 First Pressure Peak and Bursting of Diaphragm	25
2.5.2 Second-Peak Pressure	26
III EXPERIMENTAL INVESTIGATION OF EXPLOSIONS IN GLOVEBOXES	31
3.1 Experimental Apparatus	31
3.1.1 Pressure Measuring System	31
3.1.2 Gas Supply and Mixing System	31
3.1.3 Ignition and Timing System	33
3.1.4 Test Chambers	36
3.2 Balloon Explosion Results	36
3.2.1 (Balloon) Explosion in the Closed 27 cu ft Chamber	39
3.2.2 (Balloon) Explosion in the 24 cu ft Glovebox	39
3.2.3 Free-Vent versus Filters in (Balloon) Explosion Venting	39
3.3 Pressure Relief With Bursting Diaphragm	45
3.3.1 Bursting Diaphragm Explosion in the 27 cu ft Test Chamber	45
3.3.2 Bursting Diaphragm Explosion in the Cylindrical Test Chambers	52
3.4 Free-Vent Pressure Relief	54
IV DATA EVALUATION	56
4.1 Localized Explosion in A Glovebox	56
4.2 Explosion Relief With Bursting Diaphragm	56
4.2.1 Correlation of Bursting Diaphragm Data	56
4.2.2 Effect of Bursting Pressure on the Second-Peak Pressure	61
4.2.3 Effect of Geometry and Configuration	61

FACTORY MUTUAL RESEARCH CORPORATION

x		16215.1
	<u>Section</u>	<u>Page</u>
	4.3 Explosion Relief With Free-Vent or Filter	64
	4.3.1 Correlation of Free-Vent Data	64
	4.3.2 Explosion Venting With Filters	66
V	GENERAL GUIDELINES FOR EXPLOSION PROTECTION IN GLOVEBOXES	67
	5.1 General Glovebox Design Criteria	67
	5.1.1 Effect of Explosion on Filters	68
	5.1.2 Effect of Explosion on Gloves	69
	5.2 Explosion Venting With Bursting Diaphragm	72
	5.2.1 Effect of Mixture Strength and Fuel	72
	5.2.2 Determination of Vent Area	73
	5.2.3 Selection of Vent Relief Device	75
	5.2.4 Air Ventilation Obstacles and Multiple Sources of Ignition	77
	5.2.5 Confining and Exhausting the Explosion Discharge	78
	5.2.6 Design and Construction of Bursting Diaphragm Explosion Pressure Relief	79
VI	RECOMMENDATIONS FOR FURTHER STUDY	84
VII	NOMENCLATURE	85
VIII	REFERENCES	88
	APPENDIX A Mathematical Modeling of Explosion Venting Including Free Venting	
	APPENDIX B Summary of Current Safety Practices at AEC Glovebox Facilities	
	APPENDIX C Tables of Experimental Data	

LIST OF ILLUSTRATIONS

<u>Figure No.</u>	<u>Title</u>	<u>Page</u>
2-1	Burning Velocities of Methane-, Ethane-, Propane-, and n-Heptane Vapor Air Mixtures at Atmospheric Pressure and Room Temperature	5
2-2	Burning Velocities of Mixtures of Hydrogen, Oxygen, and Nitrogen at Room Temperature and Atmospheric Pressure (Jahn)	5
2-3	Variation in Burning Velocity of Stoichiometric Methane-Air and Propane-Air Mixtures with Pressure at 26°C	6
2-4	Effect of Temperature on Burning Velocities of Four Paraffin Hydrocarbons in Air at Atmospheric Pressure	6
2-5	Time-Pressure Record of Ozone Explosion in Spherical Vessel	7
2-6	Analysis of Explosion Pressure Record Shown in Figure 2-5	7
2-7	Maximum Explosion Pressure Versus Composition of the Mixture for 4-Liter Bomb and 60-cu-ft Vessel	10
2-8	A Conceptual Model of a Centrally Ignited Localized (Balloon) Explosion Inside a Spherical Chamber	12
2-9	Theoretically Predicted Pressure-Time History For a 24-in. Diameter Free-Vent in a 27 cu-ft Vessel	17
2-10	Graphical Presentation of Published Free-Vent Explosion Data	18
2-11	Flow Characteristics of Size B Flanders High Efficiency Filter Unit	20
2-12	Comparison of Flow Characteristics Between a Type B Flanders High-Efficiency Filter and a Sharp Edge Orifice at Different Temperatures and Pressures	22
2-13	A Typical Pressure-Time History For an Explosion in a Cubical Oven Vented with a Bursting Diaphragm	24

<u>Figure No.</u>	<u>Title</u>	<u>Page</u>
2-14	Effect of Turbulence on the Maximum Explosion (2nd Peak) Pressure	28
2-15	Variation of the Second-Peak Pressure with the Vent Area Parameter	29
3-1	Block Diagram Showing General Arrangement of Test Instrumentations	32
3-2	Schematic Diagram of Gas Supply and Mixing Setup I- Balloon Explosion	34
3-3	Schematic Diagram of Gas Supply and Mixing Setup II- Chamber Completely Filled With Combustible Gas	34
3-4	Schematic Diagram of Gas Supply and Mixing Setup III- Chamber Completely Filled With Homogeneous Mixture	35
3-5	Wiring Diagram of The Experimental Arrangement	35
3-6	Glovebox with Air Circulation Scheme	37
3-7	27-cu-ft Aluminum Test Chamber	37
3-8	Cylindrical Test Chambers (Configurations A and B)	38
3-9	Test Results For Localized (Balloon) Explosion in a Closed Chamber	40
3-10	Pressure-Time History of a Balloon Explosion in a Closed Chamber as Recorded by Oscillogram (Test #A-12)	41
3-11	Effect of Filters and Air Circulation on the Localized (Balloon) Explosion	42
3-12	Effect of Air Circulation on (Balloon) Explosion	43
3-13	Effect of the Combination of the Filters, Gloves and Air Circulation on the Localized (Balloon) Explosion	44
3-14	Comparison of Free-Vent Against Filters in (Balloon) Explosion Venting	46
3-15	Pressure-Time History of a Balloon Explosion inside a Chamber Provided With Free-Vent as Recorded by Oscillogram (Test #AA-101)	47

<u>Figure No.</u>	<u>Title</u>	<u>Page</u>
3-16	Pressure-Time History of a Balloon Explosion Inside a Chamber Provided With Filters as Recorded by Oscillogram (Test #AA-1577)	47
3-17	Typical Pressure-Time History Measured For an Explosion in the 27-cu-ft Chamber Vented with a 24-in. Diameter Bursting Diaphragm	48
3-18	Diaphragm Bursting Pressure (First Peak) PSI as a Function of Diaphragm Diameter	49
3-19	Second-Peak Pressure (PSI) as a Function of the Diaphragm Diameter (inches)	51
3-20	Test Setup to Simulate the Glovebox Explosion from a Gas Leak	53
3-21	Effect of Configuration (L/D) on the Explosion Pressure	55
4-1	Correlation of Localized (Balloon) Explosion Data	57
4-2	Correlation of the Theoretical and Experimental Data For Bursting Diaphragm Pressure Relief	59
4-3	Correlation of the Experimental Data Obtained From Present Study with the Published Data	59
4-4	Direct Comparison of the Experimentally and Theoretically Determined Pressure-Time Records For Stoichiometric Propane/Air Mixture Exploded in a 27-cu-ft. Chamber with a 24-in. Diameter Diaphragm	60
4-5	Maximum-Explosion Pressure versus Disc Bursting Pressure for Stationary 2.50 mol % Pentane in Air Mixtures	62
4-6	Effect of Bursting Pressure on the Second-Peak Pressure	63
4-7	Correlation of the Free-Vent Pressure Relief Data	65
5-1	Rupture of Filters and Gloves	70
5-2	Mounting of Gloves on the 3 Ft x 3 Ft Cylindrical Test Chamber (Arrangement A)	71
5-3	Mounting of Gloves on the 3 Ft x 3 Ft Cylindrical Test Chamber (Arrangement B)	71

<u>Figure No.</u>	<u>Title</u>	<u>Page</u>
5-4	Nomograph For Bursting Diaphragm Explosion Relief Design (Thin Metal Diaphragm with Bursting not much different from that shown in Figure 3-18)	74
5-5	Rupture Pressure vs. Vent Area of Various Venting Materials	76
A-1	Conceptual Model of the Explosion Venting	A3



LIST OF TABLES

<u>Table No.</u>	<u>Title</u>	<u>Page</u>
Table 1	Balloon Explosion in the 27 Ft <sup>3</sup> Aluminum Chamber	C-1
Table 2	Balloon Explosion in 24 Ft <sup>3</sup> Wooden Glovebox	C-1
Table 3	Free-Vent Versus Filter in Balloon Explosion	C-3
Table 4	Bursting Diaphragm Pressure Relief on the 27-cu-ft Cubical Chamber (Filled Completely with Non-Homogeneous Propane and Air Mixture)	C-4
Table 5	Bursting Diaphragm on the 27-cu-ft Cubical Chamber (Homogeneous Mixture, Completely Filled)	C-6
Table 6	Bursting Diaphragm Pressure Relief on the 27-cu-ft Cubical Chamber (Filled Completely with Hydrogen/Air Mixture)	C-7
Table 7	Bursting Diaphragm Pressure Relief on the 3-ft Diameter Cylindrical Test Chambers (Completely Filled with Homogeneous Propane and Air Mixture)	C-7
Table 8	Free-Vent Pressure Relief Data (Test Chambers Were Completely Filled with Homogeneous Mixture of Propane and Air)	C-7
Table 9	Factory Mutual Research Corp. Tests on Glove Bursting Pressures	C-8

INTRODUCTION

In the AEC program, gloveboxes are used principally to handle toxic pyrophoric, and radioactive material. Glovebox work at AEC facilities varies over a wide range and involves a variety of equipment. It encompasses research, development, production, and weapons fabrication activities.

A glovebox is a relatively weak structure. It is usually designed and tested to withstand about 4 in. water gauge without leaking of the contaminated gas to the operating area. Although the gloveboxes can be fabricated to withstand a much higher pressure, some of the weak components, such as windows, gloves and filters, cannot withstand more than 2 to 5 psi.

A fire or explosion in the glovebox may cause gradual or sudden pressurization, which can cause the glovebox components to fail. In order to prevent the spread of radioactivity and contamination to the operation area, the fire and explosion must be quickly and effectively extinguished or suppressed. A collection of data on methods of suppression and extinguishment of fire or explosion inside gloveboxes is given in the "Glovebox Fire Safety"<sup>(1)</sup> Guide. The problem of fire and explosion protection is complicated by the structural limitations of the glovebox and the need to apply extinguishing agents without pressurizing the glovebox. Where plutonium, enriched uranium, or other fissile materials are handled, special care is needed to avoid introducing moderator-type extinguishing agents (such as water) in a form or manner that could create a potential for nuclear criticality. Where chemicals reactive metals, etc., are handled, care is needed to avoid introducing incompatible extinguishing agents that could cause an adverse chemical reaction (e.g. water and sodium) resulting in overpressure or explosion and loss of glovebox containment.

Overpressure in a glovebox may be caused by chemical reaction, vaporization of liquids, solid and liquid fires and gaseous combustion explosions. Depending on the speed of the flame propagation or rate of the energy release, combustion explosion can be classified in two types, ordinary explosions (deflagrations) and detonations. Overpressure due to deflagration results mainly from the thermal expansion of a subsonic propagating combustion wave. The peak pressure of deflagration in a closed vessel seldom exceeds about 130 psi and it can be effectively reduced to a few psi by means of a suitable pressure relief device. Detonation is an extremely fast explosion. The flame propagates at supersonic speed. The peak pressure in detonation may reach several thousand psi. Since detonation wave velocities are many times the speed of sound, the gas cannot be vented as the result of a pressure increase caused by detonation until the wave front reaches the vent opening. Therefore, the primary interest in this phase of investigation is limited to ordinary explosion (deflagration). The current safety practices of AEC's glovebox facilities emphasize mostly preventive measures, either by eliminating the source of fuel or inerting the entire system. It was felt that explosion venting seems to be a more economic and reliable solution to this problem because overpressurization in AEC glovebox facilities may not always result from combustion processes.

Where the possibility exists of accidents that may lead to serious overpressurizations, special attention should be given to the design and selection of a pressure relief device so that the pressure loading exerted on the glovebox can be reduced to a safety level that the weakest components, such as gloves, filters and windows, can withstand. Furthermore, the ability of various glovebox components to withstand the maximum credible explosion is a problem of dynamic response rather than static loading. In order to design a safe glovebox, able to withstand the effect of accidental explosions, a method for estimating the explosion character and the dynamic response of various components is critically important. Therefore, the objective of this phase of the program has been to:

- 1) determine the integrity or limitation of present glovebox design;
- 2) explore the possibility of reducing the maximum credible explosion impulse to a controllable level by means of pressure relief devices; and
- 3) collect and generate data pertaining to the problem of explosion venting and apply them specifically to AEC glovebox operation.

## II

MECHANISM OF EXPLOSION PRESSURE RELIEF

The ability of the glovebox to withstand the effect of explosion is a function of the duration, magnitude and rate of the pressure rise. One way of reducing the explosion damage to a glovebox is to provide pressure relief vents. It is often very difficult to apply this method in practice because of lack of information on the complicated combustion process of the vented explosions. Although some, mainly empirical, data are available, they are generally applied only to certain limited applications. In general, agreement among various investigations is very poor. Even the relatively easier problem of scaling the results of practical measurements contains certain pitfalls.

The degree of success in this investigation depends upon the ability to estimate the characters of the vented explosion and the dynamic response of various exposed glovebox components. Accidental explosions are, by definition, uncontrolled; therefore, the detailed characteristics involved are complex and difficult to define. Therefore, investigation in this phase of the program must be limited to some simplified but least favorable cases. The primary purpose of this section is to review the state of knowledge on this subject and to explore further into the fundamental principles and interrelationships among various controlling parameters. The mathematical results presented can be considered as an approximation of the actual conditions that may exist. It could, at least, be used as a basis for extrapolation or scale-up of the experimental data to conditions that are commonly met with in AEC operations.

### 2.1 BURNING VELOCITY AND FLAME SPEED

If a combustible gas mixture is ignited at a point source, the flame will propagate spherically outward. Several different velocities may be associated with this flame propagation. These velocities are very important because they have a marked effect on the amount of heat which may be liberated during the combustion explosion process. The flame front, which separates the burned gas and unburned gas, moves outward symmetrically relative to a fixed observer at a flame velocity of  $S_b$ ; and the actual burning velocity which is conventionally denoted as  $S_u$ , is the velocity of the flame relative to the unburned gases or the velocity at which the combustible mixture passes into an advancing flame front. The flame velocity is actually the vector sum of four components: burning velocity; thermal expansion;

change in the number of moles; and initial velocity of the gas. If a steady-state, unlimited flame front propagates into a combustible mixture at rest, the flame velocity is equal to the burning velocity. In the case of spherical flame propagation in a closed vessel, the flame front travels at a much higher velocity than the burning velocity because of the thermal expansion of the burned gas trapped at the center of the vessel.

The burning velocities and flammability of various hydrocarbons have been measured by numerous investigators in air and other oxidants<sup>(2,3)</sup>. At one atmosphere and 26°C, the burning velocity of paraffin hydrocarbons in air ranges from a few centimeters per sec near the limits of flammability to about 45 cm per sec at the stoichiometric mixture composition. Figures 2-1 and 2-2 show the published results for four paraffin hydrocarbons-air<sup>(4)</sup> and hydrogen-air<sup>(5)</sup> mixtures at atmospheric pressure and room temperature. A change in either temperature or pressure will alter  $S_u$  for a particular mixture. It was found that an increase in pressure causes  $S_u$  of stoichiometric propane-air and methane-air mixtures to decrease in the pressure range of 0.5 to 20 atmospheres<sup>(4)</sup> (Figure 2-3). The effect of temperature is more consistent. For a given pressure and mixture composition, an increase in temperature raises  $S_u$  (Figure 2-4). For some of the paraffin hydrocarbons:

$$S_u = 10 + 0.000342 T^2 \quad (1)$$

where

$S_u$  = burning velocity, Cm/sec

T = Temperature, °K

## 2.2 EXPLOSION IN A CLOSED VESSEL

### 2.2.1 Previous Work

The combustion explosion in a small spherical vessel with center ignition has been examined by Lewis and Von Elbe<sup>(5)</sup>. A typical pressure-time relationship measured for closed vessel explosion is plotted in Figure 2-5. The pressure reaches a sharp peak over a short period,  $t_m$ . After the ignition, the flame front (combustion wave) has been found to propagate very rapidly so that convection and buoyancy effects of the hot burned gas are not noticeable. The flame front propagates spherically and arrives at the wall practically simultaneously at all points. A detailed analysis of ozone explosion in a 15-cm-diameter sphere by Lewis and Von Elbe<sup>(5)</sup> is illustrated in Figure 2-6. The radius of circles 1b, 2b, etc.

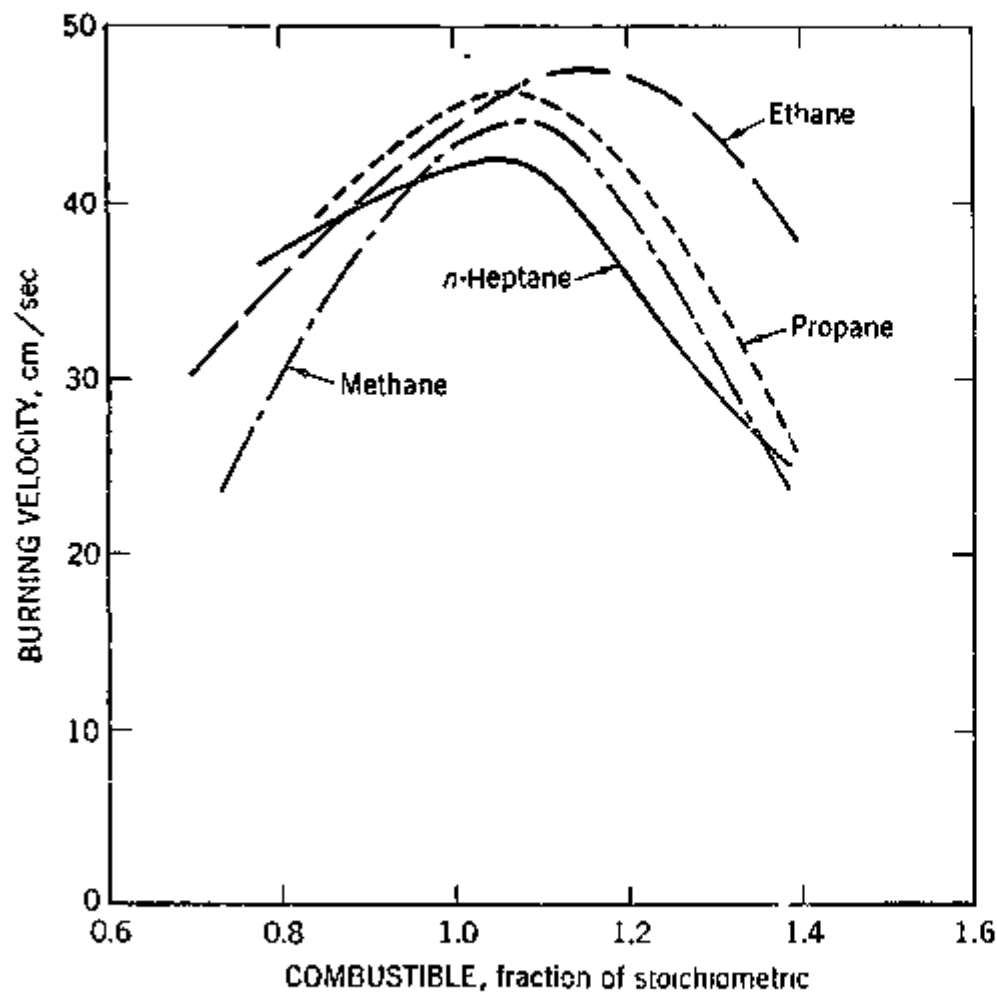


FIGURE 2-1 BURNING VELOCITIES OF METHANE-, ETHANE-, PROPANE-, AND n-HEPTANE VAPOR AIR MIXTURES AT ATMOSPHERIC PRESSURE AND ROOM TEMPERATURE. (REFERENCE 4)

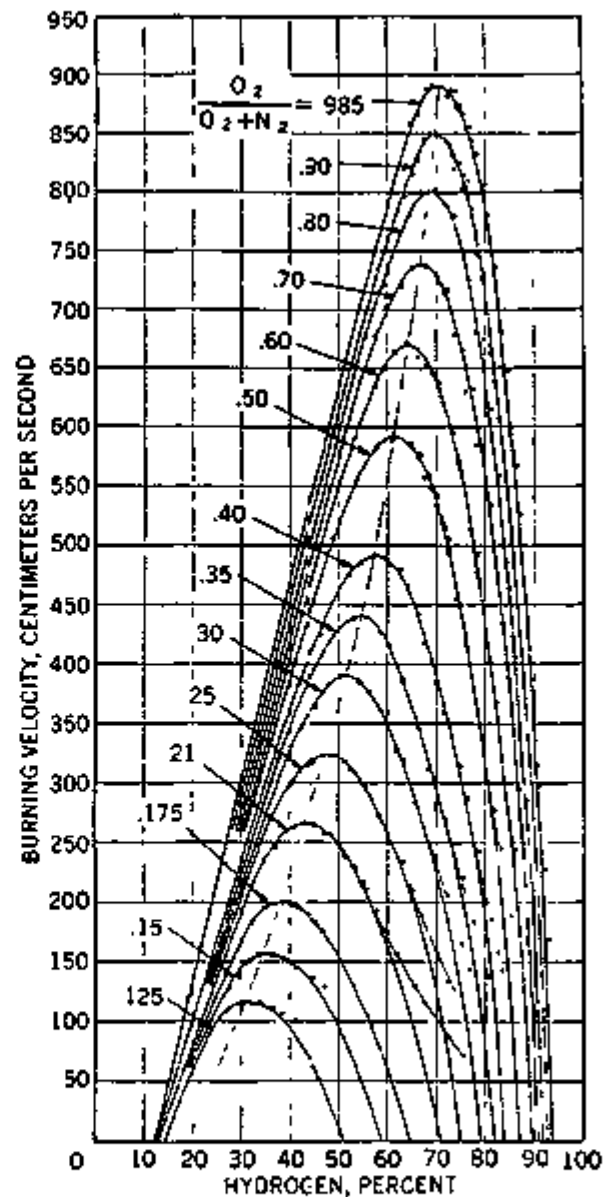


FIGURE 2-2 BURNING VELOCITIES OF MIXTURES OF HYDROGEN, OXYGEN, AND NITROGEN AT ROOM TEMPERATURE AND ATMOSPHERIC PRESSURE (JAHN). (REFERENCE 5)

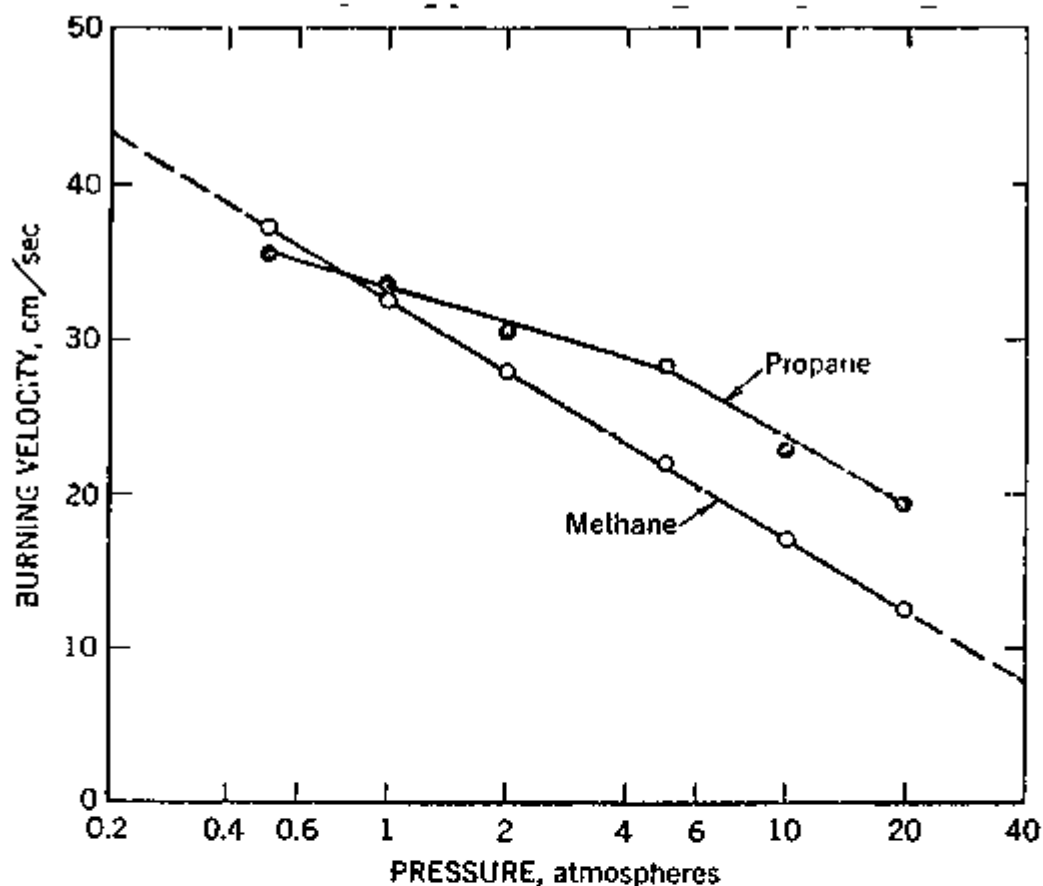


FIGURE 2-3 Variation in Burning Velocity of Stoichiometric Methane-Air and Propane-Air Mixtures With Pressure at 26° C  
(Reference 4)

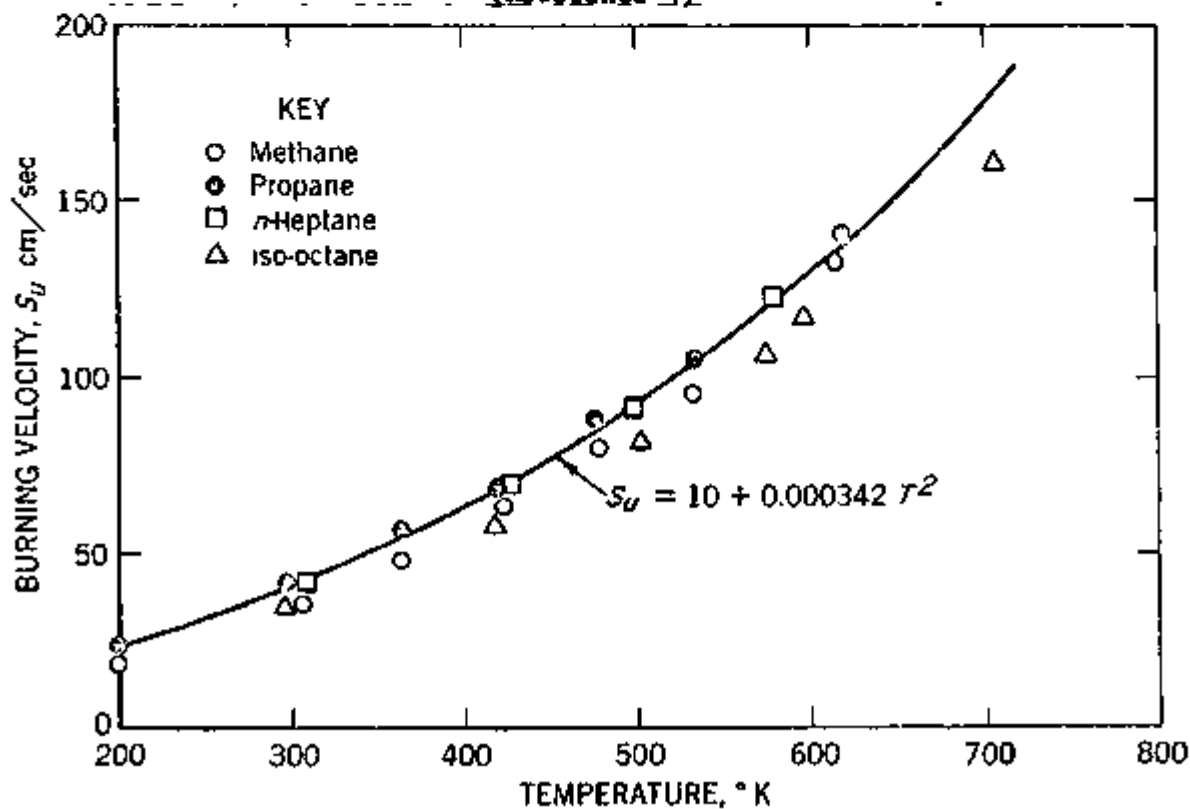


FIGURE 2-4 -Effect of Temperature on Burning Velocities of Four Paraffin Hydrocarbons in Air at Atmospheric Pressure.  
(Reference 4)

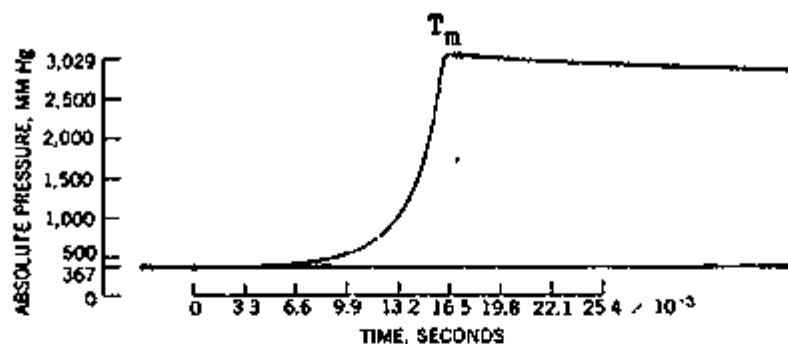


FIG. 2-5 Time-pressure record of ozone explosion in spherical vessel  
 $T_0 = 301.1^\circ\text{K}$ ;  $P_0 = 307 \text{ mm Hg}$ ; 10.00%  $\text{O}_3$  in  $\text{O}_2$   
 (Reference 5)

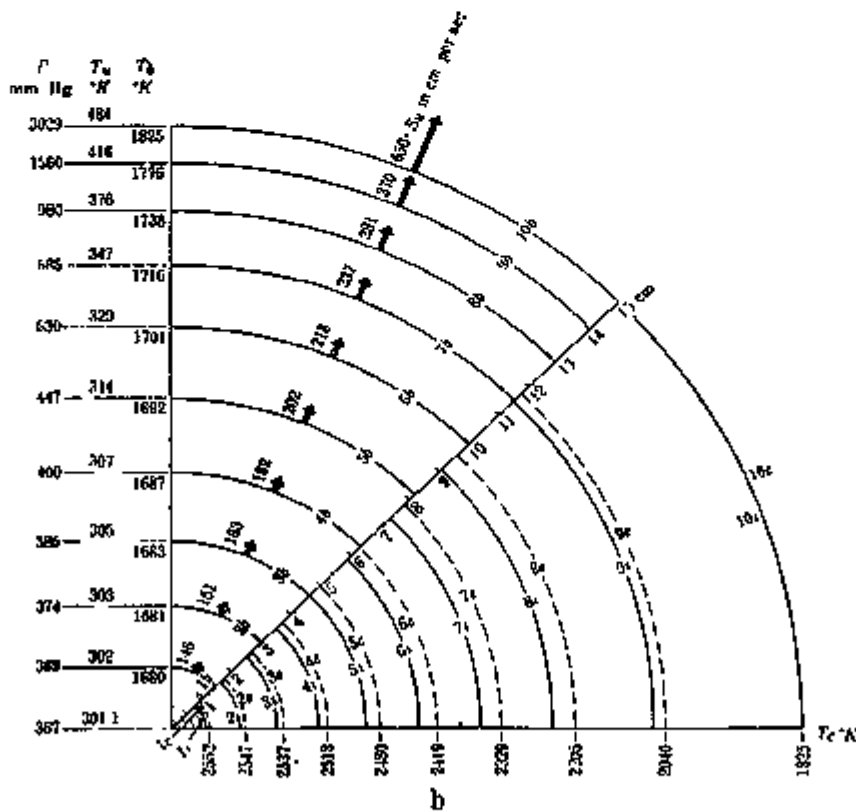


FIG. 2-6 Analysis of explosion pressure record shown in Fig. 2-5  
 (Reference 5)



are the radius of the volume which is occupied by the burned gas at time intervals of one-tenth the total explosion time,  $t_m$ . The burning velocity ( $S_u$ ), is indicated by arrow. Although not given in the figure, the actual flame speed ( $S_b$ ) is easily obtained by dividing the distance between the two circles by time interval. To each circle 1b, etc., the corresponding pressure  $P$  and temperature  $t_b$  are indicated along the ordinate, showing that at the initial stage gas burns and expands at practically constant pressure. It is subsequently compressed to nearly its original volume at the end of the combustion process. This means that the last portion of the gas to burn must be first compressed adiabatically and then expanded to approximately its original volume, as indicated by circles 9i, 9b and 9e. Toward the last stage of the process, burning velocity becomes greatest.

A mathematical model of the explosion in a closed vessel has been derived by Nagy, Conn, and Verakis.<sup>(6)</sup> Based on the equation of state and law of adiabatic expansion, the following equations were derived to express the pressure-time relationships of the explosion in a spherical vessel.

$$\frac{dP(t)}{dt} = \frac{3\gamma S_u' T_u(o)^2 P_r \beta P(m)^{2/3\gamma}}{a T_r^2 P(o)^{2-3/\gamma}} \left[ P(m)^{1/\gamma} - P(o)^{1/\gamma} \right]^{1/3} \left[ 1 - \left( \frac{P(o)}{P(t)} \right)^{1/\gamma} \right]^{2/3} P(t)^{3 - \frac{2}{\gamma} - \beta} \quad (2)$$

which will lead to a simplified expression for the maximum explosion pressure in a closed vessel<sup>(6)(7)</sup>

$$\frac{P(m)}{P(o)} = \frac{M_u T_b}{M_b T_o} \quad (3)$$

where

- $a$  \* radius of enclosure.
- $\gamma$  \* ratio of specific heat of the gas at constant pressure to constant volume.
- $S_u'$  = burning velocity at the reference level of temperature and pressure
- $M_u, M_b$  = average or effective molecular weights of unburned and burned gases.
- $\beta$  = exponent indicating dependence of transformation velocity on pressure.
- $P(m)$  \* final explosion pressure, maximum pressure in a closed vessel, absolute
- $P(o)$  = initial pressure, absolute
- $P_r$  = reference pressure level, 14.7 psia.

- R = universal gas constant.
- $T_u(o)$  = initial temperature.
- $T_r$  = reference temperature level, 537° R.
- $T_b(o)$  = adiabatic flame temperature or temperature of the burned gas at  $P(o)$

Cousins and Cotton<sup>(8)</sup> measured explosion pressure of 5% propane-air mixture in a 3-cu-ft. tank at 90 psi. Harris<sup>(9)</sup> reported a pressure of 117 psi for a 3% pentane-air mixture. A complete tabulation of explosion data for various vapors and gases is available in NFPA Pamphlet No. 68<sup>(10)</sup> and Engineering Bulletin of Purdue University<sup>(11)</sup>.

As concluded by Harris<sup>(9)</sup> in his investigation of combustion explosion in closed vessels of 4 liter and 60 ft<sup>3</sup> in size, the maximum pressure of the most explosive pentane-air mixtures (slightly richer than stoichiometric) remained constant, while the pressure generated in lean and in very rich mixtures decreased with the increase in vessel size (see Figure 2-7). The explanation for lower peak pressure in lean and very rich mixtures in the large vessel size is probably caused by considerable increase in heat loss through the vessel walls occurring during the long reaction time. It was also found that for a fairly well defined concentration region (2.7 to 4.0 mole percent) in a large vessel, a vibrating pressure curve trace was observed. The mixture burned with a screeched pattern instead of the normally silent combustion. The rate of pressure  $dp/dt$  for the vibratory combustion was considerably higher than the combustion at the stoichiometric concentration.

These vibratory explosions have been observed by a number of workers, but only in large vessels. The explanation for this effect is not known, but it is possible that pressure waves travelling ahead of the flame are reflected from the vessel walls and cause distortion of the flame front.

The effect of turbulence on closed vessels was also investigated by Harris<sup>(9)</sup>. It was found that a high degree of turbulence, caused by a fan of 18-in. diameter, turning at 200 rpm in a 60 ft<sup>3</sup> vessel causes a marked increase in the rate of pressure rise,  $dp/dt$ . This increase in the rate of pressure rise has no effect on the maximum explosion pressure for the mixture between 2.7 to 4 mole percent but has a marked increase for the lean and very rich mixtures.

### 2.2.2 Maximum Explosion Pressure resulting from a Localized Explosion

The explosion pressure in a confined gaseous combustion explosion is governed by three independent processes: 1) gas expansion due to temperature rise; 2) gas expansion due to increase in molecular weight or number of moles resulting from the combustion reaction; and 3) the stagnation pressure created at the walls by sudden deceleration of the combustion wave (flame front). For the ordinary explosion (deflagration) of a hydrocarbon-air mixture which has a flame speed of less than 20 ft per sec, the stagnation pressure is less than 0.004 psi; therefore, only the first two processes indicated above will be considered.

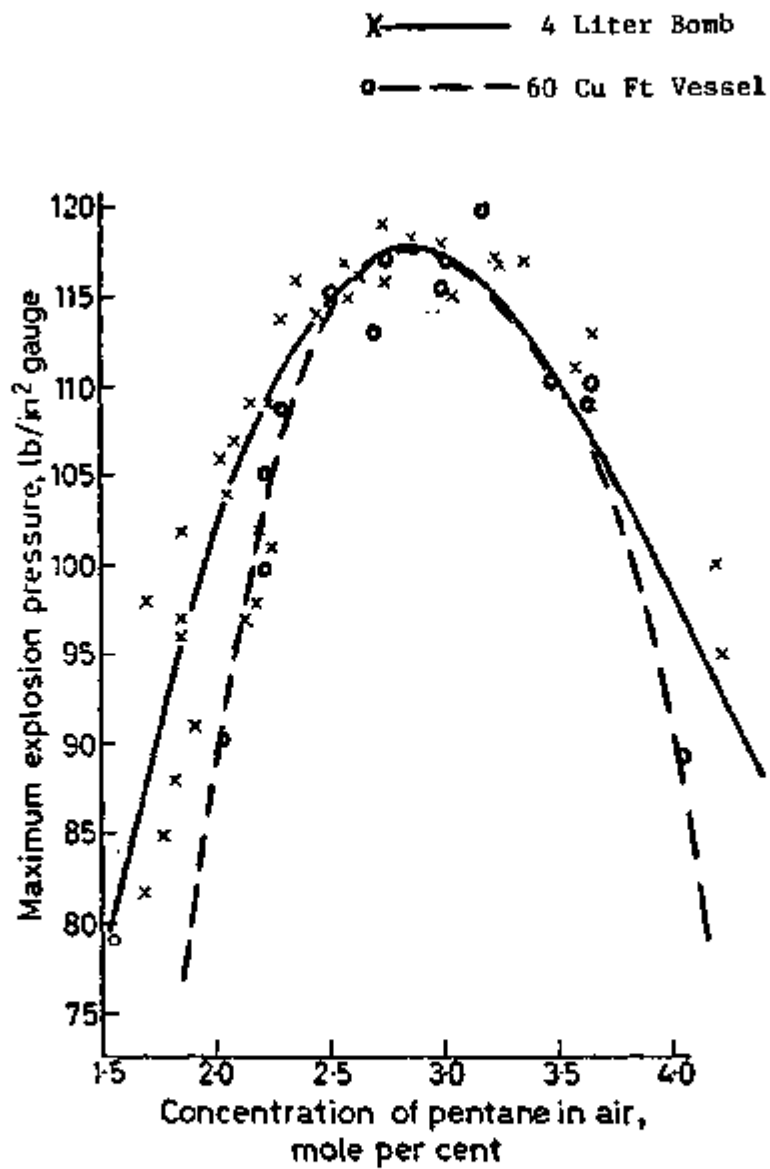


FIG. 2-7 MAXIMUM EXPLOSION PRESSURE VERSUS COMPOSITION OF THE MIXTURE FOR 4-LITER BOMB AND 60-CU-FT VESSEL.

(Reference 9)

Suppose that a combustible gas mixture at the initial volume of  $V_u(o)$  is ignited at the center of a closed vessel which has a volume of  $V$  and, at the end of the combustion process, the products of combustion are expanded from  $v(o)$  to  $V_b(e)$ , as shown in Figure 2-8. The gas outside the flame volume  $v_u(e)$  is then being compressed adiabatically to a pressure of  $p(e)$ . Applying the law of adiabatic compression to the gas space outside the flame volume, we find

$$P(o) \left[ V - V_u(o) \right]^\gamma = P(e) \left[ V - V_b(e) \right]^\gamma \quad (4)$$

Employing the ideal gas law to the combustible mixture,  $V_u(o)$ , before and after the combustion reaction, we have

$$P(o) V_u(o) = \frac{m_o}{M_u} R T_u(o) \quad (5)$$

$$P(e) V_b(e) = \frac{m_o}{M_b} R T_b(e) \quad (6)$$

where

$m_o$  = Initial mass of the gas mixture

Combining the above three equations and rearranging the terms, we find

$$V_u(o) \left\{ \frac{M_u T_b(e)}{M_b T_u(o)} \left[ \frac{P(e)}{P(o)} \right]^{\frac{1-\gamma}{\gamma}} - 1 \right\} = V \left\{ \left[ \frac{P(e)}{P(o)} \right]^{\frac{1}{\gamma}} - 1 \right\} \quad (7)$$

In the case of localized gaseous combustion explosion, which is probably close to the condition of most of the accidental explosions, the relationship between the ratio of the volume of the combustible mixture and the volume of the vessel,  $V_u(o)/V$ , and the maximum explosion pressure  $p(e)$ , can be expressed as

$$\frac{V_u(o)}{V} = \left\{ \left[ \frac{P(e)}{P(o)} \right]^{\frac{1}{\gamma}} - 1 \right\} \left/ \left\{ \frac{M_u T_b}{M_b T_u} \left[ \frac{P(e)}{P(o)} \right]^{\frac{1-\gamma}{\gamma}} - 1 \right\} \right. \quad (8)$$

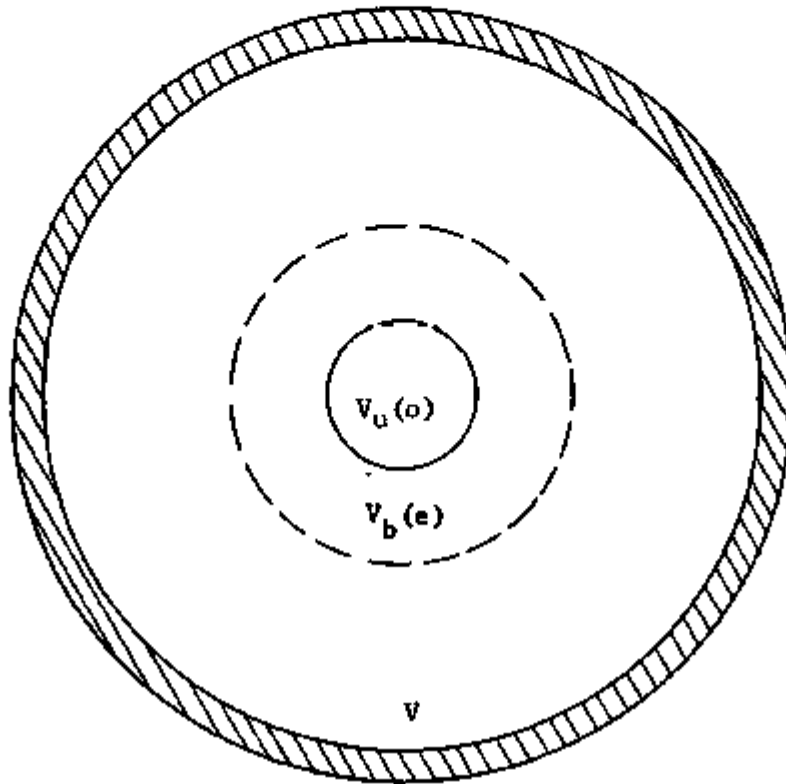


FIG. 2-8 A CONCEPTUAL MODEL OF A CENTRALLY IGNITED LOCALIZED (BALLOON) EXPLOSION INSIDE A SPHERICAL CHAMBER.

For the case of explosion in a vessel which is being filled completely with a combustible mixture, the same expression shown in equation (3) can be obtained by substituting  $V_u(o) = V$  into equation(8).

$$\frac{P(m)}{P(o)} = \frac{M_u T_b}{M_b T_u} = \frac{n_b T_b}{n_u T_u} \quad (9)$$

For stoichiometric propane/air mixture,  $M_u/M_b = \frac{n_b}{n_u} = 1.04$  and  $T_b = 2265^\circ\text{K}$ <sup>(11)</sup> and for hydrogen/air mixture  $M_u/M_b = 0.84$  and  $T_b = 2490^\circ\text{K}$ .

### 2.3 EXPLOSION RELIEF WITH FREE-VENT

In closed vessel explosions, it has been seen that the maximum pressure developed is practically independent of volume and depends almost entirely on the nature of the combustible for a given initial temperature and pressure. In open vent explosions, the maximum pressure developed depends also on flow characteristics through the opening and pressure drop across it, so that the rate of pressure rise inside the enclosure is an important factor in determining the pressure and time relationship resulting from an open vent explosion. The actual pressure rise is balanced by two opposing factors. First, there is the rise in pressure due to the temperature rise resulting from the propagation of flame, and second, there is a continuous falling in pressure due to the escape of the gas through the openings.

#### 2.3.1 Previous Work

Benson and Burgoyne<sup>(12)</sup> derived a simplified expression to predict the peak explosion pressure for a given vent area  $A_v$ , in a spherical vessel by equating the maximum rate of volume increase, when the flame front reaches the wall, to the rate of efflux of the unburned gas through the opening under a pressure head of peak pressure difference across the opening:

$$\frac{P(e)}{P(o)} = \left\{ \left[ \frac{4\pi a^2 \sigma_w}{CA_v} \right]^2 \frac{1}{2P(o)\rho_u(o)} \left( \frac{\gamma-1}{\gamma} \right) + 1 \right\}^{\frac{\gamma}{\gamma-1}} \quad (10)$$

up to the critical pressure of  $P(e)/P(o) < 1.59$

Where

$a$  = equivalent radius of the enclosure, ft

$C$  = Orifice discharge coefficient

$\sigma$  = Expansion ratio,  $\sigma = P(m)/P(o)$

$\omega$  = Mass burning speed,  $\omega = g\rho_u(o)S_u$ , lb/sec ft<sup>2</sup>

$A_v$  = Vent area, ft<sup>2</sup>

$\rho_u(o)$  = mass density at initial conditions, lb sec<sup>2</sup>/ft<sup>4</sup>

Jones (13) introduced a simplified equation to predict the pressure-time relationship of a dust explosion in a vented enclosure based on the assumption of a constant mass burning rate. However, none of these equations has ever been verified with experiments.

### 2.3.2 Mathematical Model

In view of the lack of understanding on the principles of the vented explosion, an attempt has been made to derive a mathematical model based on the spherical flame propagation theory, conservation of mass and adiabatic compression. Details of the derivations are presented in Appendix A, which shows that the pressure-time relationship of a free-vent explosion can be expressed by the following three simultaneous non-linear ordinary differential equations:

$$\frac{d\zeta}{d\tau} = 3\chi\gamma(\nu-1)\zeta^{\frac{3\gamma-2}{3\gamma}}\xi^{2/3} - \alpha(\nu\psi_b + \nu^{\frac{1}{2}}\psi_u)\gamma\zeta^{\frac{\gamma-1}{\gamma}}\sqrt{\frac{\gamma}{\gamma-1}(\zeta^{\frac{\gamma-1}{\gamma}} - 1)} \quad (11)$$

$$\frac{d\xi}{d\tau} = 3\chi\zeta^{\frac{1}{3\gamma}}\xi^{\frac{2}{3}} - \psi_b\alpha\sqrt{\frac{\gamma}{\gamma-1}(\zeta^{\frac{\gamma-1}{\gamma}} - 1)} \quad (12)$$

$$\frac{d\lambda}{d\tau} = -3\chi\zeta^{\frac{1}{3\gamma}}\xi^{2/3} - \psi_u\alpha(\nu)^{\frac{1}{2}}\sqrt{\frac{\gamma}{\gamma-1}(\zeta^{\frac{\gamma-1}{\gamma}} - 1)} \quad (13)$$

The above dimensionless parameters are defined as

$$\zeta = \frac{P(t)}{P(o)} \quad (14)$$

$$\tau = \frac{t S_u v^{2/3}}{a} \quad (15)$$

$$\alpha = \frac{2CA_v a}{S_u n_o} \left(\frac{1}{v}\right)^{7/6} \left(\rho_u(o) P(o)\right)^{1/2} = \frac{2CA_v a}{S_u v} \left(\frac{P(o)}{\rho_u(o)}\right)^{1/2} \left(\frac{1}{v}\right)^{7/6} \quad (16)$$

$$\xi = \frac{m_{rb}(t)}{m_o} \quad (17)$$

$$\lambda = \frac{m_{ru}(t)}{m_o} \quad (18)$$

$$v = \rho_u(o) / \rho_b(o) \quad (19)$$

$$\psi_b + \psi_u = 1 \quad (20)$$

Where

$\lambda$  is the dimensionless unburned gas remaining

$\xi$  is the dimensionless burned gas remaining

$m_{rb}$  is the burned gas remaining in enclosure;

$m_{ru}$  is the unburned gas remaining in enclosure;

$m_o$  is the initial gas mass;

$\zeta$  is the dimensionless pressure;

$\tau$  is the dimensionless time;

$\chi$  is the turbulence correction factor, and

$\psi_b$  and  $\psi_u$  are the fraction of the total opening area from which the burned and unburned gases are flowing out.

$v$  is the dimensionless density

$\alpha$  is the explosion venting parameter for spherical vessel



The first term on the right hand side of equation (11) represents the pressure rise due to the flame propagation and the second term represents the falling in pressure due to the escape of burned and unburned gases through the opening. Equations 11, 12 and 13 also indicate that the explosion pressure is a function of four independent dimensionless parameters;  $\alpha$ ,  $\nu$ ,  $\psi_b$  and  $\chi$ .

$\alpha$  and  $\nu$  consist of a number of well defined geometrical and physical properties;  $\psi_b$  and  $\chi$  have to be determined experimentally. The above equations have been programmed for the 360 IBM computer using the fourth order Runge-Kutta integration method for two different cases.

Case I. Only the unburned gases are flowing out, i.e.:

$$\psi_u = 1 \quad ; \quad \psi_b = 0 \quad (21)$$

Case II. The quality of the out-flowing gases is directly proportional to the ratio of burned and unburned gases remaining inside the vessel at the instant,  $t$ , i.e.:

$$\begin{aligned} \psi_b &= \xi / (\xi + \lambda) \\ \psi_u &= \lambda / (\xi + \lambda) \end{aligned} \quad (22)$$

Figure 2-9 shows the pressure-time curve predicted for a 24-in. diameter free-vent on a 27 cu. ft. vessel at two different turbulence levels using the computer program for Case I. In comparison with the closed vessel explosion curve, the free-vent explosion pressure rises slowly to a peak of 0.59psi and then reduces back to the base line.

### 2.3.3 Discussion

It has been customary to specify explosion venting data in terms of maximum pressure as a function of a ratio vent area/volume of the vessel, (1)(8)(10) Recently, Maisey<sup>(7)</sup> and Palmer and Rogowski<sup>(14)</sup> showed experimentally that a more logical method of specifying vent area is to express it as a vent area factor,  $K$

$$K = \frac{A}{A_v} = \frac{\text{cross sectional area of side containing the vent}}{\text{area of vent}} \quad (23)$$

For the purpose of correlation or scale-up of experimental data which is conducted with a known gas mixture in a cubical vessel, controlling variables  $\nu$ ,  $\psi_b$  and possibly  $\chi$  become constants. The only controlling parameter  $\alpha$  can be further reduced into:

$$\alpha = f \left( \frac{A_v A}{V} \right) = f_1 \left( \frac{A_v}{A} \right) = f_2 (K)^{-1} \quad (24)$$

Figure 2-10 is a graphical presentation of the published free-vent explosion pressure versus  $K$  ratio. The figure shows that the data obtained correlate very well with the  $K$  factor for different volumes of vessels. However, the large difference between the data of Cousins and Cotton<sup>(8)</sup> and that of Palmer and Rogowski<sup>(14)</sup> is not explainable at the present time.

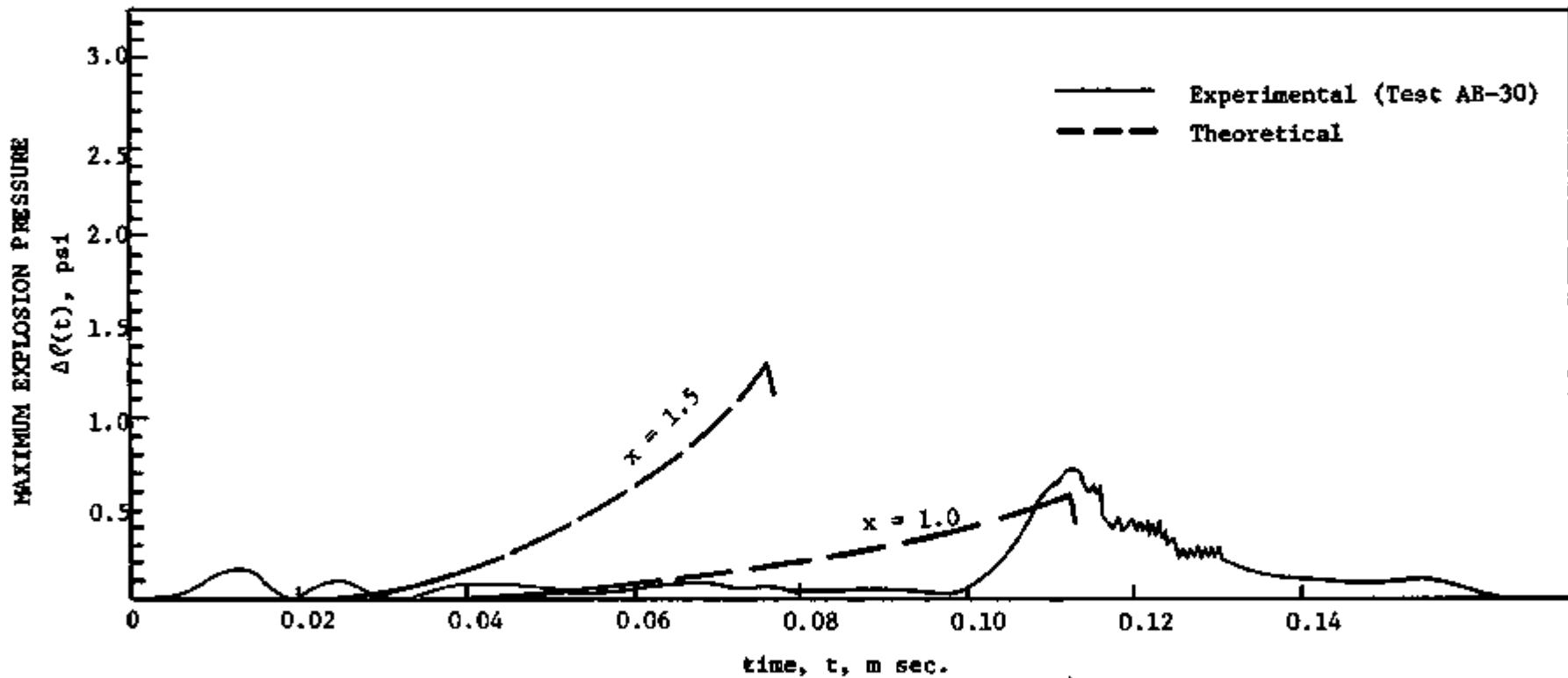


Figure 2-9 Theoretically Predicted Pressure-Time History For a 24 in. Diameter Free-Vent in a 27 cu. ft. Vessel

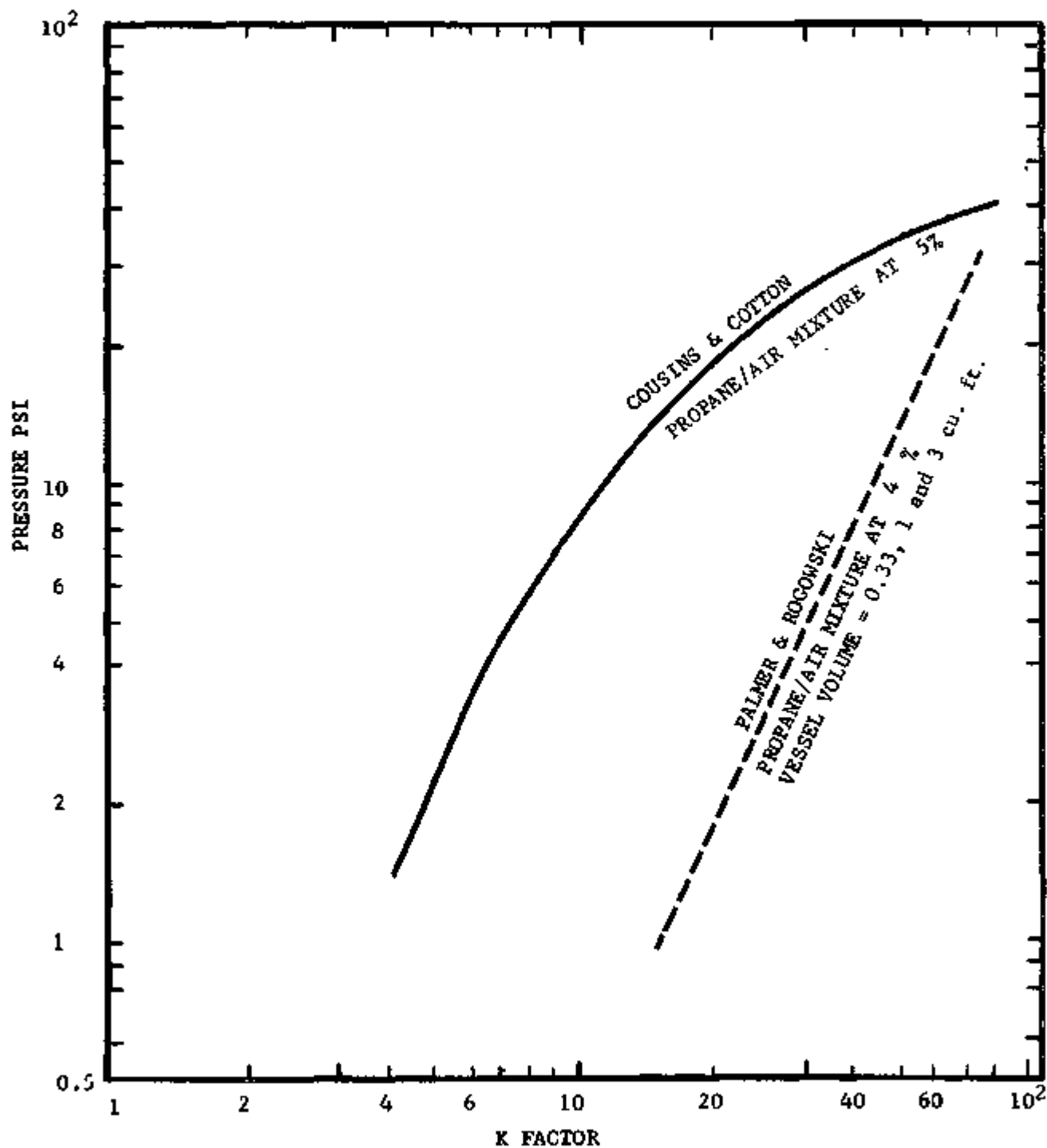


FIG. 2-10 GRAPHICAL PRESENTATION OF PUBLISHED FREE-VENT EXPLOSION DATA

#### 2.4 EXPLOSION RELIEF WITH FILTERS

The basic principle of explosion relief through filters is very much similar to that described earlier for open vent except that the gas in this case escapes through the filters.

Two major theoretical approaches<sup>(15,16)</sup>, channel theory and drag theory, have been followed to calculate the flow through filters in the viscous flow region. The equation derived agrees very well with experimental data in this region when the Reynolds number,

$$N_{re} = \frac{d_f v' \rho}{\mu} \frac{1}{1-z} < 10$$

Where

$d_f$  = diameter of the filter fibers

$\rho$  = density of the air

$\mu$  = viscosity of the air

$z$  = void fraction

$v'$  = actual face velocity across the filter media surface

These equations can be expressed in a simple form:

$$C_1 [P(t) - P(o)] = \mu v_s \quad (25)$$

Where  $C_1$  is characteristic of the geometrical parameters such as  $d_f$ ,  $z$  etc.  $v_s$  is the superficial velocity based on the cross-sectional area of the filter unit and  $\mu$  is the dynamic gas viscosity which is independent of pressure but approximately proportional to temperature.

For the turbulent flow region,  $N_{re} = \frac{d_f v_s \rho}{\mu} \frac{1}{1-z} > 1000$ , gas flowing through a filter can be expressed by:

$$C_2 [P(t) - P(o)] = \mu v_s^2 \quad (26)$$

Where the geometrical parameter  $C_2$  is a function of  $d_f$ ,  $z$ , Filter thickness, etc.

By summing up equations (25) and (26), equation for a fibrous filter over the entire flow region can be expressed by:

$$P(t) - P(o) = \frac{1}{C_1} \mu v_s + \frac{1}{C_2} \mu v_s^2$$

Where the geometrical parameter  $C_1$  and  $C_2$  for a given filter can be estimated from pressure versus flow-rate data points which are usually supplied by the filter manufacturer, (see Figure 2-11).  $C_1$  is calculated more accurately at lower values of  $N_{re}$  and  $C_2$  is calculated more accurately at higher values of  $N_{re}$ .

For the commonly used AEC absolute filters with average fiber diameter of less than 1 micron, under the conditions pertaining to this study,  $p(t) - p(o) < 4$  psi,  $N_{re}$  is much smaller than 1. Therefore, the laminar

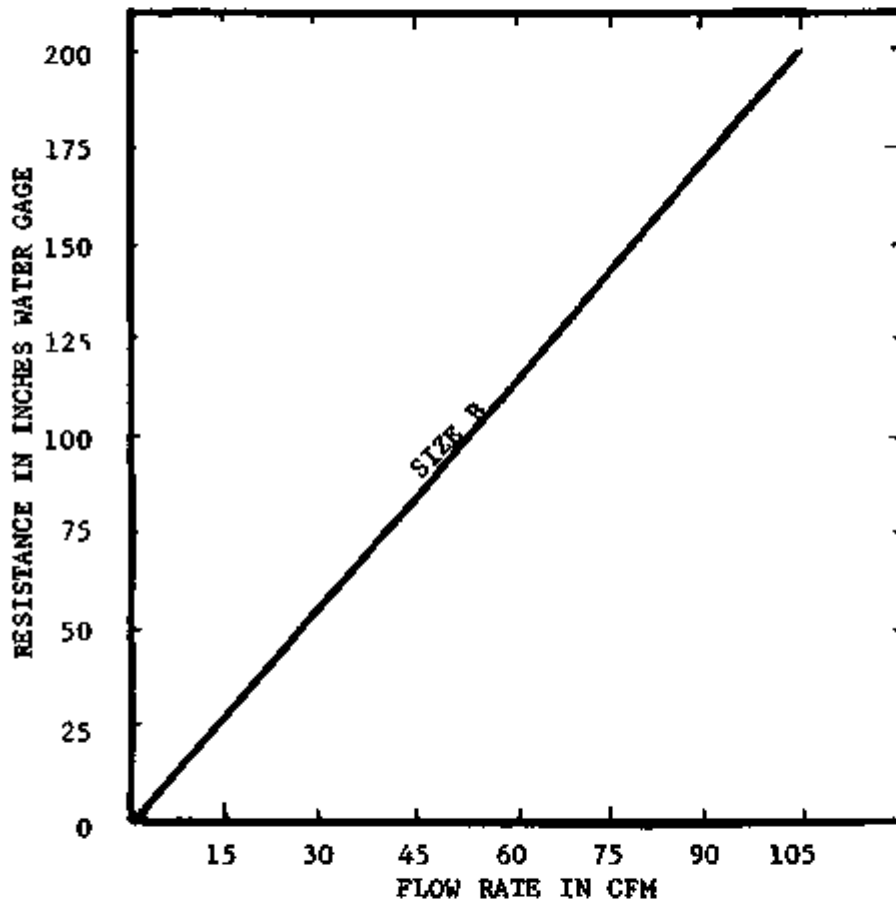


FIG. 2-11 FLOW CHARACTERISTICS OF SIZE B FLANDERS HIGH EFFICIENCY FILTER UNIT

gas flowing through the filter can be expressed as:

$$\frac{dm}{dt} = C_1 A_F \rho \frac{[P(t) - P(o)]}{\mu} \quad (27)$$

where  $m$  is the mass flow,

$A_F$  is the cross-sectional area of the filter unit.

The flow characteristics of a size B Flanders high-efficiency filter is compared with that for a sharp edge orifice in Figure 2 12. This figure shows that for a given pressure drop of 2 psi the free orifice is about 3.6 times more effective than a type B Flanders high-efficiency filter in venting 60°F air and 3.32 times more effective in venting 1000°F air. However, the advantage of a free orifice over a filter in venting gradually reduces for higher pressure ranges. In order to vent equal amounts of air at 1000°F, the filter has to be 3.3 times larger than the free orifice at the pressure differential of 4 psi, and 2.1 times larger at 4 psi.

The governing differential equations for pressure response for explosion venting with filters has been derived in the Appendix A as

$$\frac{d\xi}{d\tau} = 3\chi\gamma(\nu-1)\xi^{\frac{3\gamma-2}{2\gamma}}\xi^{2/3} - (\psi_b + \nu\psi_u)\alpha_F\gamma\xi^{\frac{1}{\gamma}}(\xi-1) \quad (28)$$

$$\frac{d\xi}{d\tau} = 3\chi\gamma(\nu-1)\xi^{\frac{1}{3\gamma}}\xi^{2/3} - \frac{\psi_b\alpha_F}{\nu}\xi^{\frac{2-\gamma}{\gamma}}(\xi-1) \quad (29)$$

where the explosion venting parameter for filter is defined as:

$$\begin{aligned} \alpha_F &= \frac{C_1 A_F^a}{S_u m_o} \left( \rho_u(o) P(o) \right) \left( \frac{1}{\nu} \right)^{5/3} \\ &= \frac{C_1 A_F^a}{S_u V} \left( P(o) \right) \left( \frac{1}{\nu} \right)^{5/3} \end{aligned} \quad (30)$$

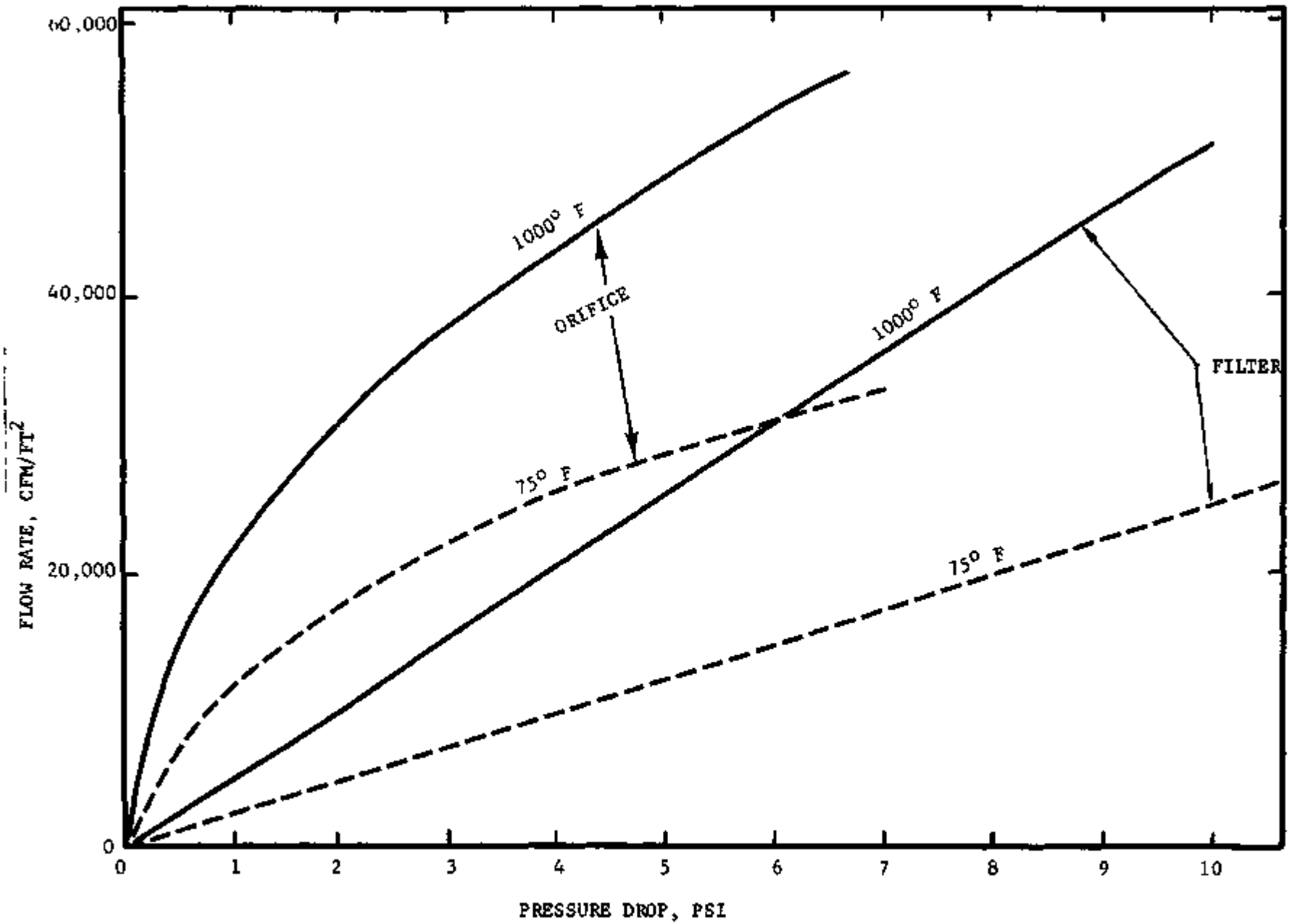


FIG. 2-12 COMPARISON OF FLOW CHARACTERISTICS BETWEEN A TYPE B FLANDERS HIGH-EFFICIENCY FILTER AND A SHARP EDGE ORIFICE AT DIFFERENT TEMPERATURES AND PRESSURES.

## 2.5 EXPLOSION RELIEF WITH BURSTING DIAPHRAGM

As previously described, explosion pressure can be reduced considerably by the provision of free-vents through which explosion gases can be released. In AEC glovebox operations, such a vent opening has to be covered for normal operations. Therefore, knowledge is required not only of the area of relief necessary in relation to the size and strength of the glovebox components, but also of the manner and the condition in which the relief is to be uncovered. Theoretical treatment of the subject presents a number of difficulties and in the present state of knowledge it is not possible to predict the relief requirements from theoretically sound principles.

Some data, mainly empirical, are available, particularly for explosion relief using bursting diaphragms in short cylindrical or cubical vessels; this work has been reviewed by Maisey<sup>(7)</sup>. In general, the measured pressure-time records show distinctive double-peak characteristics. A typical pressure-time record (measured by Simmonds and Cabbage<sup>(17)</sup> for an explosion in a cubical oven vented with a bursting diaphragm pressure relief) is presented in Figure 2-13.

This double pressure peak characteristic associated with the bursting diaphragm explosion can be explained mathematically by solving the general differential equations (11), (12) and (13) for the following initial and boundary conditions:

- 1) Initial condition

$$\tau = 0$$

$$\zeta = 1$$

- 2) up to the point of bursting  $0 < \tau < \tau_b$

$$\tau = \tau_b \text{ when } P = P_b$$

$$\alpha = 0$$

- 3) Assume that only the unburned gas is leaking through the opening, after the bursting of the diaphragm, that is

$$\psi_u = 1$$

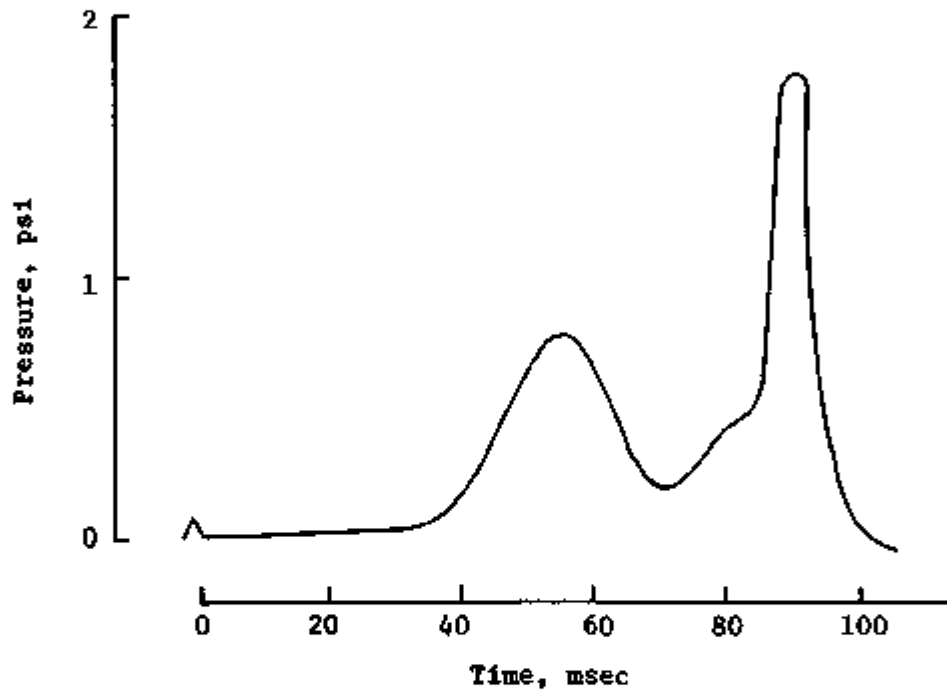
$$\psi_b = 0$$

The computation can proceed until all the unburned gas mixture inside vessel is consumed; i.e.,

$$\lambda = 0$$

- 4) After the flame front reaches the wall,  $\lambda = 0$ , the first term on the right hand side of equations (11), (12) and (13) will be dropped out.





Oven Volume = 4.6' x 4.6' x 4.6'

Vent Area = 9 ft<sup>2</sup>

Bursting Diaphragm = Rubberized Asbestos

Figure 2-13 A Typical Pressure-Time History for an Explosion in a Cubical Oven Vented With a Bursting Diaphragm (Reference 17)

A program to obtain numerical solution from these equations and boundary conditions using the 4th Order Runge Kutta integration method on an IBM 360 computer has been completed. The theoretically predicted pressure-time curve will be compared with the experimentally measured curve later in Section 4.2.1 of this report.

### 2.5.1 First Pressure Peak and Bursting of Diaphragm

If a combustible gas mixture is ignited at the center, the flame will propagate spherically outward as the case in closed vessel explosions. Depending upon the size of the vessel and type of gas mixture, a rapidly increasing pressure load is exerted on the diaphragm until failure occurs. This bursting pressure is represented by the first pressure peak in Figure 2-13.

The static bursting pressures of diaphragms of pure metals (18) at atmospheric temperature follow the function of

$$P_b = \frac{4\delta\sigma_b}{d} \quad (31)$$

where  $P_b$  is the bursting pressure,  $d$  is the diameter of the diaphragm,  $\delta$  is the thickness of the diaphragm, and  $\sigma_b$  is the bursting strength. For the case of a static bursting of a diaphragm, the bursting strength, in fact, is a variable which is expressed (19) as

$$\sigma_b = \frac{4E\delta^2}{d^2} \left[ \frac{2}{1-\epsilon} \left(\frac{y}{\delta}\right) + \frac{1}{2} \left(\frac{y}{\delta}\right)^2 \right] \quad (32)$$

and

$$y = \sqrt{\frac{\sigma_d d^2}{4 (0.976E)}} \quad (33)$$

where  $y$  = Maximum deflection at the center

$E$  = Young's modulus

$\sigma_d$  = Ultimate strength

$\epsilon$  = Poissons Ratio

$\delta$  = Thickness

Under the actual explosion relief condition, the diaphragm material is strain rate dependent. The dynamic response of linear impact on a structural member is treated classically by using the analogy of a weight suspended by a spring in a frictionless environment. It has been shown that the yield stress for the dynamic case is approximately twice that of the static case. (20). Further study in this area is recommended.

### 2.5.2 Second-Peak Pressure

The second-peak pressure and the shape of the pressure-time curve may be explained by consideration of the course of events after the bursting of the diaphragm. As described earlier, for a constant burning speed, the rate of formation of products, and consequently, the rate of rise of pressure, depends on the surface area at which combustion can take place. This area increases rapidly as the combustion front spreads outwards. For a low pressure release diaphragm the combustion flame front area at the time of bursting of the diaphragm is relatively small. A relatively small size opening will be sufficient to provide the venting needed to rapidly reduce the pressure. Depending upon the opening size, strength of the mixture, and the possible inertia force associated with the bursting of the diaphragm, a pressure built-up inside the vessel to a second pressure peak has been experienced as the combustion process is continued (see Figure 2-13). The rapid increase in pressure is caused by

- 1) the rapid increase in the formation of products especially when the flame approaches the wall of the vessel as expressed in Appendix A, and
- 2) the sudden or gradual increase in burning velocity after the bursting of the diaphragm due to the turbulent and vibratory flame propagation effects.

1. Turbulence Effect- Vibratory pressure propagation has been observed in explosions in large vented and unvented vessels (9) (21) (22) and in long ducts (23) (24). A vibratory pressure response has also been noted in pressure traces obtained in experiments during the present program. Markstein (25) associates vibratory pressure wave propagation with a cellular flame front of increased surface area and the subsequent increase in burning velocity. Burgoyne and Wilson (21) provide other possible reasons for this phenomenon. They recognize vibrations as a result of combustion instability. Partial explanations for this phenomenon are as follows:

- 1) instability by the relative diffusion rates of fuel and oxygen through the flame.
- 2) oscillation of the burning gas by vibration of the vessel and auxiliary equipment.
- 3) interaction of shock or pressure waves with the flame front.

- 4) onset of turbulent flow conditions in the unburnt gas ahead of the propagating flame.
- 5) turbulent burning front induced by the flowing of exhaust unburned gas which travels in a direction perpendicular to the flame propagation.

As described in Section 2.2.3, turbulence and vibratory combustion were found to accelerate the flame propagation speed and burning rate. These effects can be induced in an explosion chamber in many different ways such as bursting of a diaphragm, interaction between the propagating flame and the occupying gases, placing obstacles along the direction of the flame propagation or stirring with a fan. Harris and Briscoe<sup>(22)</sup> made an extensive study of the effect of turbulence on the bursting diaphragm explosion over a range of concentration of pentane-air mixtures using a 60-cu-ft cylindrical vessel. Turbulence was produced by operating a four-blade 19-in. diameter fan driven at speeds up to 2000 rpm. The material of the bursting diaphragm was varied so that a constant 17 psi bursting pressure (first-peak) was achieved regardless of the vent size. The measured maximum pressure (second-peak) is presented in Figure 2-14 as a function of degree of turbulence, expressed in terms of fan operating speed. The pressure rose to maximum with the increase in fan speed for a small vent, but for larger vents the explosion pressure did not reach a maximum at the highest attainable speeds of 2000 rpm. Although these data are not directly applicable to the low pressure relief case which is the primary interest of this study, they demonstrate the effect of turbulence or increase in rate of burning on the explosion pressure (second-peak).

2. Effect of Geometry and Configuration - The explosion pressure (second pressure peak) is customarily expressed as a function of the vent ratio, vent area/volume of the vessel. Recently, Simmonds and Cabbage<sup>(17)</sup> correlated the measured second pressure peak as a function of the vent area factor K (cross-sectional area of the wall containing the vent / vent area). The variation of measured second-peak pressure,  $P_2$  (psi) with the parameter K is shown in Figure 2-15. It is reported that for design purposes in a cubical oven with the rubberized asbestos sheet as the bursting diaphragm, the value of second-peak pressure is given simply by

$$P_2 = K = A/A_v$$

This relationship has been verified for town gas explosion in an oven of 8 to 98 cu ft in size for a K value of 1 to 3.

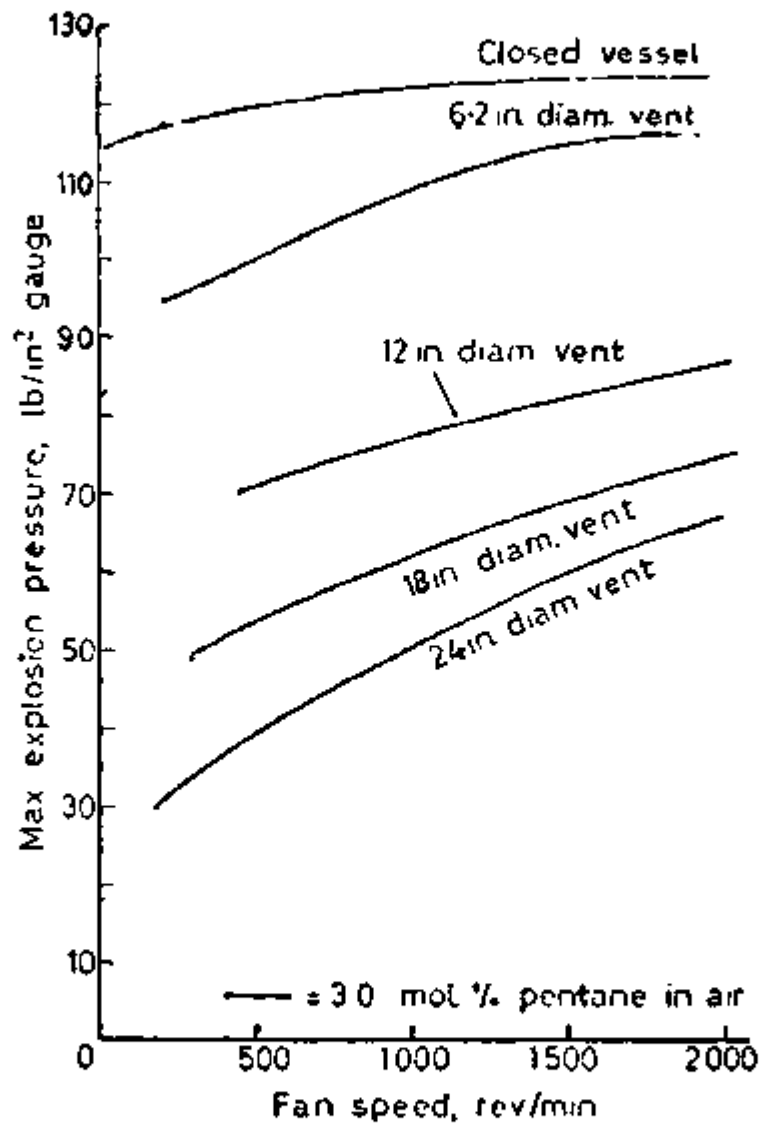


FIG. 2-14 EFFECT OF TURBULENCE ON THE MAXIMUM EXPLOSION (2ND-PEAK) PRESSURE

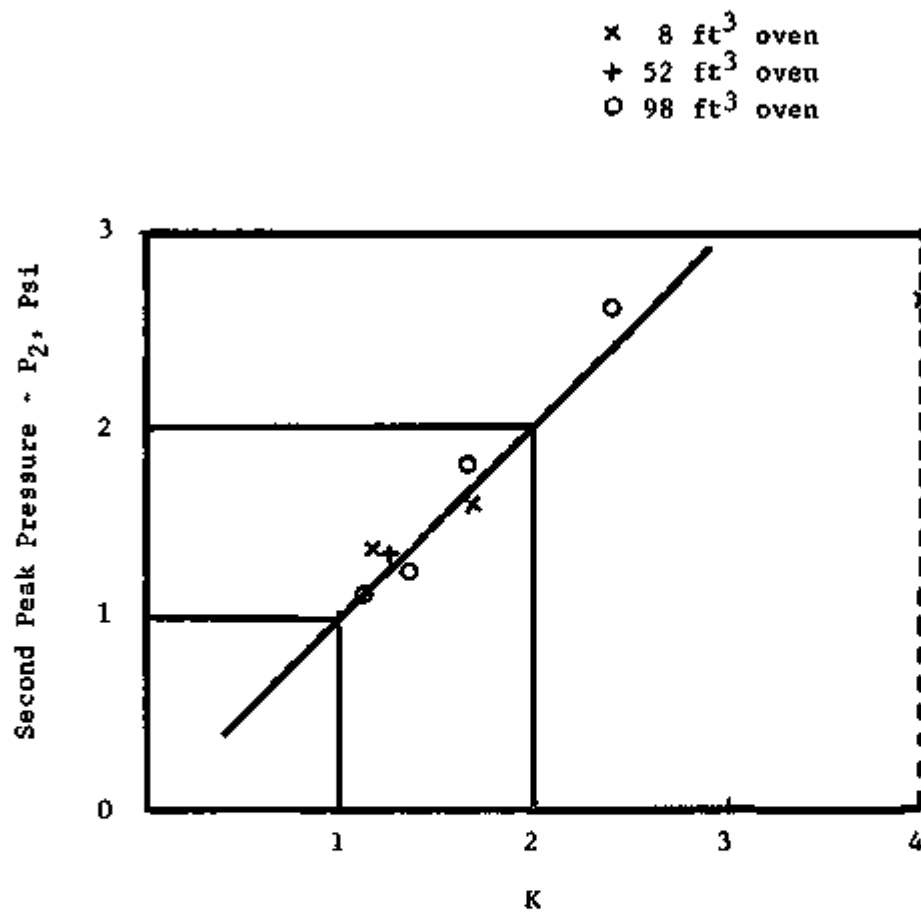


FIG.2-15 VARIATION OF THE SECOND-PEAK PRESSURE WITH THE VENT AREA PARAMETER

A correlation was performed by Rasbash<sup>(26)</sup> of pressure versus  $K$  and  $L/D$ . The correlation was based on the work of Rasbash<sup>(23)</sup>, Simmonds<sup>(17)</sup> and Cousins and Cotton<sup>(8)</sup>. The factor  $K$  was varied from  $K=1$  to  $K=32$  and  $L/D$  was varied from  $L/D = 1$  to  $L/D = 30$ . Pressure increased with  $K$  at fixed  $L/D$  as expected. At larger values of  $K$  ( $K=4$  to  $32$ ) pressure increased with  $L/D$  to a constant value at values of  $L/D=6$ . However, for values of  $K$  approaching 1, pressure is nearly invariant with  $L/D$  to values of  $L/D = 3$  and increases for larger values of  $L/D$ . The reason given for the increase in pressure when  $L/D > 3$  was that the turbulent flow was becoming established along the axis of the long path which increased the burning velocity and flame spread. An ordinary deflagration of acetylene/air mixture will develop into a serious detonation when the  $L/D$  ratio is larger than 40.<sup>(27)</sup>

## III

EXPERIMENTAL INVESTIGATION OF EXPLOSIONS IN GLOVEBOXES

The experimental program was developed to evaluate the variables associated with overpressurization that could occur in gloveboxes as a result of igniting an accumulation of combustible gas systems.

Data, in the form of pressure as a function of time, was obtained for a series of explosive conditions and experimental configurations. The primary combustible gas mixture was a slightly higher than stoichiometric mixture of propane/air (4 to 5 percent by volume). A second mixture, hydrogen/air mixture (40 percent by volume), was used to represent the maximum foreseeable incident.

### 3.1 EXPERIMENTAL APPARATUS

The experimental apparatus consisted of: 1) pressure measuring system; 2) gas supply and mixing system; 3) ignition and timing system; and 4) test chamber. Figure 3-1 shows the general arrangement of the experimental instrumentations.

#### 3.1.1 Pressure Measuring System

The pressure transducer was a Consolidated Electrodynamics Corporation Type 4-393, having a 0-15 psi range. Later in the program a Dynisco PT-25, 0-10 psi transducer was also used. These devices are unbonded types of strain gages and require an external voltage supply to the variable-resistance bridge arm. The transducers were located centrally on the side panels of the test vessel. The output voltages of these devices which are analogs of the pressures generated within an enclosed volume, are presented as an electrical signal to the vertical deflection plates of a Tektronix dual-trace cathode ray oscilloscope. A Type 1A1 two-channel plug-in amplifier unit was used with the oscilloscope. The pressure-time data associated with the confined explosion was acquired on Polaroid Type 3000 speed film from the phosphorescent screen of the CRO by a Tektronix Type C-12, trace recording camera. A Honeywell Visicorder was paralleled to the Tektronix to acquire longer time histories and better resolution as the program continued.

The Dynisco pressure transducers had high thermal sensitivity which affected the pressure output significantly. This effect was minimized by a 1/4 in. coating of Dow Corning high vacuum grease sprayed with a silicone aluminum aerosol spray.

#### 3.1.2 Gas Supply and Mixing System

The propane used in this study was commercially pure (99.6%) gas obtained from Matheson, Inc. This analysis was obtained from FMRC's gas



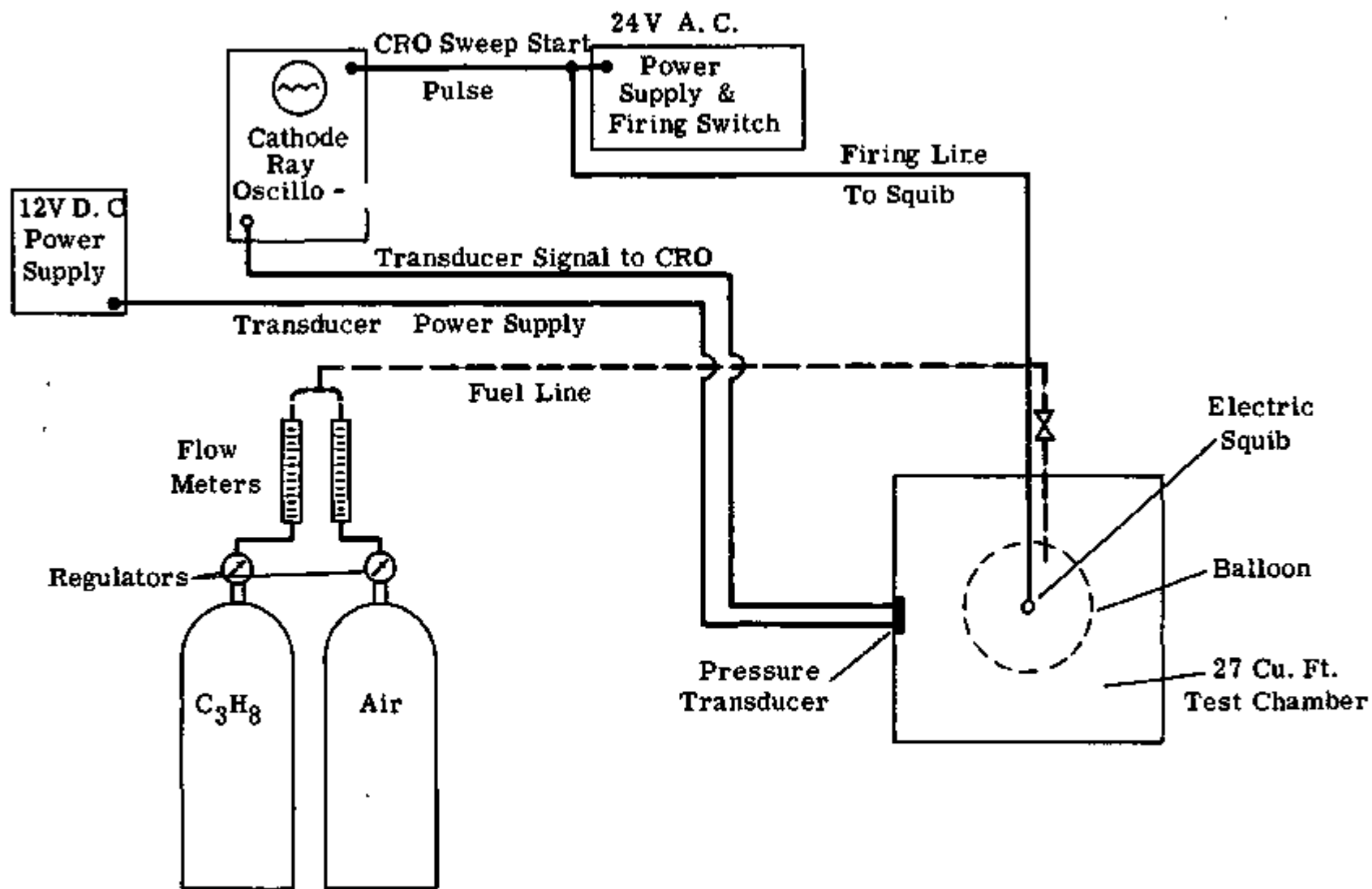


FIGURE 3-1: BLOCK DIAGRAM SHOWING GENERAL ARRANGEMENT OF TEST INSTRUMENTATIONS

chromatograph and verified the analysis of the supplier. Arrangements used to meter and mix the propane/air mixtures are shown schematically in Figures 3-2, 3-3, and 3-4. Figure 3-2 was designed to introduce the measured quantities of propane and air into the balloon through a single 1/4-in. copper line of about 15 ft length. The mixing of propane and air is accomplished in the feeding line.

In the event that the entire chamber was to be filled with a gas mixture, the arrangement shown in Figure 3-3 was used in the earlier part of the work. A measured quantity of propane was metered and fed into the test chamber. An 8-in. diameter propeller, situated near the center of one vertical wall, was used for mixing and could be run during an explosion to provide turbulence. The normal propane filling time was about 3 min. The fan was used for the greater part of the test series, during the filling period. Later, the method of filling and mixing was modified as shown in Figure 3-4. Proper quantities of propane and air, measured with two separate flowmeters, passed through a Selas mixer, Selas type B No 310 gas combustion controller and a solenoid valve into the test chamber. A volume of gas mixture equal to about ten changes of the entire chamber was purged through the chamber for each experiment. Periodically gas samples were collected at the feeding line as well as at the exhaust line to assure proper mixing.

### 3.1.3 Ignition and Timing System

Figure 3-5 is a schematic of the wiring for ignition and timing system. The experiment was started when the firing switch, S1, was closed. The single sweep of the oscilloscope was started and voltage was supplied to the initiating squib. A delay of approximately 1.5 to 1.8 milliseconds was generally experienced between the start of the scope sweep and initiation of the gaseous mixture. When high speed motion pictures were required, a second switch, S2, was placed in Series with S1. The function of the switch S2 was to start the initiation train after the inertia of the camera was overcome and the film was brought up to the required speed. This was accomplished by adjusting the closing time of a microswitch. The microswitch has an extension rod which actuated the switch upon sensing a given amount of film on the unexposed reel. The necessary amount of unexposed film which had to be passed to overcome the inertia of the camera was determined from calibrations supplied by the manufacturer. The camera was a Hycam Model K20SIE-115 high-speed camera manufactured by Red Lake Laboratories, Santa Clara, California. The gas mixtures were ignited by a type S6H0 electrical squib manufactured by Hercules Incorporated or a type M-100 electric match made by Atlas Chemical Industries.

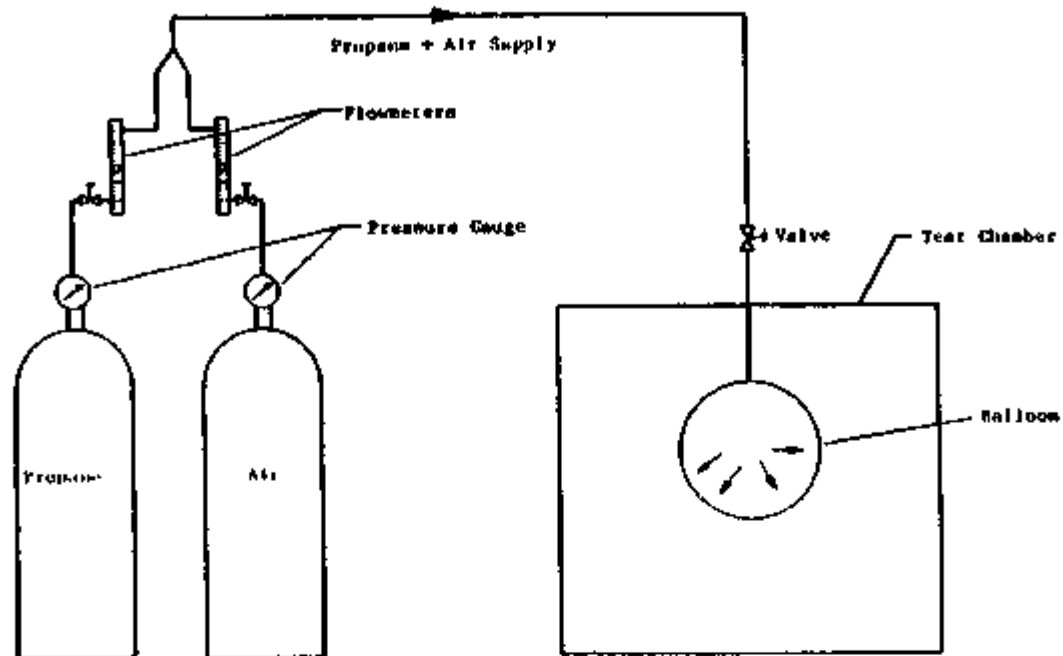


FIGURE 3-2 SCHEMATIC DIAGRAM OF GAS SUPPLY AND MIXING SETUP I--BALLOON EXPLOSION

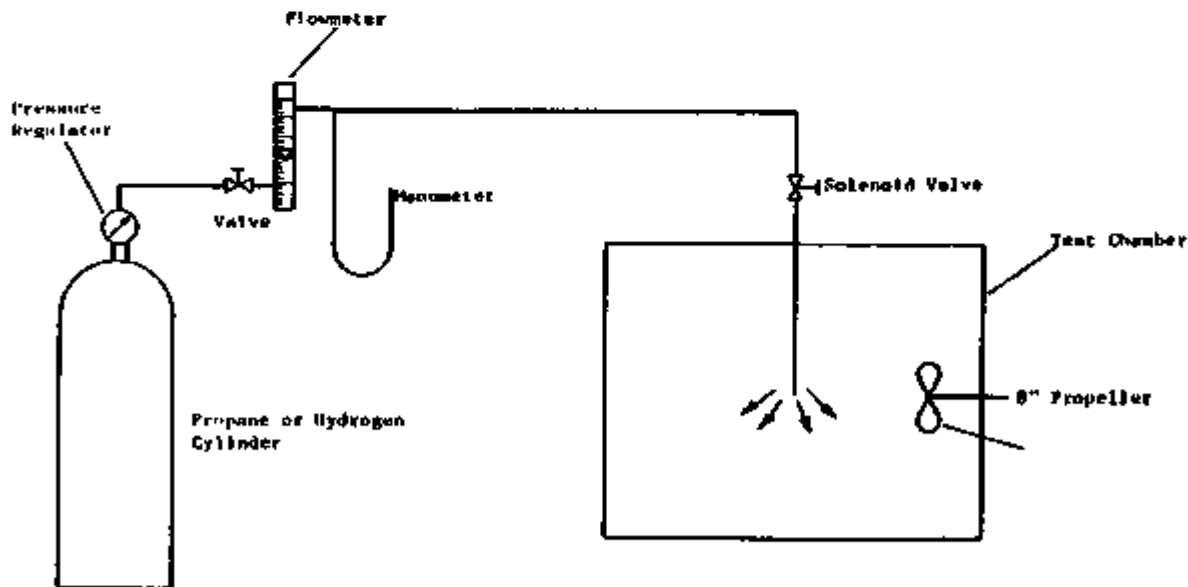


FIGURE 3-3 SCHEMATIC DIAGRAM OF GAS SUPPLY AND MIXING SETUP II--CHAMBER COMPLETELY FILLED WITH COMBUSTIBLE GAS

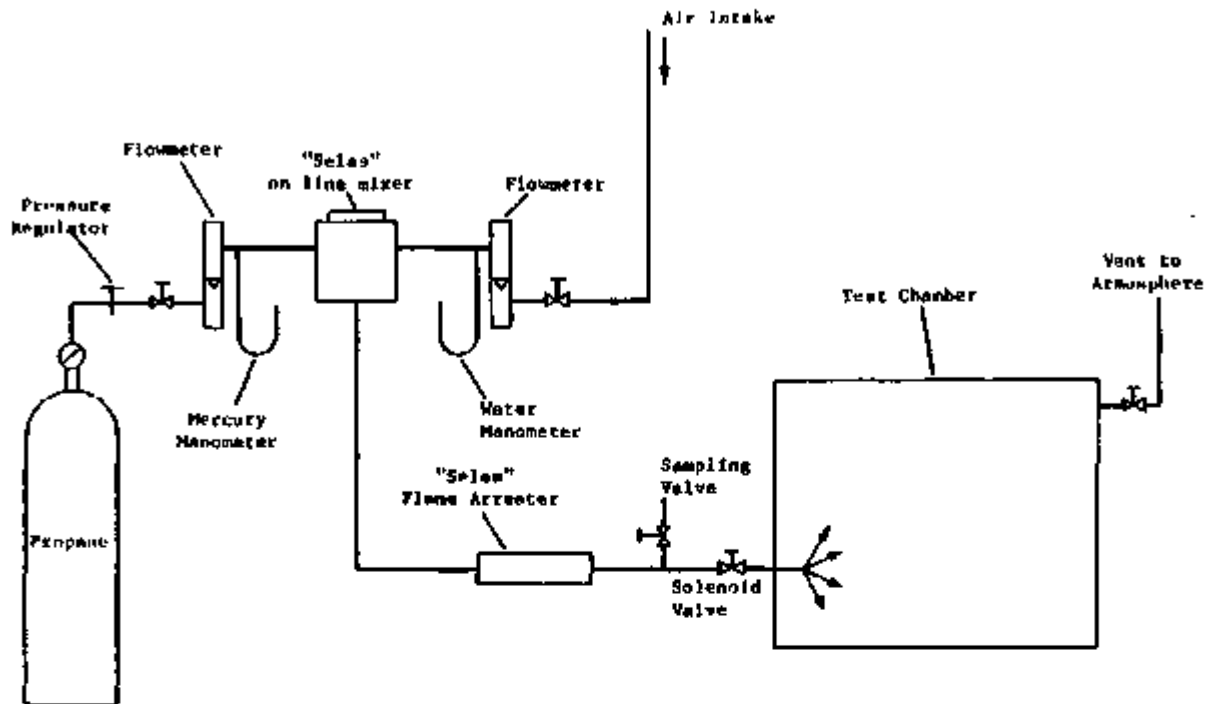


FIGURE 3-4 SCHEMATIC DIAGRAM OF GAS SUPPLY AND MIXING SEVID III-- CHAMBER COMPLETELY FILLED WITH HOMOGENEOUS MIXTURE

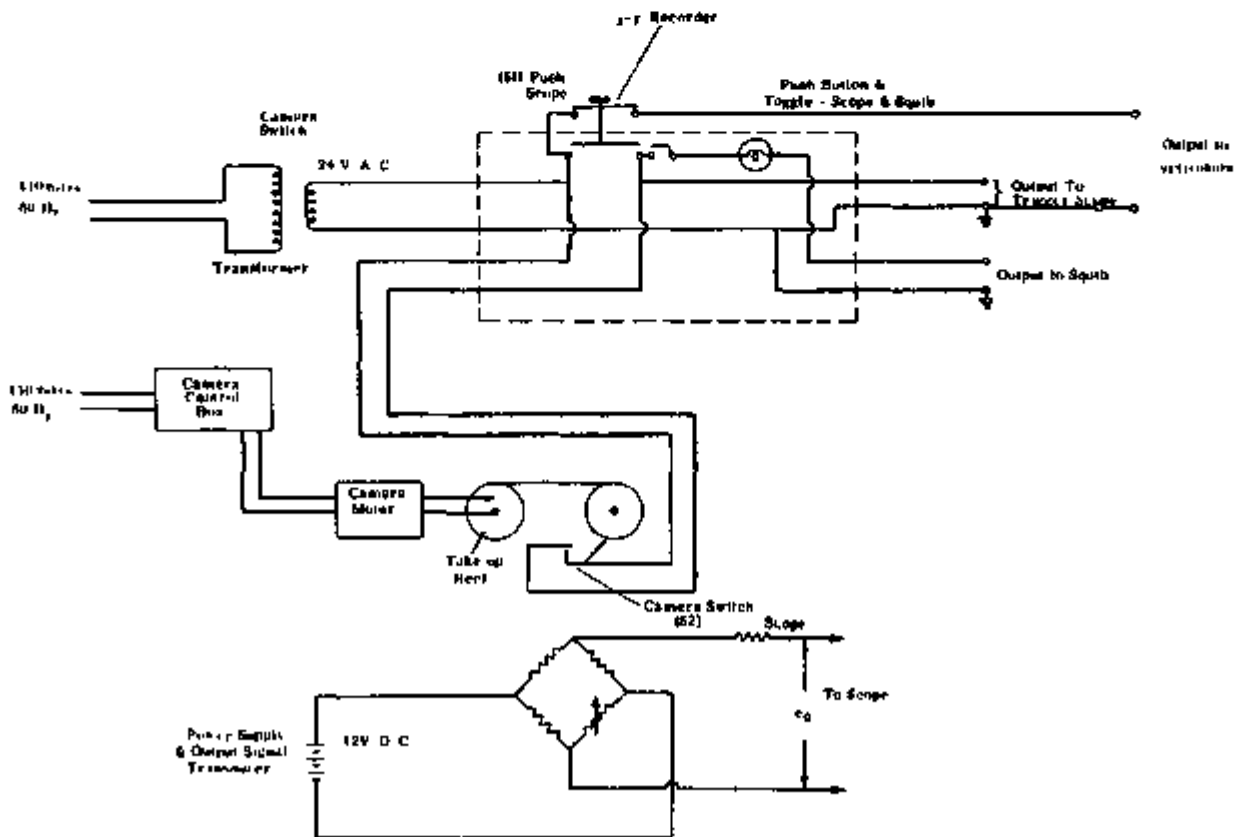


FIGURE 3-5 WIRING DIAGRAM OF THE EXPERIMENTAL ARRANGEMENT

### 3.1.4 Test Chambers

#### 1. 24 Cu Ft Wooden Glovebox

A 24 cu ft (2ftx3ftx4ft) simulated wooden glovebox, used in earlier investigations of the fire problem in gloveboxes(1) was used initially as a test chamber. This configuration as shown in Figure 3-6 was desirable from the point of view of geometry as well as being readily available. However, it became evident after several series of tests were performed that this chamber was not suitable for explosion experiments because of its excessive leakage and weakness in construction.

#### 2. 27 Cu Ft Test Chamber

Figure 3-7 shows the design of the 27 cu ft air-tight aluminum chamber (3ftx3ftx3ft). Several interchangeable front panels and matching flanges were fabricated. These panels could be attached on the front wall permitting the investigation of a large number of variables under controlled conditions.

#### 3. Cylindrical Test Chamber

In order to determine the effect of geometry and configuration and to provide a means of evaluation, two 3-ft diameter cylindrical test chambers (one 3 ft and one 6 ft in length) were designed so that additional sections could be added to vary L/D significantly. Figure 3-8 shows two different configurations used in this program. The bursting diaphragm can be mounted on either front or side openings to investigate the effect of vent location on explosion characteristics.

## 3.2 BALLOON EXPLOSION RESULTS

Propane and air were passed through the flow meters at a pre-determined rate so that a stoichiometric propane/air mixture (4 percent and 96 percent by volume) at a given volume could be achieved in a centrally located meteorological balloon prior to ignition (see Figure 3-2). Resultant pressures exerted on the wall of the test chamber were recorded by the pressure measuring system. The above procedure was followed in subsequent tests performed in the 24 cu ft wooden glovebox as well as the 27 cu ft aluminum chamber. The objectives of balloon explosion experiments were to: 1) determine the upper limit of explosive volume which can be safely handled by the present glovebox design; 2) to verify the localized explosion theory described in Section 2.2.1 of this report; and 3) to explore the pressure relief effect of the high-efficiency filters in relation to free-vent.

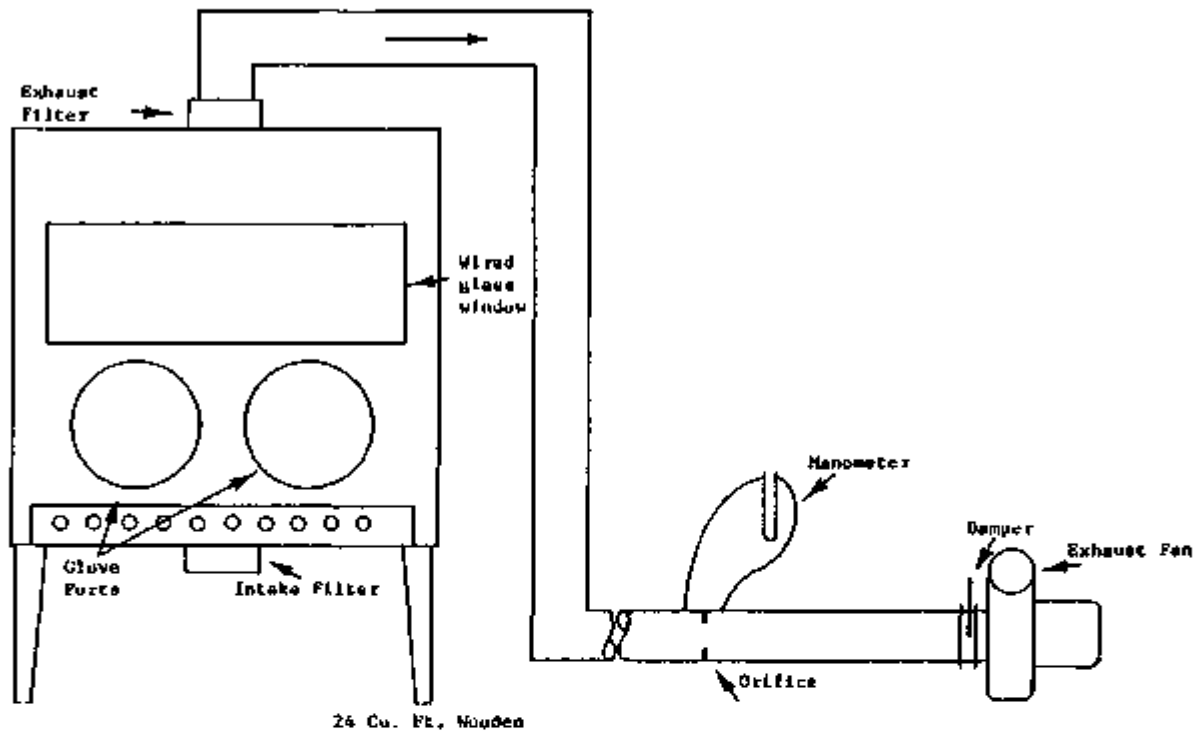


FIG. 3-6 GLOVEBOX WITH AIR CIRCULATION SCHEME

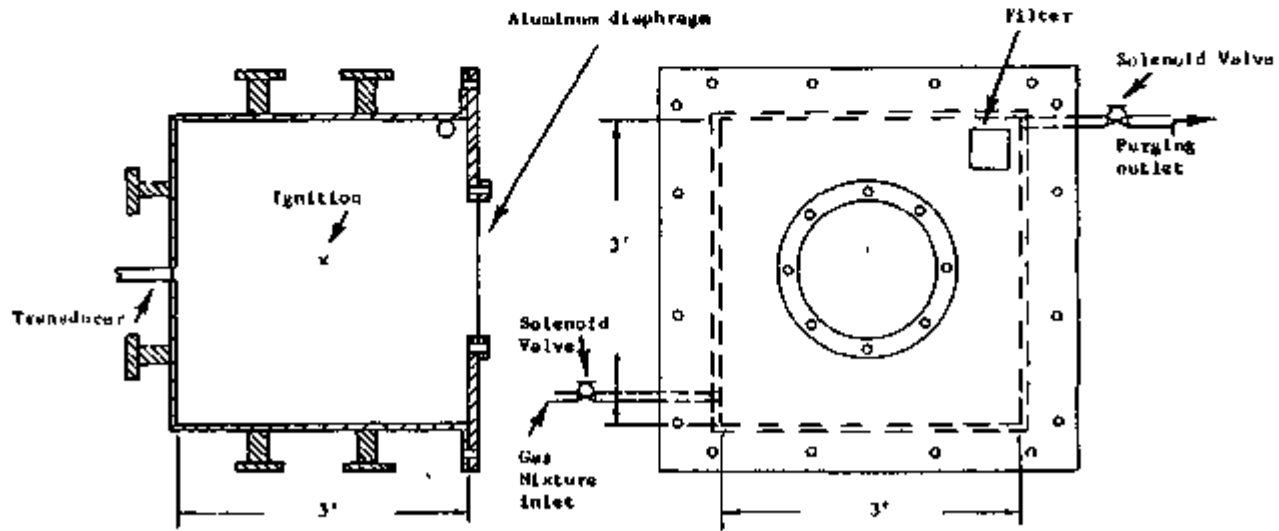
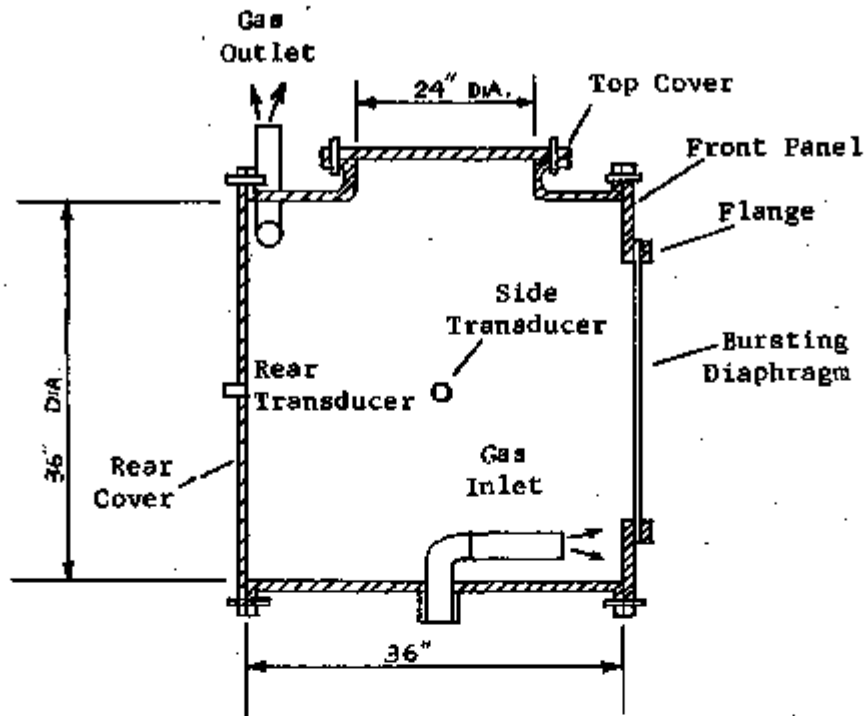


FIG. 3-7 27 CU. FT. ALUMINUM TEST CHAMBER

CONFIGURATION A



CONFIGURATION B

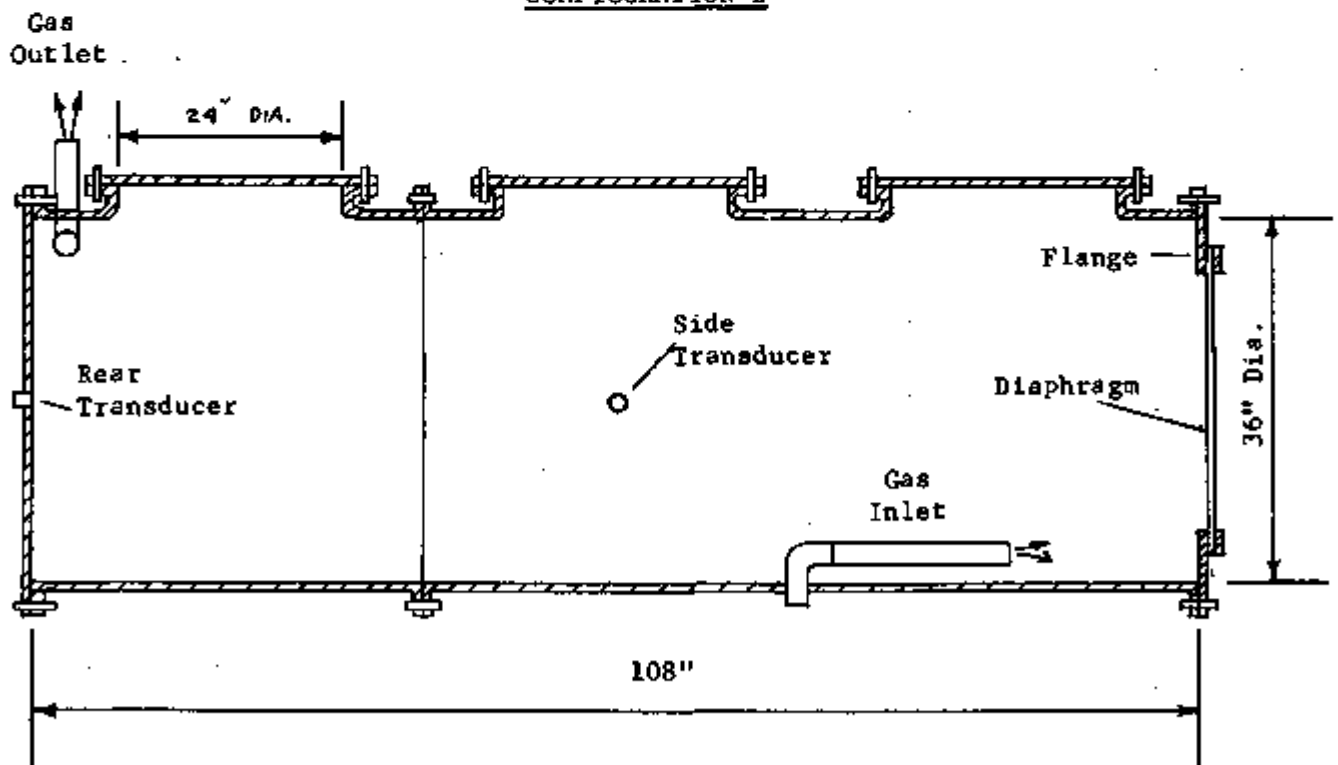


FIG. 3-8 CYLINDRICAL TEST CHAMBERS

### 3.2.1 (Balloon) Explosion in the closed 27 cu ft chamber

Because the 24 cu ft wooden glovebox was not air tight, the closed chamber balloon explosion tests were performed in the 27 cu ft aluminum test chamber. Data are given in Table 1 (Appendix C) and represented by the points in Figure 3-9, in terms of maximum explosion pressure versus the dimensionless volume ratio of  $V_u(o)/V$ . Figure 3-10, an oscillogram of test No. A-12, shows that the pressure curve for a 0.35 cu ft balloon rises to a maximum of about 2 psi at about 60 milliseconds after ignition.

### 3.2.2 (Balloon) Explosion in the 24 cu ft Glovebox

Experiments were performed in the 24 cu ft wooden glovebox to determine the effect of gloves, filter, air circulation and duct work, as well as combinations of these elements on the explosion characteristics. Data obtained from this series of experiments appear in Table 2 (Appendix C). Figure 3-11 is a plot of maximum explosion pressure as a function of balloon volume/chamber volume ratio for different air circulation rates in the wooden glovebox with two filters, and Figure 3-12 is a plot of maximum explosion pressure as a function of air circulation rate for a fixed balloon size of 0.53 cu ft. These figures seem to indicate that air circulation up to 48 cfm (two air changes per min.) does not contribute noticeable change in explosion pressure. Some trend of increase in explosion pressure is indicated at the higher air circulation rates.

Test results obtained in the same glovebox but mounted with two filters and two gloves (one 15-mil Neoprene and one 10-mil Latex) are plotted in both Figures 3-12 and 3-13. In comparison with the data obtained without the gloves, the existence of gloves on the glovebox seems to have no effect on the explosion pressure. These tests were initiated with the gloves protruding inside the glovebox. Over the range of conditions tested, the pressure rose to a peak of about 2 psi over a period of less than 10 millisecond, and the gloves could only extend about 2/3 of their full length. Obviously, one could not expect the full attenuating effect until the gloves were fully inflated. The gloves appear to withstand much higher than 2 psi under the dynamic loading condition tested.

### 3.2.3 Free-Vent versus Filters in (Balloon) Explosion Venting

Explosion venting effects of free-vent and high-efficiency filters are compared experimentally in the 27 cu ft aluminum chamber. As tabulated in Table 3, a total of about 70 tests were performed by exploding a fixed volume (0.53 cu ft) of propane/air mixture inside the vented test chamber. The size of free-vent varied from 1-in. diameter to two 6 1/2 in. x 6 1/2 in. squares. The filters used in these experiments were standard 8 in. x 8 in. x 6 in. Flanders size-B high-efficiency filter units, having an opening area of  $A_f = 6 \frac{1}{2}$  in. x  $6 \frac{1}{2}$  in. The number of filters used ranged from one to six. Data obtained from these experiments are plotted in Figure 3-14 as maximum explosion pressure versus the vent area parameter, K. The figure shows that both curves approach the maximum pressure of 3.4 psi as the vent areas reduce to zero ( $K = \infty$ ) which is equivalent to the maximum explosion pressure for an 0.53 cu ft balloon [ $V_u(o)/V = 1.97\%$ ] in a closed chamber (see Figure 3-9).



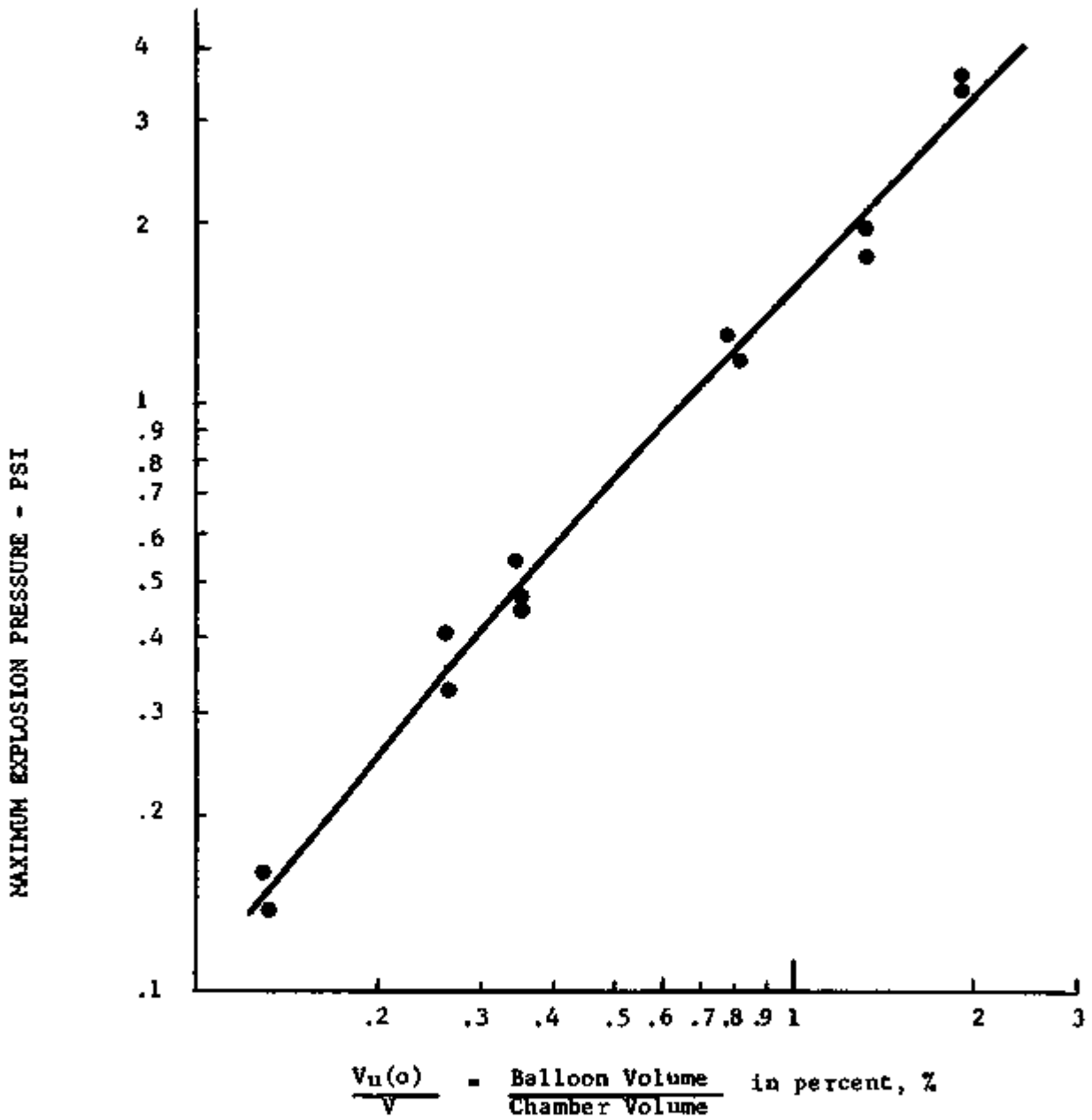


FIG. 3-9 TEST RESULTS FOR LOCALIZED (BALLOON) EXPLOSION IN A CLOSED CHAMBER

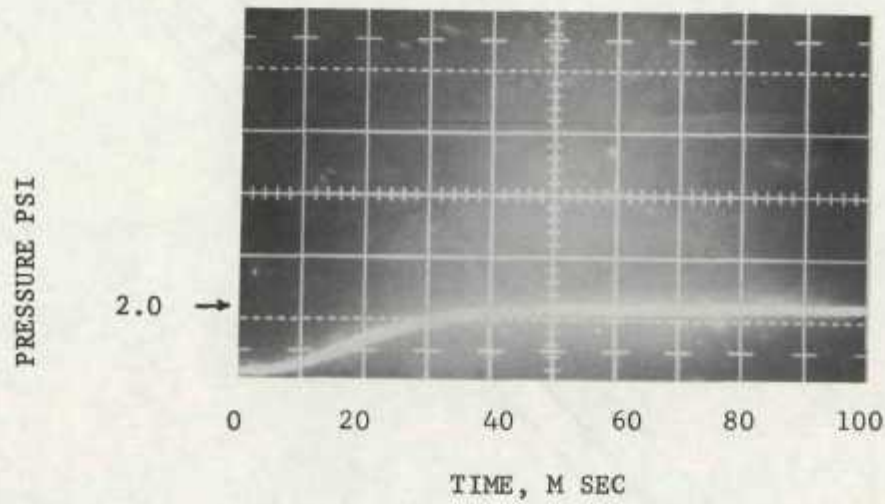


FIG.3-10 PRESSURE - TIME HISTORY OF A BALLOON EXPLOSION IN A CLOSED CHAMBER AS RECORDED BY OSCILLOGRAM (TEST # A-12)

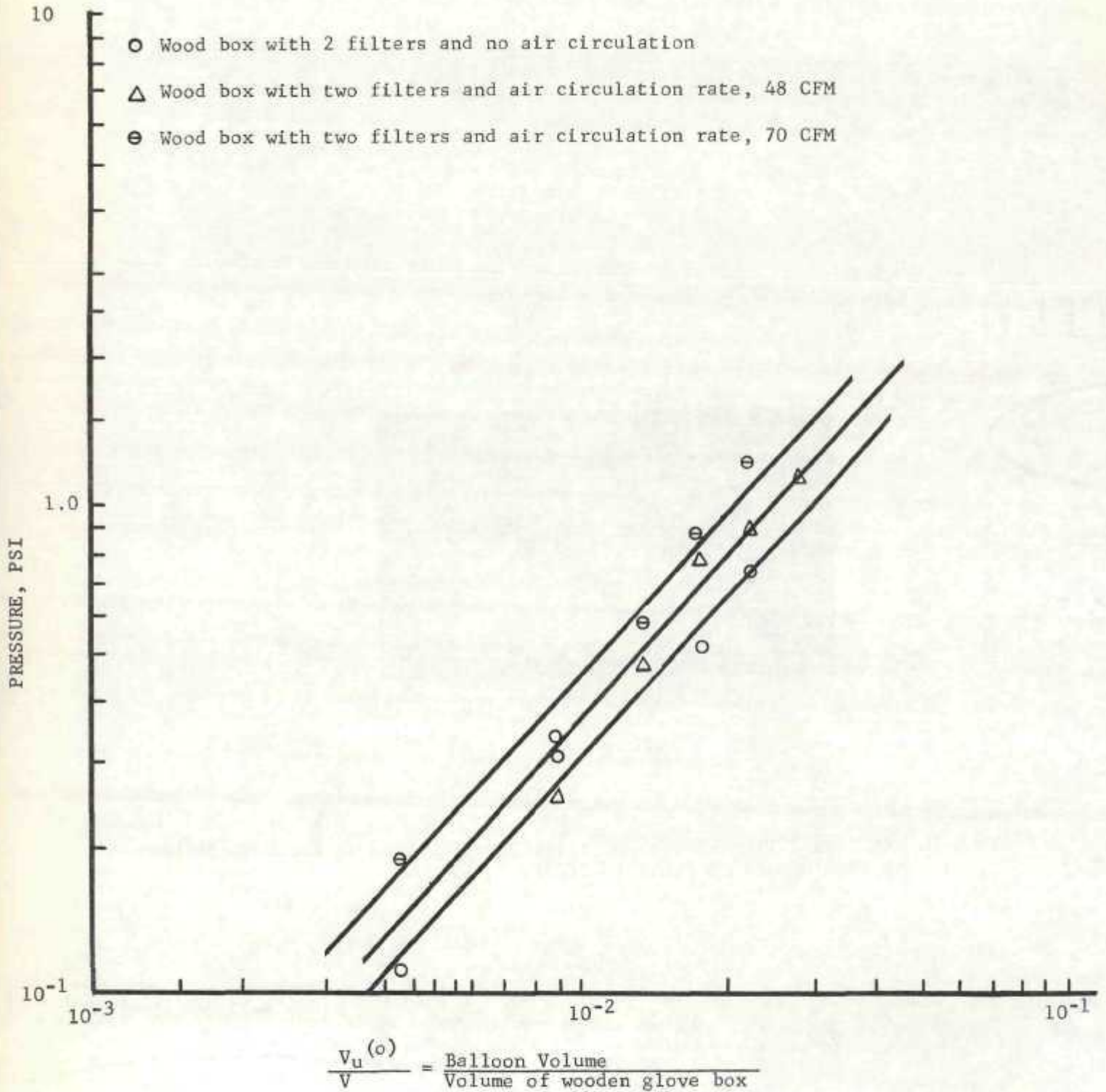


FIG. 3-11 EFFECT OF FILTERS AND AIR CIRCULATION ON THE LOCALIZED (BALLOON) EXPLOSION

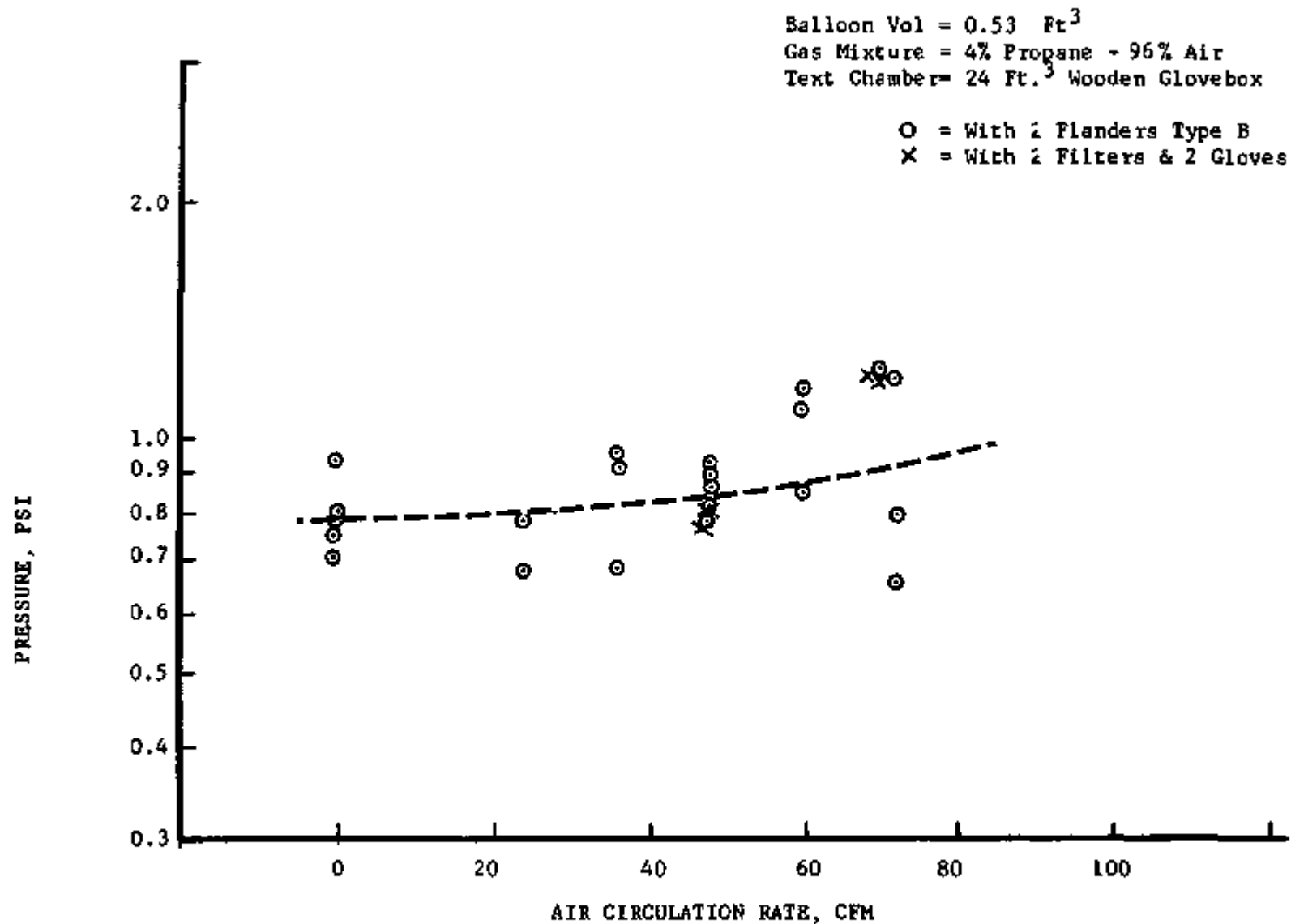


FIG. 3-12 EFFECT OF AIR CIRCULATION ON (BALLOON) EXPLOSION

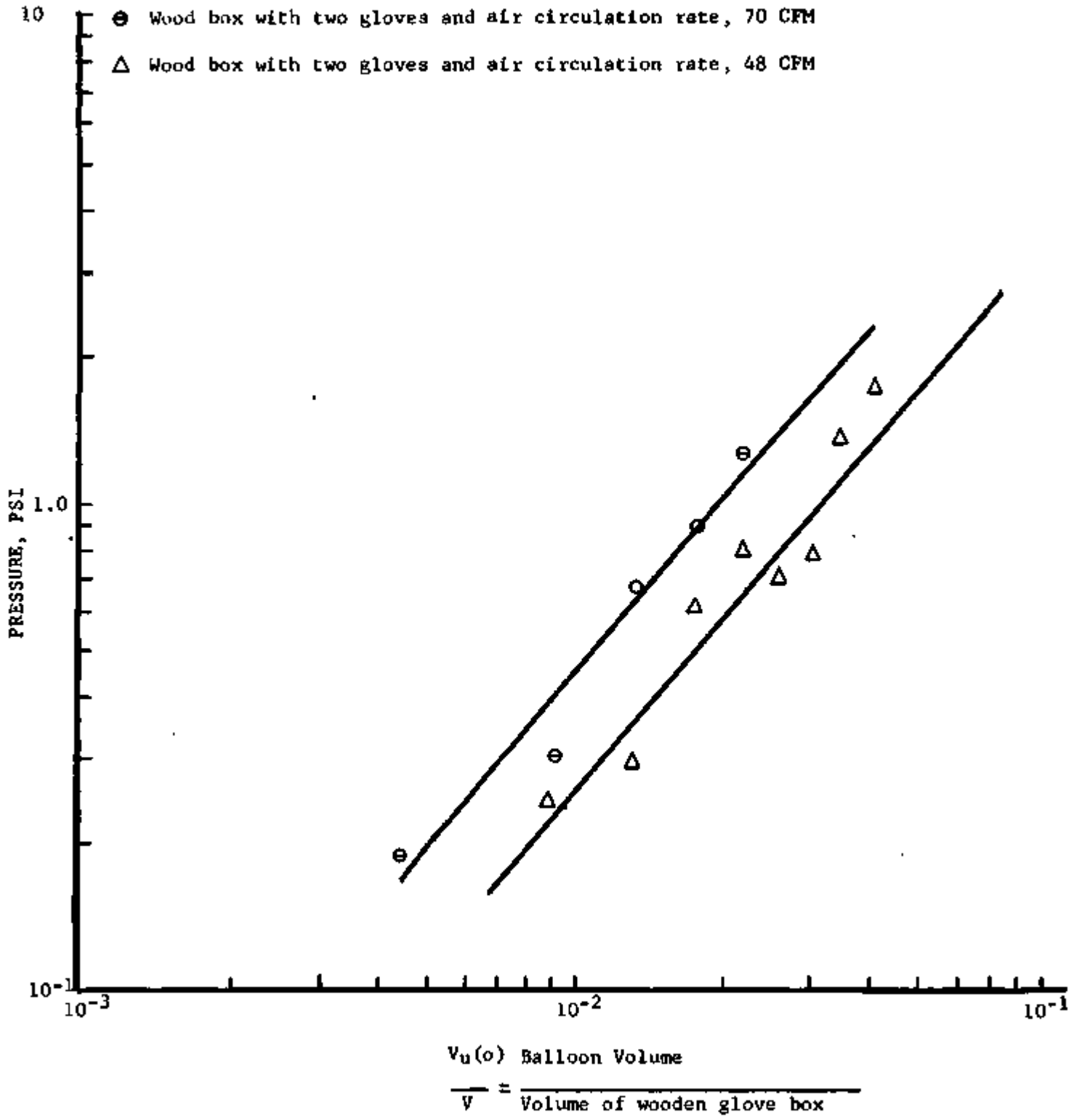


FIG. 3-13 EFFECT OF THE COMBINATION OF THE FILTERS, GLOVES AND AIR CIRCULATION ON THE LOCALIZED (BALLOON) EXPLOSION

Direct comparison of the pressure curves in Figure 3-14 shows that in order to achieve the same effectiveness as the free-vent, explosion venting with filters would require about four times greater cross-sectional area.

Oscillograms of Test No. AA-101 for one 6 1/2-in. x 6 1/2-in. free-vent and Test No. AA-157 for three 6 1/2-in. x 6 1/2-in. opening filters are presented in Figures 3-15 and 3-16. In view of the differences in the time scale used in these two figures, the pressure-time record measured with one 6 1/2-in. x 6 1/2-in. free-vent is slightly lower than that measured for three 6 1/2-in. x 6 1/2-in. filters.

### 3.3 PRESSURE RELIEF WITH BURSTING DIAPHRAGM

Experiments were continued to investigate the explosion venting characteristics in the 27 cu ft and the 3-ft diameter cylindrical test chambers with the entire chamber filled with the combustible gas mixture. The bursting diaphragm used in this study is 1-mil-thick, Type 5-1100 aluminum foil. The objectives of this test series were to: 1) determine the effect of various controlling variables associated with the bursting diaphragm on the explosion characteristics; and 2) verify the explosion venting theory described in Section 2.5.

#### 3.3.1 Bursting Diaphragm Explosion in the 27 cu ft Test Chamber

Non-Homogeneous Propane/Air - The earlier experiments were performed with the setup as shown in Figure 3-3. Propane gas was introduced to the chamber at the rate of 0.36 cfm. A 4-percent concentration would require a filling time of 3 min. During this filling time the 8-in. propeller was running to enhance the mixing. Since we are not sure whether homogeneous mixing of the propane and air were achieved during these tests, test results obtained from this mixing arrangement are tabulated in Table 4-A as non-homogeneous data. The typical pressure-time record measured from the 24-in. diameter bursting diaphragm on the 27 cu ft chamber (Tests AA-277, AA-279) is presented in Figure 3-17. The figure shows the distinctive double-pressure peaks. The first peak is identified as the bursting pressure of the diaphragm. After bursting of the diaphragm, the sudden release of gases causes the falling of pressure. Depending on the opening size and bursting pressure, the pressure started to build up to a second peak, as described earlier in Section 2-5. The measured non-homogeneous first-peak pressures (bursting pressure) are represented by the dotted vertical lines in Figure 3-18 as a function of diaphragm diameter. In general, the first peak (bursting pressure) decreases with the increase in the diaphragm diameter. The  $\pm 20$  percent scattering in measured points can be attributed to the fact that we could not stretch and mount the large diameter thin foil on the chamber the same way for each test. It was also observed that the foils were not always bursting in the same fashion each time. In most cases, the diaphragm burst out as a whole piece and sometimes ruptured into 10 or 20 small pieces. Unexpectedly, the measured

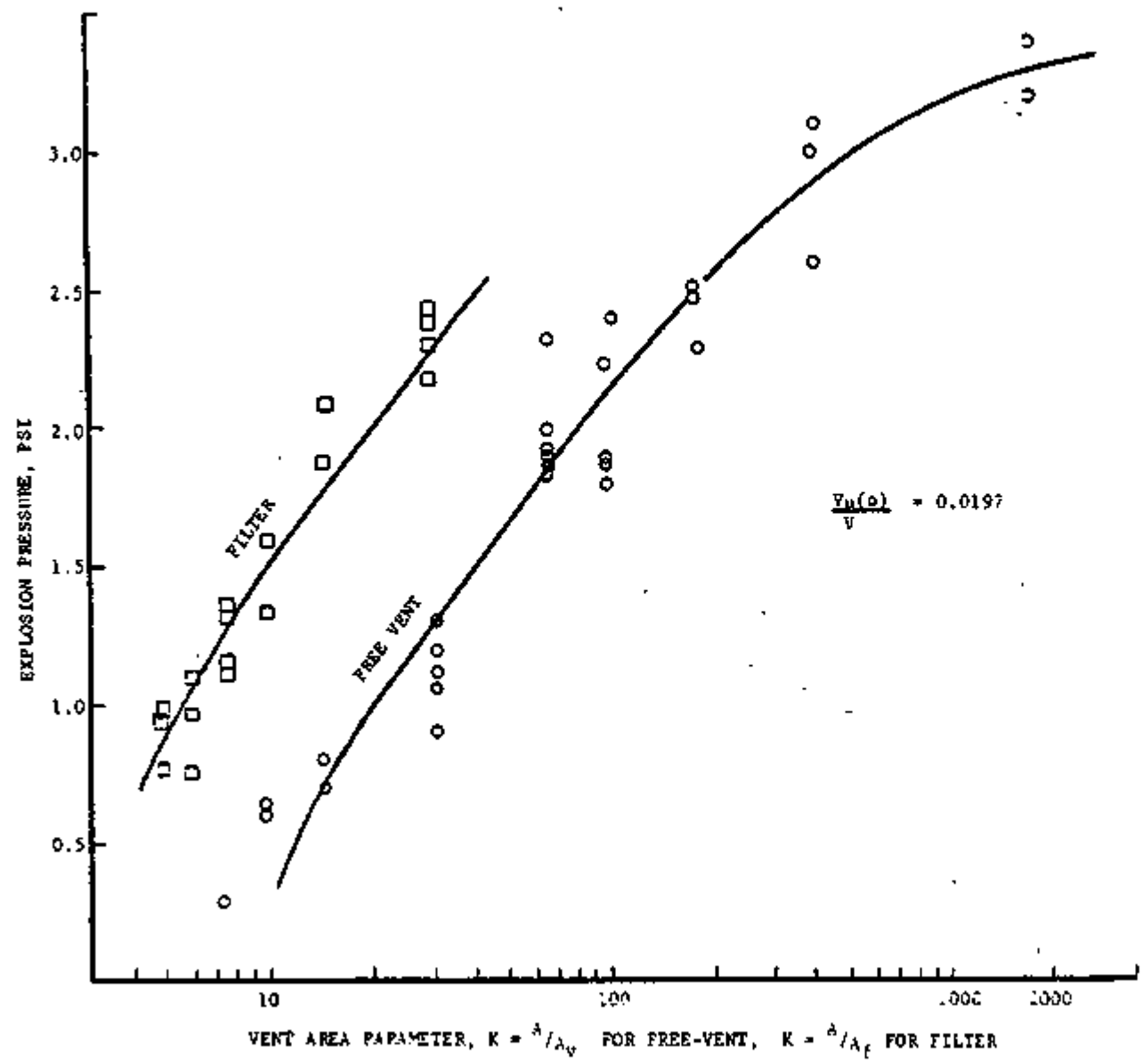


FIG. 3-14 COMPARISON OF FREE-VENT AGAINST FILTERS IN (BALLOON) EXPLOSION VENTING

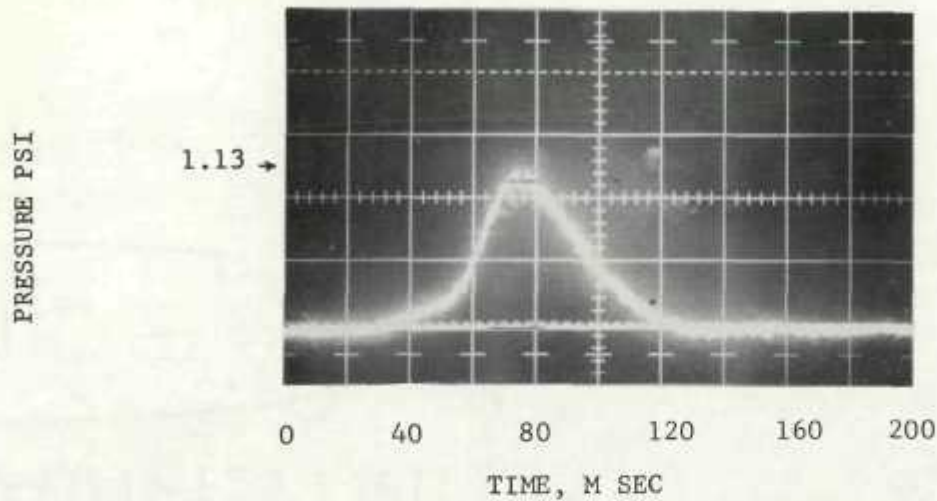


FIG.3-15 PRESSURE - TIME HISTORY OF A BALLOON EXPLOSION INSIDE A CHAMBER PROVIDED WITH FREE VENT AS RECORDED BY OSCILLOGRAM (TEST #AA-101)

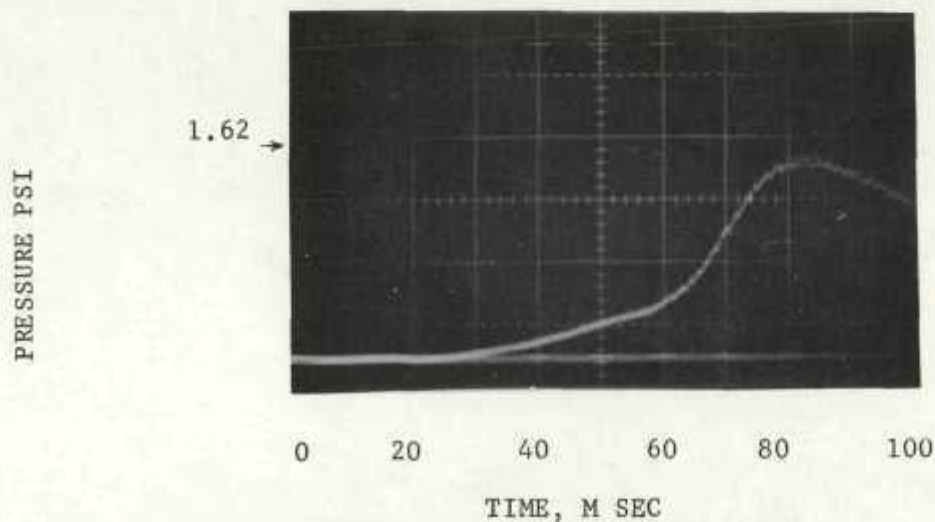


FIG.3-16 PRESSURE - TIME HISTORY OF A BALLOON EXPLOSION INSIDE A CHAMBER PROVIDED WITH FILTERS AS RECORDED BY OSCILLOGRAM (TEST # AA-1577)



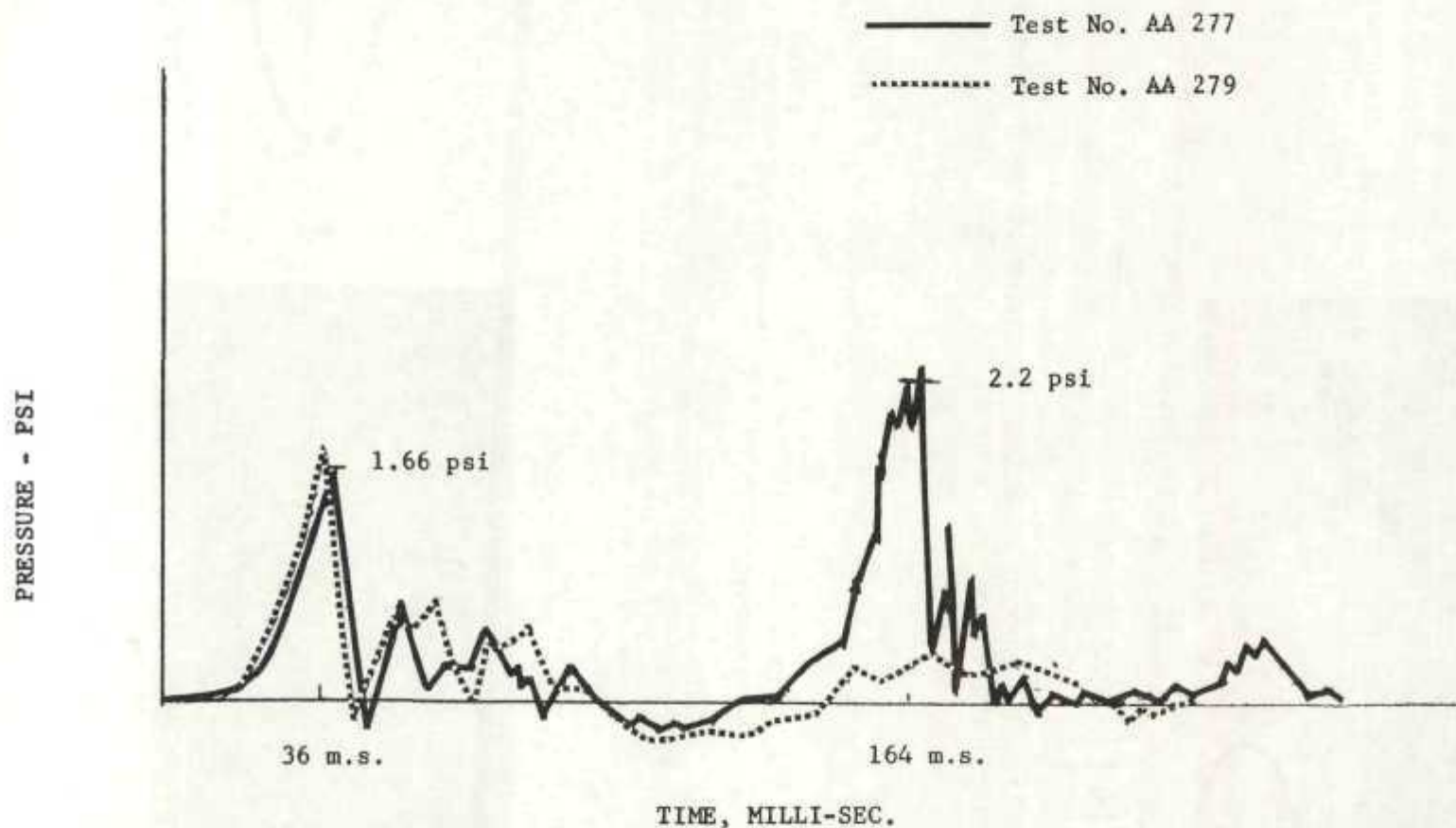


FIG. 3-17 TYPICAL PRESSURE-TIME HISTORY MEASURED FOR AN EXPLOSION IN THE 27 CU. FT. CHAMBER VENTED WITH A 24 IN. DIAMETER BURSTING DIAPHRAGM

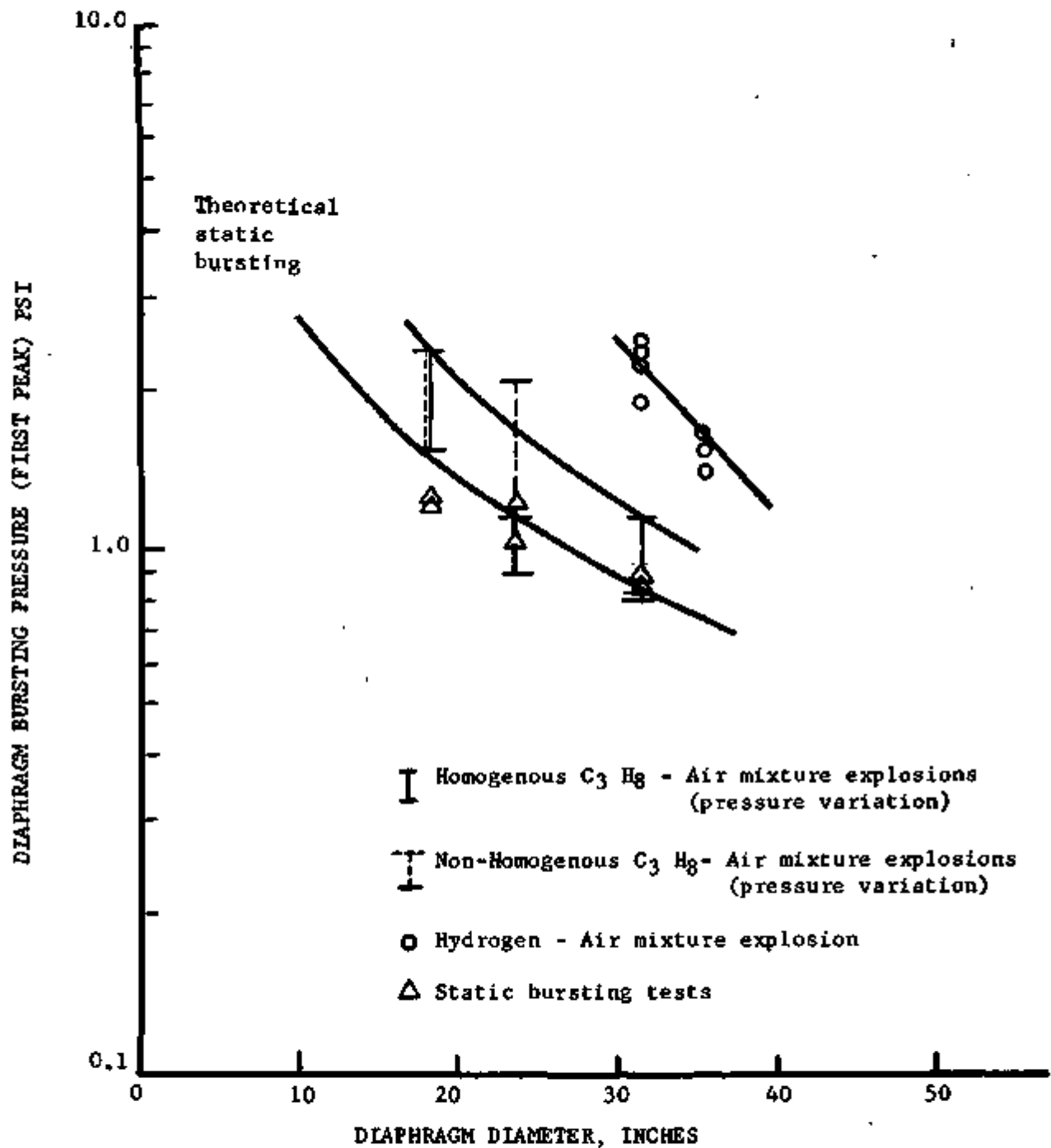


FIG. 3-18 DIAPHRAGM BURSTING PRESSURE (FIRST PEAK) PSI AS A FUNCTION OF DIAPHRAGM DIAMETER

second-peak pressure varied considerably even under the same test condition. The non-homogeneous second-peak pressure is represented by the dotted vertical lines in Figure 3-19 as a function of the vent area ratio,  $K=A/A_v$ . Samples of pressure-time records with high second-peak pressure (Test No. 277) and low second-peak pressure (Test No. 279) under the same test condition are compared in Figure 3-17. The difference in second-peak pressure is attributed to the turbulence effect induced by the difference in bursting condition. In general, high second-peak data usually associated with the test in which the diaphragm burst into many small pieces.

Homogeneous Propane/Air Mixture - In view of the wide range of scattering in second-peak pressure data, it was decided that a better mixing setup should be used to ensure the homogeneity of the mixture at a richer than stoichiometric condition so that the maximum hazard condition could be reached. Homogeneous mixture tests were conducted with the setup shown in Figure 3-4. The Selas mixer is not only used as a mixer but it also served as a blower which draws about 455 cfh of air from the atmosphere to mix with a measured amount of gas to form the required concentration at the feeding line. The propane concentration used in these tests was varied from 4 to 6.6 percent. The purging time for the 27 ft vessel was 20 min. A 30-sec. delay after the filling was usually employed to stabilize the mixture inside the test chamber. However, in several test runs, ignition was initiated while the purging was still in progress. Data obtained from this series of tests are tabulated in Table 5-A as the homogeneous mixture, and indicate that 5.08% concentration seems to give the highest second-peak pressure. The measured first- and second-peak pressure for this homogeneous case is plotted also in Figures 3-18 and 3-19, denoted by the solid lines. It was found that the homogeneous mixture at higher concentration did not affect the first-peak pressure, but it did raise the second-peak pressures to a much higher level. For the purpose of pressure relief design, it is reasonable to use the upper envelope line of Figures 3-18 and 3-19 as the first- and second-peak explosion pressure curve.

Hydrogen/air mixture - In order to determine the effect of mixture strength (burning speed) on the bursting diaphragm explosion relief performance, a series of experiments were carried out on the 27 cu ft test chamber filled completely with a richer than stoichiometric mixture of hydrogen/air (40 mole percent). Although the same non-homogeneous gas supply and mixing setup as shown in Figure 3-3 was used during this test series, the results obtained should not be very different from those obtained with the homogeneous mixing arrangement. Crovich's<sup>(9)</sup> explosion tests indicated little difference in rate of pressure rise between mixtures containing 30, 40 and 50 percent of hydrogen. Furthermore, the large quantity of hydrogen was injected downward through a small nozzle over a long period of about 30 minutes; thus it is believed that the hydrogen concentration variation inside the test chamber should not be beyond the 30 percent to 50 percent limits. Data obtained are tabulated in Table 6 and plotted together with the propane/air explosion data in Figures 3-18 and 3-19. Comparison of hydrogen/air explosion with that obtained for propane/air explosion for

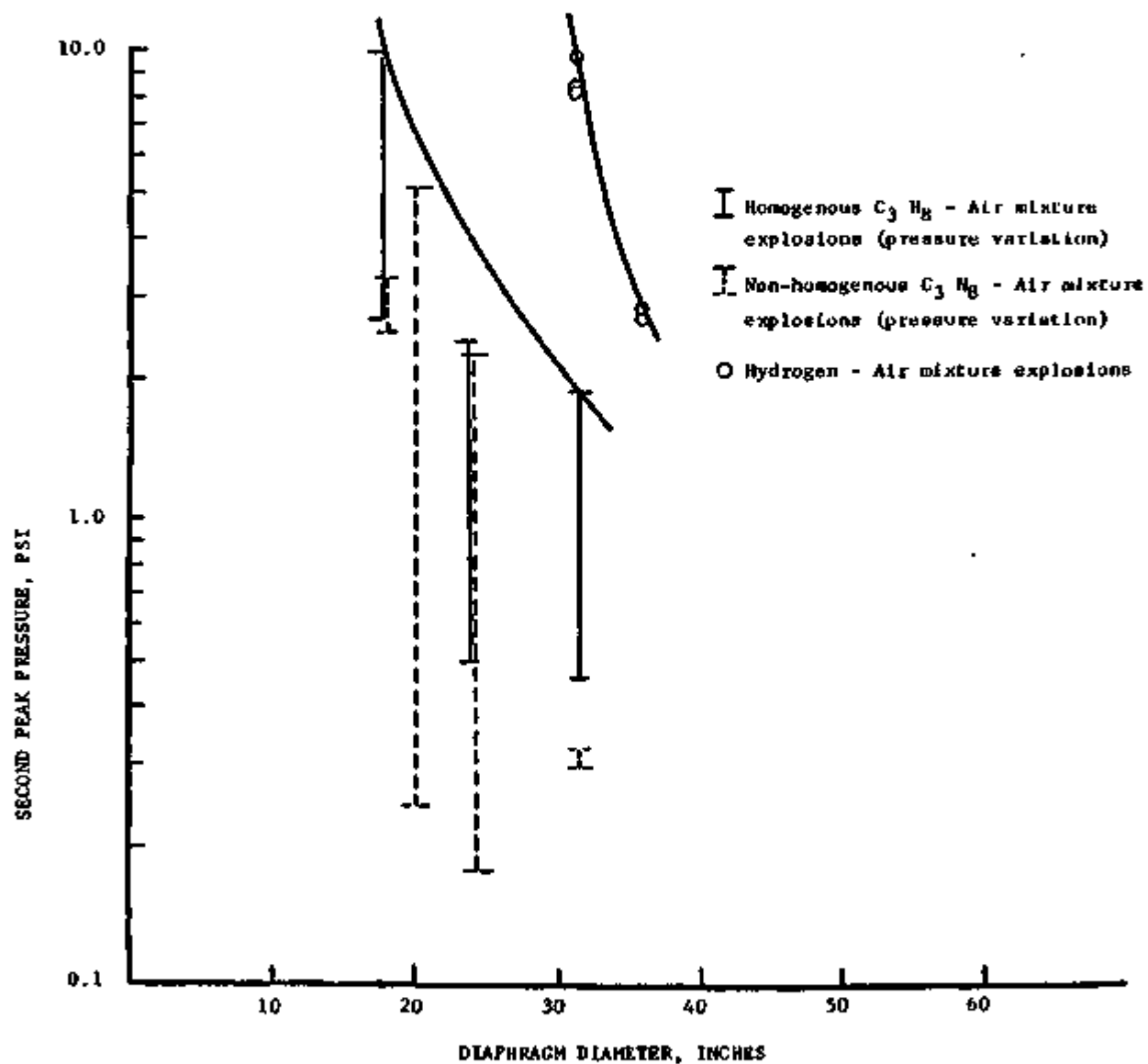


FIG.3-19 SECOND PEAK PRESSURE(PSI)AS A FUNCTION OF THE DIAPHRAGM DIAMETER( INCHES)

the same diaphragm diameter of 32 in. indicated that the flame of hydrogen/air mixture propagates about six times faster and the first-peak pressure is about two times higher, while the second-peak pressure is about five times higher than in a propane/air explosion.

Effect of Obstacles, Filters and Air Circulation - A 3ftx3ft, 16-gauge, 1/2-in. diamond expanded metal screen located very near to the inside of the diaphragm, did not contribute any noticeable increase in explosion pressure (see Test No. AB-27 and AB-28 of Table 5-B).

Attempts were also made to investigate the effect of obstacles, filters or combinations of these on the bursting diaphragm explosions. Data obtained with the non-homogeneous mixture setup are tabulated in Table 4-B. All the tests with 27 cfm air circulation rate were conducted to simulate the explosion resulting from a gas leak inside a ventilated glovebox. Figure 3-20 shows the test setup. A constant propane discharge rate of 1.08 cfm is introduced to mix with the incoming air at a constant rate of 27 cu ft. Ignition was initiated after about 30 minutes of continuous circulation. Comparing data in Table 4-B with that in Table 4-A shows that under practical operating conditions the explosion pressure (second-peak) would be much lower than that expressed by the pressure curve in Figure 3-19.

A limited number of tests were also conducted to investigate the effect of filters under the homogeneous mixture condition. These tests were carried out using a setup very similar to that in Figure 3-4. After the normal 20 minutes of purging with the homogeneous concentration of propane/air mixture at the rate of 455 cfh, the ignition was initiated while the purging was still in progress. In comparison with test No. AB-23 through AB-29, the combination of filters and air circulation seems to have no significant effect on the explosion pressures.

### 3.3.2 Bursting Diaphragm Explosion in the Cylindrical Test Chambers

In order to evaluate the geometrical effects on bursting diaphragm performance, a series of tests were performed in the cylindrical test chambers. Specifically, the following changes in geometry for a horizontal cylindrical chamber were examined: 1) change in L/D ratio with fixed cross-section; and 2) comparison of location of vent near the source of ignition (side vent) or remote from the ignition (front vent).

The configurations A and B as shown in Figure 3-8 were employed in the program. Configuration A (a three-foot diameter by three-foot long chamber) was used alternately with 18-in., 30-in., and 36-in. front-vent, and 18-in. top-vent; and configuration B (a three-foot diameter by nine-foot long chamber) was used alternately with 18-in. and 30-in. front-vent and distributed three 18-in. top-vents. The ignition source is located at the center of each configuration. Positions of pressure transducers are also shown. In contrast to previously described tests, two centrally located pressure

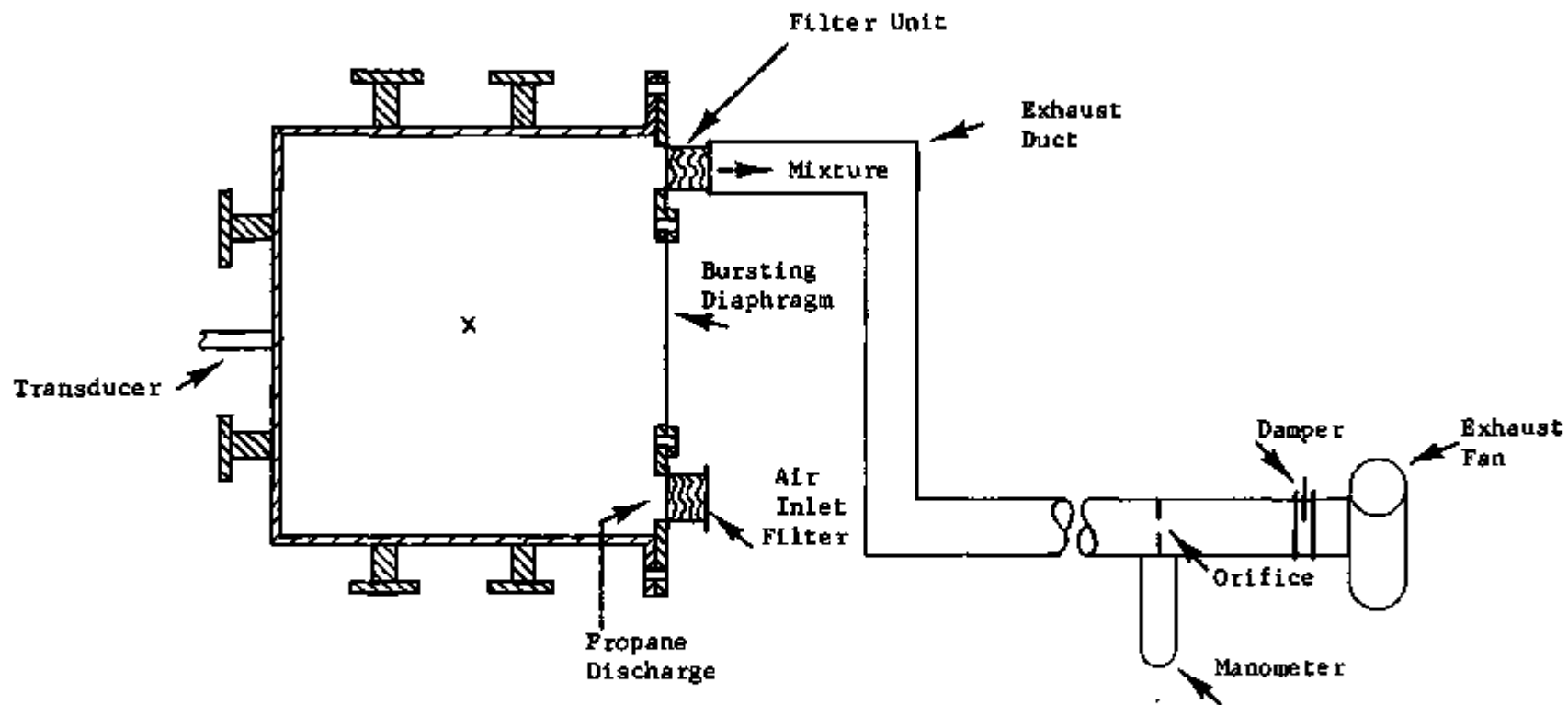


FIG. 3-20 TEST SETUP TO SIMULATE THE GLOVEBOX EXPLOSION RESULTING FROM A GASLEAK

transducers, one at the side wall and one at the end wall, were mounted on the chamber to measure the pressure variation at these two points. Test data and conditions employed are tabulated in Table 7. Since the pressures recorded by the side and the rear transducers were about the same, only the higher pressure recorded by the two transducers are presented in Figure 3-21. Figure 3-21 contains plots, the first-peak pressure versus L/D and the second-peak pressure versus L/D. In summary, the data show that:

- 1) Propane concentration in the range of 4.5 to 5.1 percent does not produce noticeable effect on the explosion characteristics;
- 2) In both the 3ftx3ft and 3ftx9ft cylinders, almost the same pressures were recorded from both side and end transducers. This means that explosion pressure is exerted equally on all walls of the chamber independent of the distance from the source of ignition;
- 3) For a given K factor increase in L/D ratio up to 3, slight increase in first-peak pressure and insignificant effect on the second-peak pressure are experienced.

#### 3.4 FREE-VENT PRESSURE RELIEF

Free-vent experiments were performed in the 27 cu ft cubical chamber and 3ftx3ft and 3ftx9ft cylindrical chambers with homogeneous propane/air mixture at 5.08 percent concentration. Data obtained are tabulated in Table 8. Direct comparison of these data with second-peak pressure of bursting diaphragm explosion tests on the same chambers shows that the maximum free-vent explosion pressure is about six times lower than the second-peak pressure measured with a bursting diaphragm. A typical free vent pressure-time record is presented in Figure 2-9.

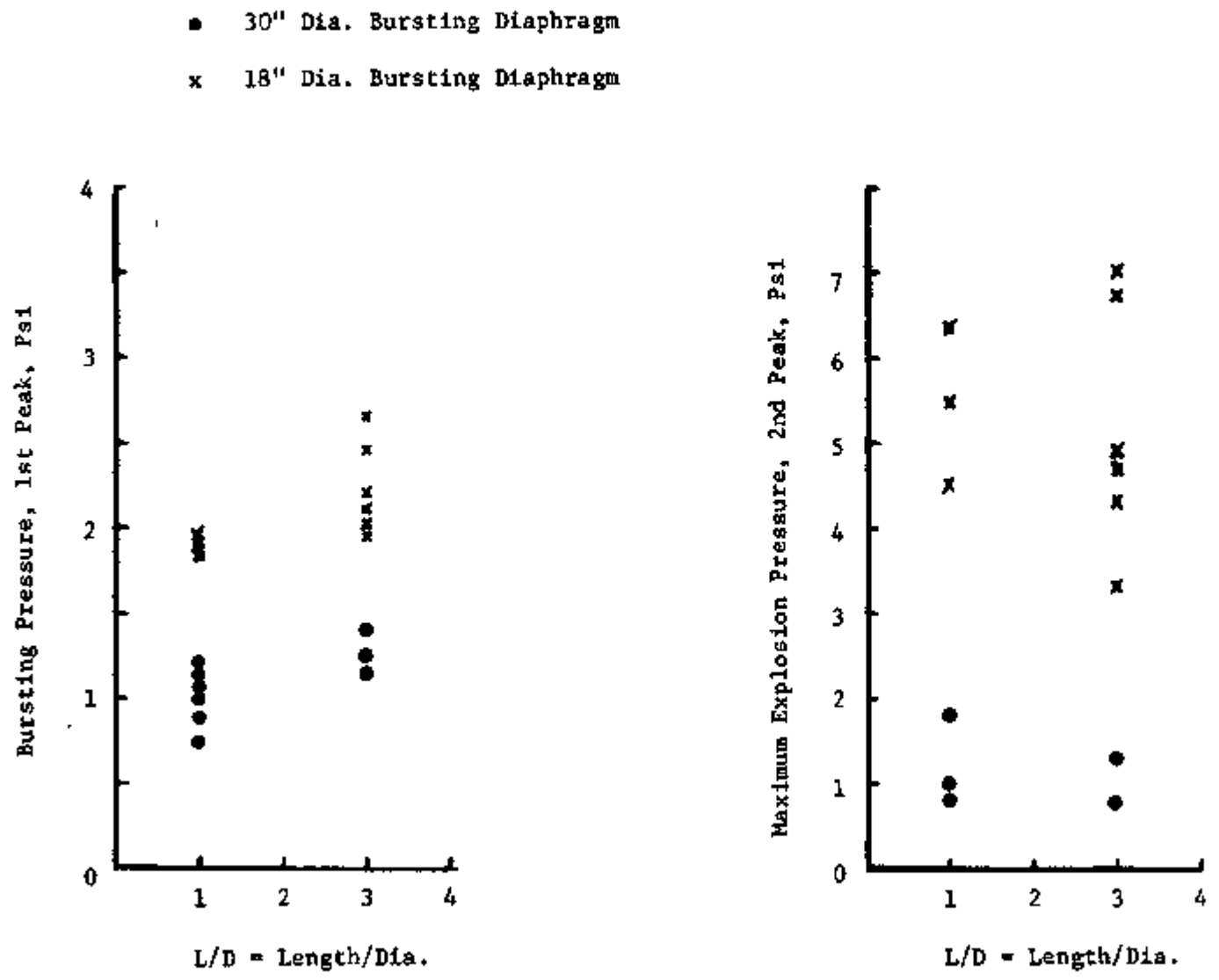


FIG. 3-21 EFFECT OF CONFIGURATION (L/D) ON THE EXPLOSION PRESSURE



## IV

DATA EVALUATION

## 4.1 LOCALIZED EXPLOSION IN A GLOVEBOX

Balloon explosion data for the 27 cu ft closed test chamber (Test Nos. A-1 to A-12 in Table 1) and the 24 cu ft wooden glovebox with one and two filters (Test Nos. W-1 to W-11 of Table 3) are replotted together with the theoretical results for a closed chamber explosion calculated from equation (8) in Figure 4-1 as maximum explosion pressure versus combustible gas volume ratio,  $V_u(o)/V$ . The good agreement between the test data and the theoretical curve for a closed chamber explosion confirms some of the explosion principles and mechanisms described earlier in this report. Furthermore, at the point of  $V_u(o)/V = 1$ , the theoretical curve agrees also very well with published experimental data(8)(10) for explosion in a 3 cu ft closed vessel filled completely with propane/air mixture. The pressure difference between the closed chamber explosion and those with filters represents the venting effect of the filter on the localized explosion in the glovebox. Actually the number of filters can be expressed as the dimensionless vent area parameter, such as  $C_F$  or K factor. In practice, the filters may be located at any one or two walls of the glovebox. Modification is required in order to take into account the second opening in a different wall.

Comparison of these curves shows that the intake and exhaust filters normally used on the gloveboxes can be quite effective in venting the localized explosion; however, the effectiveness diminishes as the explosive volume increases.

## 4.2 EXPLOSION RELIEF WITH BURSTING DIAPHRAGM

Bursting diaphragm explosion relief is one of the most commonly used devices. Diaphragms of many different kinds of materials have been used or are available for use as an airtight cover on explosion vent openings. The thin aluminum foil of 1 mil. thick was selected for this experimental investigation on the basis of convenience, low bursting pressure, heat resistance, compatibility with most AEC glovebox environments and, most of all, because bursting of thin aluminum foil would provide minimum hazard to persons and equipments nearby. The primary criterion in choosing a diaphragm is that its bursting strength must be considerably less than the weakest component of the glovebox. There is no doubt that many other materials may prove to be equally or more desirable for various special operational requirements.

4.2.1 Correlation of Bursting Diaphragm Data

The predicted theoretical bursting pressure for the one-mil-thick aluminum diaphragm is plotted, together with the experimentally determined first-peak pressure and static bursting pressure data, in Figure 3-18. The lower theoretical curve was calculated from static loading equations (31), (32), and (33). However, the measured static bursting pressure curve agrees very well with the theoretical result.

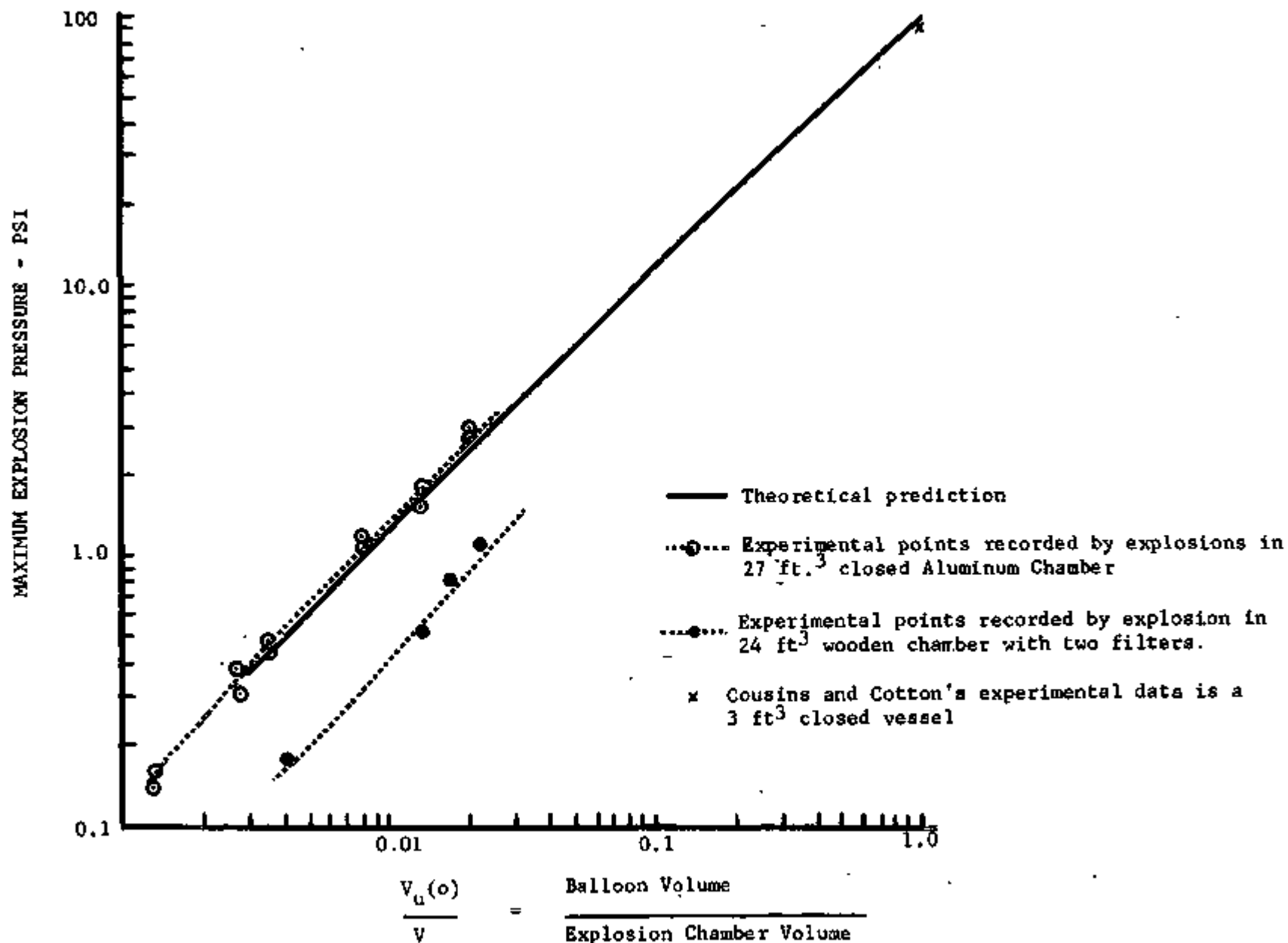


FIG. 4-1 CORRELATION OF LOCALIZED (BALLOON) EXPLOSION DATA

The second-peak pressure can be calculated from either of two cases, as shown in equations (21) and (22). As a first approach, case I, leakage of unburned gas alone, is to be considered. The second-peak pressure predicted by using the computer program described in Section 2-5 of this report is plotted in Figure 4-2 together with the highest measured pressure data obtained for the 27 cu ft cubical test chamber and the 3ftx3ft cylindrical test chamber. Data is presented as second-peak pressure versus the  $\alpha$  parameter. The venting parameters,  $\alpha$ , were calculated from equation (16) using a constant orifice discharge coefficient of  $C = 0.6$  except for the Point A. A coefficient of  $C = 1$  was used for Point A because this test was conducted for a 36 in. diaphragm, mounted on a 36 in. diameter wall (Test No. AB-82 of Table 8-A).

The measured second-peak pressure seems to fit very well into the theoretical data calculated by using the turbulent factor of  $2 < X < 3$ . The higher degree of turbulence seems to be induced at the lower  $\alpha$  value slightly more than the higher ones.

In comparison with the published data on bursting diaphragm pressure relief, as a function of the K factor, Figure 4-3 shows that the second-peak pressure measured from this study is somewhat higher than Simmonds and Cabbage's<sup>(17)</sup> experimental results and lower than the Burgoyne and Wilson<sup>(21)</sup> data. One of the possible reasons for the discrepancy is that Burgoyne and Wilson's ignition source, high voltage discharge through a thin aluminum wire, was found to throw off many small particles of aluminum; however, the electrical squib used in this study was also found through photographs to throw off, occasionally, one or two burning particles which may start separate ignition points.

Figure 4-4 shows the direct comparison of the experimentally and theoretically determined pressure-time record for the stoichiometric propane/air mixture exploded in a 27 cu ft chamber with a 24-in. diameter aluminum bursting diaphragm 1 mil. thick. Figure 4-4 shows the general characteristics of the double peak pressure record, but the measured explosion record indicated a much longer burning time than the theoretical value. The high speed movie shows that shortly after the bursting of the diaphragm the flame propagation might be temporarily slowed down or stopped because there was no sign of gas discharge through the opening until a few milli-seconds before the second pressure peak. A gradual increase in flame propagation speed may result from the effect of multiple ignition or large distortion of the flame envelope and other disturbance brought about or induced by the various possible factors listed in Section 2.5.2. It is quite possible that the turbulence factor  $X$  is actually a variable which increases with time at an unknown function.

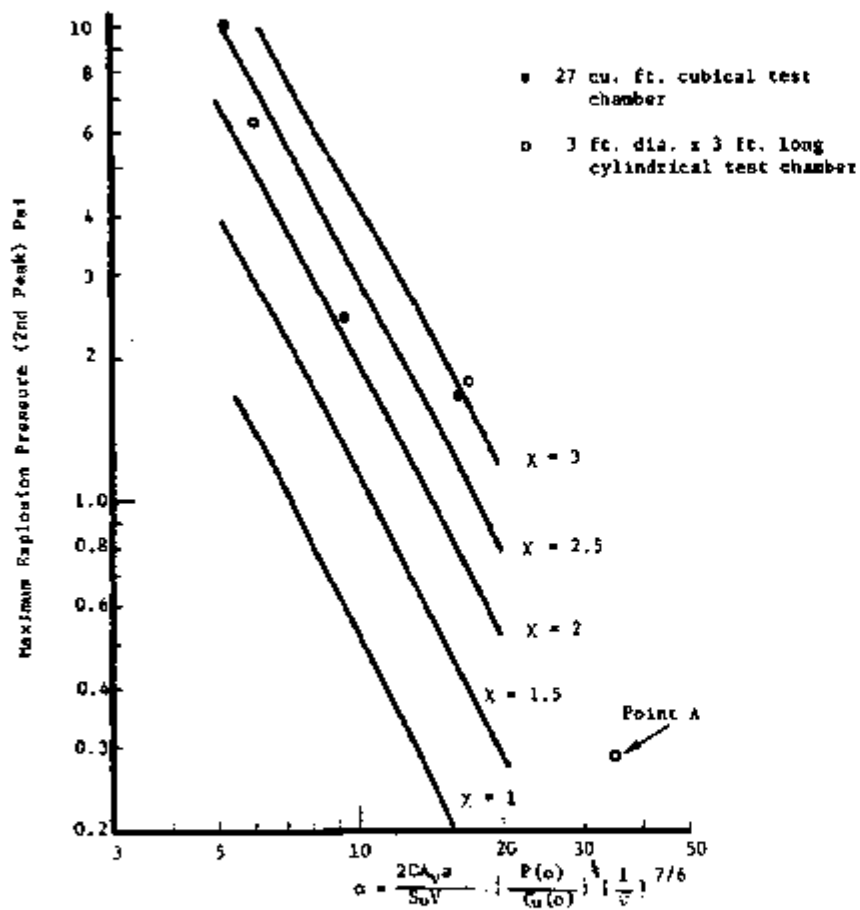


FIG. 4-2 CORRELATION OF THE THEORETICAL AND EXPERIMENTAL DATA FOR BURSTING DIAPHRAGM PRESSURE RELIEF

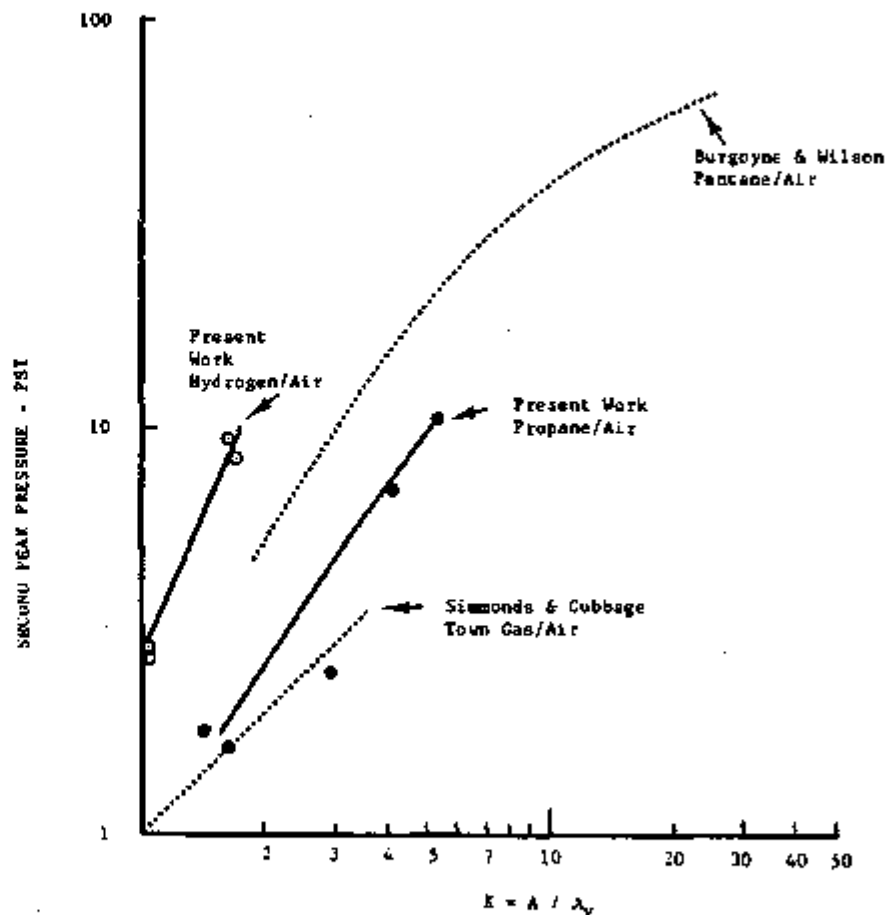


FIG. 4-3 CORRELATION OF THE EXPERIMENTAL DATA OBTAINED FROM PRESENT STUDY WITH THE PUBLISHED DATA.

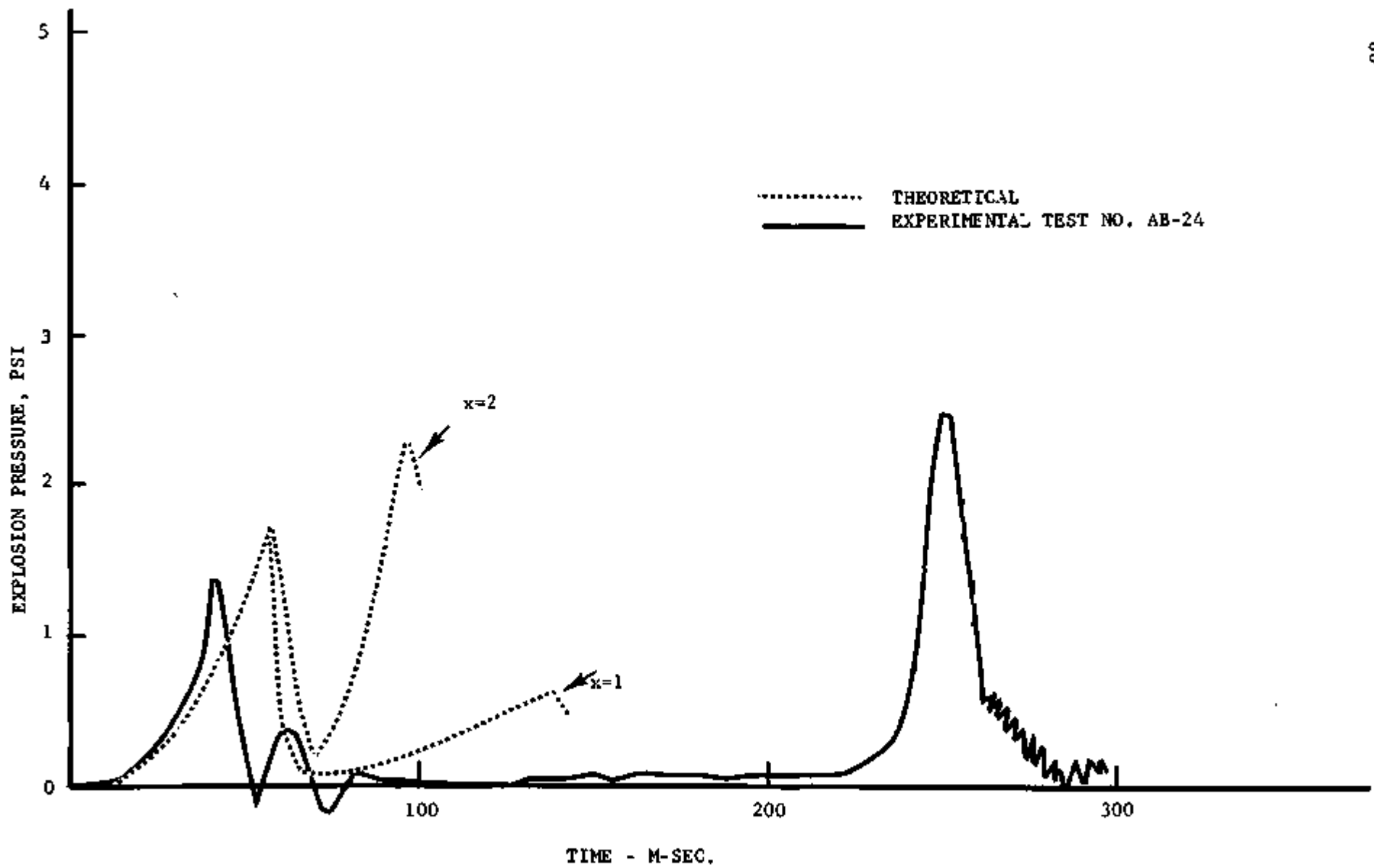


FIG. 4-4 DIRECT COMPARISON OF THE EXPERIMENTALLY AND THEORETICALLY DETERMINED PRESSURE-TIME RECORDS FOR STOICHIOMETRIC PROPANE / AIR MIXTURE EXPLODED IN A 27-CU. - FT. CHAMBER WITH A 24-IN. DIAMETER DIAPHRAGM.

#### 4.2.2 Effect of Bursting Pressure on the Second-Peak Pressure

Tests conducted thus far have not been able to determine the relationship between the first-peak and second-peak pressure. Simmonds and Cabbage<sup>(17)</sup> treated the two pressure peaks as two independent phenomena. Maisey<sup>(7)</sup> even correlated the second-peak pressure obtained with the bursting diaphragm with the maximum pressure measured with the free-vent explosion and ignored the first-pressure peak completely. The effect of bursting pressure has been studied by Harris and Briscoe<sup>(22)</sup> in correlating the maximum explosion pressure for a particular vent area with the diaphragm bursting at different pressures. This bursting pressure variation was achieved by using different kinds of diaphragms of varying thicknesses. The results of 2.5 mole percent pentane/air mixture are replotted in Figure 4-5 as the maximum explosion pressure versus the bursting pressure for different vent diameters. The most interesting feature of these results is the unexpected presence of dips in some of the curves. In order to correlate these high-pressure range explosion data with low-pressure range results obtained from this study, Figure 4-5 is transformed in Figure 4-6 in log-log scale as maximum explosion pressure versus bursting pressure for different K factors. The solid line represents Harris and Briscoe's data; the dotted lines represent the writer's interpretation and extrapolation. The limited quantity of test data obtained from this program is also plotted in this graph. Compared with the free-vent explosion data, it seems indicated that the phenomenon of explosion venting is really not yet well investigated. Simmonds and Cabbage's<sup>(17)</sup> correlation of  $P_2 = K$  seems only to apply to the range of test conditions involved. Considerable caution should be given not to extrapolate the data too far beyond the range.

It can be seen that all the maximum explosion pressure curves will essentially fall on the same straight line toward the right hand side of the figure. For these higher bursting pressure diaphragms it is apparent that the vent size is adequate to relieve the explosion and the measured value of the maximum explosion pressure is the same as the bursting pressure of the diaphragm.

#### 4.2.3 Effect of Geometry and Configuration

Gloveboxes have been designed and fabricated in many sizes and shapes to meet special operational requirements. From the point of view of shape, gloveboxes may be generalized into three basic categories; 1) those having all three dimension of the same order (cubical); 2) those having one dimension much longer than the other two (several cubical gloveboxes connected in series); and 3) those having one dimension much smaller than the other two. The examination of glovebox construction at Argonne National Laboratory showed that most of the very large gloveboxes are in the third category, having demensions such as 3ftx9ftx18ft.

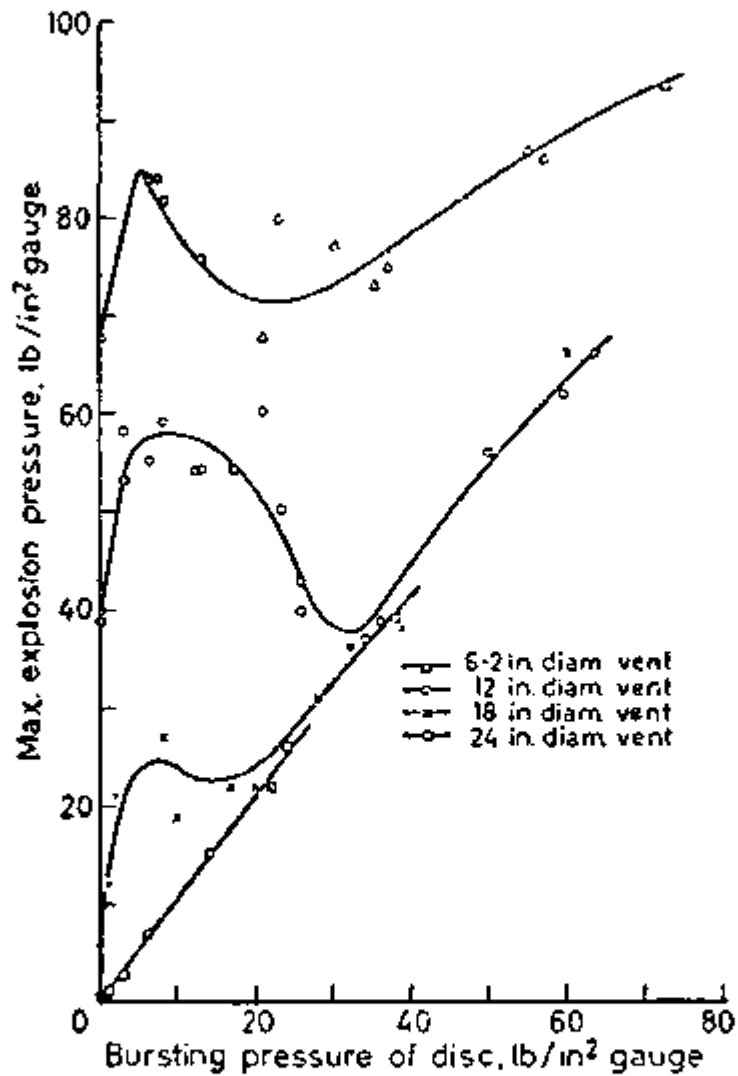


Figure 4-5 Maximum-explosion pressure versus disc bursting pressure for stationary 2.50 mol. % pentane in air mixtures

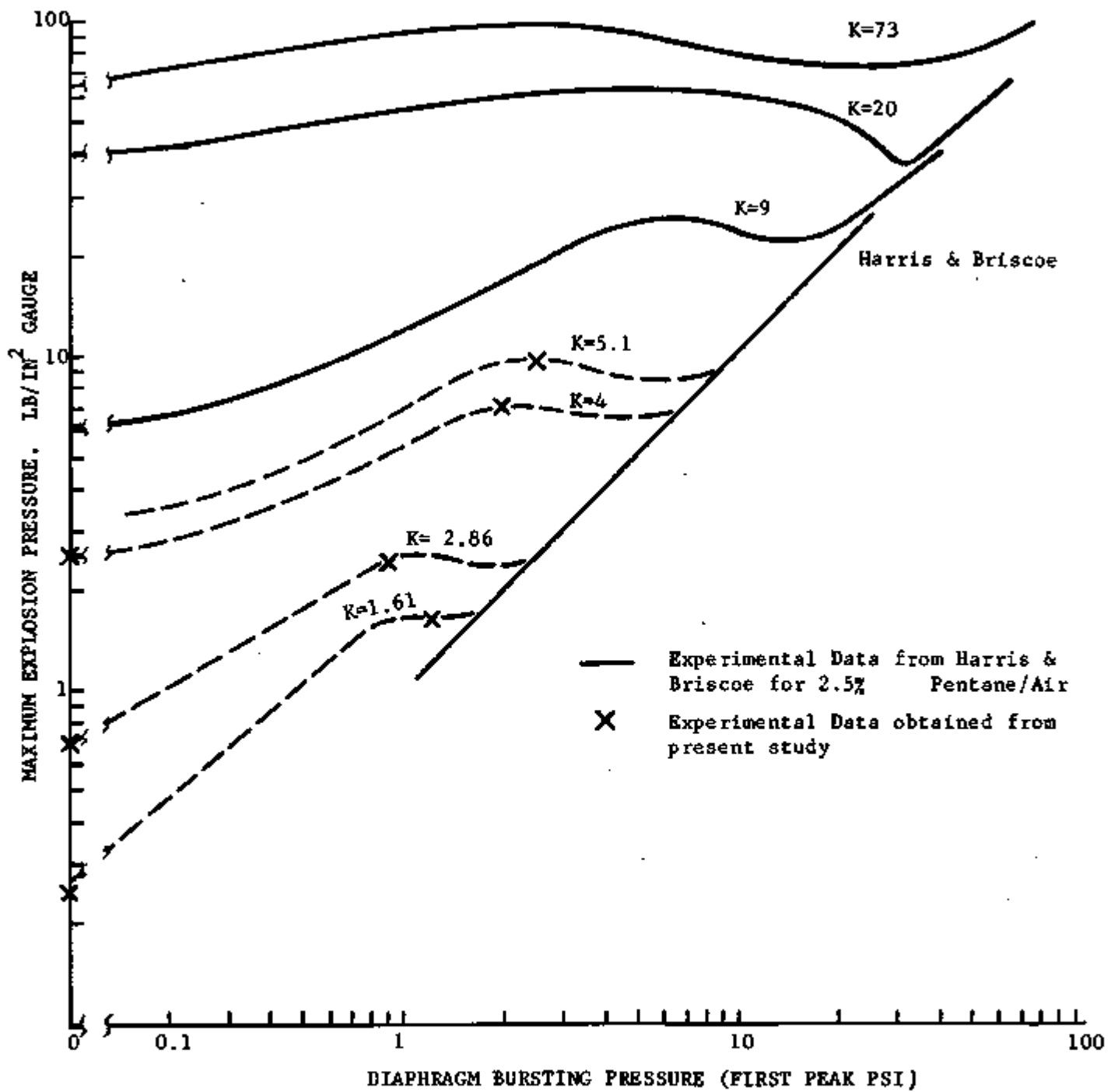


FIG. 4-6 EFFECT OF BURSTING PRESSURE ON THE SECOND-PEAK PRESSURE



Explosion pressure has been customarily correlated as a function of the vent ratio

$$A_v/V = \text{area of the vent/volume of the vessel}$$

As described previously, the rate of pressure rise is an important factor in determining the maximum explosive pressure for a vented explosion. Obviously the rate of pressure rise decreases with increasing volume, because the time taken to reach a given pressure is proportional to the cubic root of the volume. Consequently, a smaller vent ratio,  $A_v/V$ , will be required in the large gloveboxes than the smaller gloveboxes. A more logical geometrical scaling parameter has been used satisfactorily to correlate the experimental results obtained from vessels of different volumes, i.e.:

$$K = A/A_v = \frac{\text{cross section area of side containing the vent}}{\text{vent area}}$$

In Simmonds and Cabbage's<sup>(17)</sup> experimental results with four, 100-cu-ft volume enclosures of different shapes, the dimension ratio ranges from 1:1:1 to 1:2:3. In these experiments, the same bursting diaphragms were used to cover one entire wall,  $K=1$ , throughout the test program. It was concluded that no matter on which side the diaphragm was mounted, the first- and second-peak pressures were always less than those obtained in the cubical enclosure. Thus, the design of reliefs could with safety be based on the result for cubical test chambers. Rasbash's<sup>(26)</sup> attempt at a correlation of results by various workers shows that for small  $K$  factors, up to  $K=4$  the second-peak pressures are not affected by the  $L/D$  ratio.

Experiments conducted in the present program are all in the first two categories, cubical and cylindrical test chambers. As shown in Figures 3-20 and 3-21, for a  $K$  factor of 1.44 and 4, an increase in  $L/D$  from 1 to 3 contributed very little effect on the first and second pressure peaks. However, the second-peak pressure for  $K=4$  seems to show a trend of slightly increasing pressure when the  $L/D$  ratio approaches 3.

#### 4.3 EXPLOSION RELIEF WITH FREE-VENT OR FILTER

Explosion relief with a filter is a very attractive idea for AEC gloveboxes. A filter is the only material which can vent the explosion continuously, like a free opening, but without the danger of causing radioactive contamination to the atmosphere. Data obtained for explosion relief with free-vent and direct comparison between free-vent and filters in balloon explosion experiments indicate that explosion venting with a filter might be the best solution for AEC glovebox application.

##### 4.3.1 Correlation of Free-Vent Data

The experimental and theoretical data for free-vent explosion relief are compared with published free-vent data in Figure 4-7. The figure shows

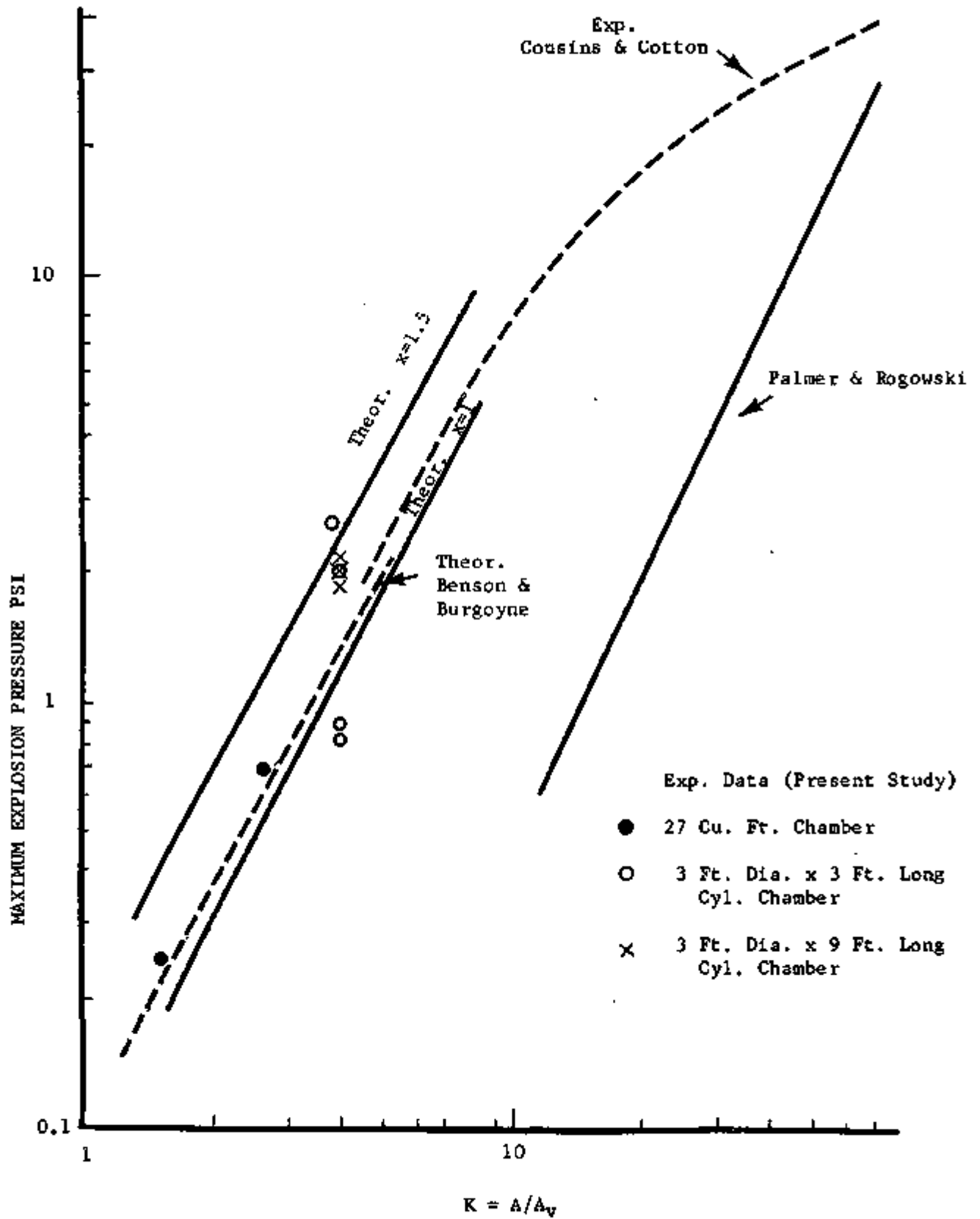


FIG. 4-7 CORRELATION OF THE FREE-VENT PRESSURE RELIEF DATA

that the maximum explosion pressure measured from this study is just slightly higher than the theoretical results based on the laminar flame propagation,  $\chi = 1$ , and agrees very well with Cousins and Cotton's<sup>(9)</sup> free-vent explosion curve. It will be noted also that the free-vent explosion data obtained by Palmer and Rogowski<sup>(14)</sup> are considerably lower than those given by Cousins and Cotton (9) and by the present study. This is surprising because all of these data were obtained with the propane/air mixture.

Explosion relief with free-vent seems to represent the best possible and most effective method, and starts to vent the gases at the very initial state of combustion. Minimum level of agitation, turbulence and discontinuity are induced in the combustion process and, therefore, lower explosion pressure should be expected.

#### 4.3.2 Explosion Venting with Filters

In view of the advantage of free-vent over the bursting diaphragm in reducing the turbulence effect, and the encouraging results obtained from the comparison test between free-vent and filters in the balloon explosion experiments, further work in this area is recommended.

Data obtained thus far seem to indicate that the maximum explosion pressure for filter venting could be correlated with the free-opening venting by using an equivalent vent area of  $F A_f$  in the K factor. The K factor for filter explosion relief may be approximated as

$$K = A/A_v = A/F A_f$$

where  $A_f$  is the cross-section area of the filter unit, and F is the correction factor for equivalent area in relation to the free opening.

Due to the difference in flow characteristic between free orifice and filter, the correction factor for equivalent opening area, F, may prove to be a variable. However, over the low pressure range of 0.5 to 3 psi, F is expected to be in the order of about 0.2 to 0.3.

### GENERAL GUIDELINES FOR EXPLOSION PROTECTION IN GLOVEBOXES

Explosion as referred to in this report is commonly known as "deflagration", a subsonic propagating combustion wave accompanied by pressure effects. Most industrial explosions start as deflagrations and relatively few develop into the more severe detonations. In protecting gloveboxes against explosion, the procedure is to arrest and minimize the effect of a deflagration. It is important to take measures at the early stage in the development of the explosion before damage or detonation has developed.

Glovebox design is influenced by the toxicity, form and quantity of the materials to be handled, type of operations, radiological risk, safety requirements, and economic considerations. There has been a wide diversity in design and construction; many gloveboxes have been designed and fabricated to meet special requirements.

Most gloveboxes are designed to withstand normal working conditions. They are usually designed and tested to limit leakage, and to withstand specified positive and negative pressures up to 4 in. water gauge (0.144 psi). There are no design criteria available which take into consideration the over-pressurization resulting from explosion inside the gloveboxes.

The current safety practices of AEC's glovebox facilities emphasize mostly preventive measures, elimination of the conditions which permit the formation of an explosive mixture and provision of sensible alarm instrumentation. It is equally necessary to apply effective protection measures. As a result of the knowledge gained from the present study and review of other published information, the following guidelines for explosion protection in gloveboxes are presented.

#### 5.1 GENERAL GLOVEBOX DESIGN CRITERIA

Several unique features must be considered in the application of explosion venting data presented in the previous sections of this report in designing the complete glovebox system: 1) size and shape of the glovebox; 2) construction strength; 3) air flow patterns; 4) type and size of the filters; 5) type and location of the gloves; 6) window material and size; 7) atmosphere control; and 8) penetration requirements (i.e. openings for ducts; piping etc.). Therefore, the proper design procedure to provide adequate protection from explosion is presented as follows:

(1) Predetermine the maximum credible explosion condition and its causes, i.e., type of fuel, source and rate of emission and location of the ignition sources. If this required information is not available, then the maximum credible explosion condition would be the central ignition in the glovebox filled completely with combustible mixture at the concentration which gives a maximum explosion pressure.

(2) Design the ventilation rate and flow pattern to confine the combustible vapor inside the glovebox to the smallest possible volume.

(3) Use equation (8) or Figure 4-1 to predict the maximum explosion pressure.

(4) If the calculated pressure is slightly higher than the safety level of the glovebox, additional low-pressure relief devices or larger filter area should be provided.

Most gloveboxes designed for 4 in. water gauge (0.144 psi) cannot withstand more than 0.3 percent in explosive volume ratio,  $V_{u(o)}/V$ . With proper design and relocation of components, the glovebox can be upgraded to a higher level of 2 to 4 psi to cope with a much larger explosive volume ratio of 4 to 9 percent. However, if there is any doubt that the entire glovebox volume may be involved, a low pressure explosion relief, such as a bursting diaphragm, should be installed.

#### 5.1.1 Effect of Explosion on Filters

The primary criteria in selecting filters for the AEC gloveboxes are: particulate matter collection efficiency; strength; durability and ability to resist fire, heat, moisture and special chemicals. The most commonly used fire resistive high-efficiency filter units are constructed of glass-fiber media with metal or asbestos separators and noncombustible adhesives. The ability to withstand overpressure of regular filters and dust loaded filters was tested in the 180-ft. Conical Shock Tube at the Naval Research Laboratory (28). A summary of the test results is presented as follows:

<u>Filter size, in.</u>	<u>Regular filter Failure pressure (psi)</u>	<u>Dust load filter Failure pressure (psi)</u>
8x8x3	3.6	
8x8x6	4.5	3.93
12x12x6	3.6	
24x24x6	2.2	
24x24x12	3.2	2.9

It can be seen from these data that the smaller the individual unit and the thicker the unit of a given size, the better is its ability to withstand the shock wave. Shock pressures near the failure pressures resulted in adhesive cracking or small leaks at the media - adhesive bond. Shock pressures of 2.5 to 1 psi greater than the failure pressure resulted in blow-out slits in the downstream ends of the filter pleats. Shock pressures of more than 2 psi greater than the ultimate failure pressures caused extensive damage to the filter unit.

The loaded filters were artificially loaded with talc dust to simulate a filter approaching the end of its useful service life. It is reported

that a five-fold increase in air resistance due to the dust loading shows a 15-percent drop in the shock wave resistance capability. It was also concluded that stronger adhesives and means to support the center area of the larger filter units would improve the blast resistance markedly.

The 8x8x6 filter has been exposed to various explosion pressures in some of the present test runs. Up to an explosion pressure of 4 psi (Test No. AA-264 in Table 4-B) no sign of blowout or rupture of the filter media was observed. In order to test the strength of the filters and gloves, a total of six filters and two latex gloves were mounted on the front funnel of the 27 cu ft cubic test chamber. The first-peak pressure was slightly higher than 7 psi, which was the calibrated upper limit of the visicorder. Figure 5-1 shows the ruptured filters and gloves after the test.

#### 5.1.2 Effect of Explosion on Gloves

Loss experience and FMRC tests show that internal pressure buildup from explosion, fire and unregulated supply of gas from a high-pressure source may cause gloves to rupture. Table 9 shows the static bursting pressure of various gloves commonly used in AEC gloveboxes (1). These tests were performed pneumatically at FMRC, based on a pressure rise of not more than 0.1 psi per sec in comparison with the rate of about 100 psi per sec in actual explosion cases. In view of the difference between dynamic and static rupture characteristics described in the previous sections, the ability to withstand explosion pressure of the neoprene one-piece 0.015-in. thick glove and latex were tested in this study. The following is a summary of the findings.

- 1) The gloves appear to withstand much higher pressure in dynamic conditions than when tested under static conditions.
- 2) Both the neoprene, one-piece, 0.015-in. thick glove and the latex glove, at normal working conditions (protruding inside glovebox) could withstand a pressure of more than 2 psi. The same gloves rupture at 0.56 psi and 0.28 psi under static test conditions.
- 3) The same neoprene glove mounted on the top flange of the cylindrical chamber as shown in Figure 5-2 did not rupture at a dynamic pressure of 1.5 psi.
- 4) The same neoprene glove mounted on the top flange of the cylindrical chamber with the hand hanging down as shown in Figure 5-3 ruptured at 1.3 psi. As shown on the high-speed movie, the sleeve of the glove was pinched by its own weight. The sleeve was expanded and ruptured near the root, like an elastic bursting diaphragm before the remaining portion of the glove had a chance to be inflated.
- 5) The pressure relieving effect due to the stretching or expansion is not noticeable in these tests.



TEST NO. AA-263

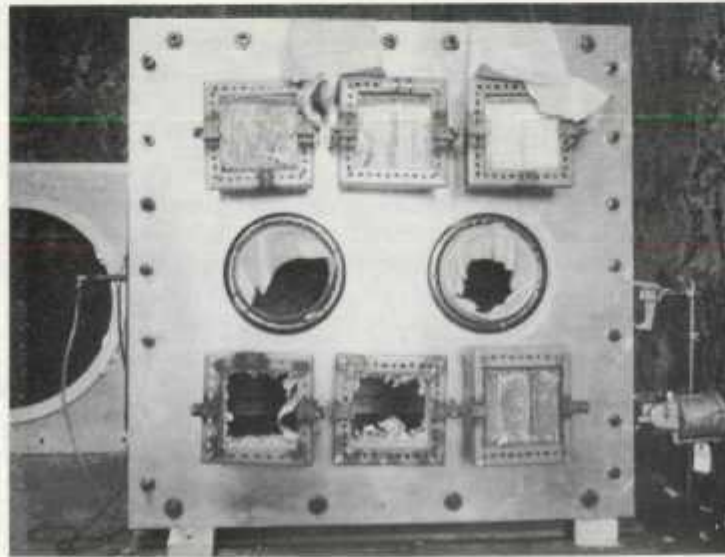


FIG. 5-1 RUPTURE OF FILTERS AND GLOVES



FIGURE 5-2 - MOUNTING OF GLOVES ON THE 3ft x 3ft  
CYLINDRICAL TEST CHAMBER (Arrangement A)



FIGURE 5-3 - MOUNTING OF GLOVES ON THE 3ft x 3ft  
CYLINDRICAL TEST CHAMBER (Arrangement B)



6) The dynamic rupture pressure of the thicker gloves may well be up to 4 psi. Exact dynamic rupture pressures of various gloves is not known. The rupture pressure is a function of the material, thickness, construction, as well as how the gloves are mounted.

Recommended practices are:

1) Avoidance of any means to pinch or prevent the glove from free expansion to a full attenuation. Tying two gloves together at the outside of the glovebox when the gloves are not in use may cause the gloves to rupture at a much lower pressure in case of explosion.

2) The use of outside metal glove port covers when not in use.

## 5.2 EXPLOSION VENTING WITH BURSTING DIAPHRAGM

Gloveboxes containing or handling flammable gases and vapors should be vented according to the contents, operating conditions and the type of construction. As described in previous sections, a large vent area or small K factor are required for the more hazardous materials having a high burning velocity and rapid rate of pressure rise. In general, smaller gloveboxes are more hazardous than the larger gloveboxes, because, in the event of accident, a larger portion of the space may be involved with maximum explosive mixture strength, whereas in a large ventilated glovebox there is a greater chance of having a localized explosion rather than a completely filled explosion.

In the design of a suitable explosion pressure relief, the following factors should be considered:

- 1) Strength of the glovebox structure and its components.
- 2) Strength and homogeneity of the combustible mixture accumulated inside the glovebox, i.e., concentration, burning velocity, rate of pressure rise, explosive volume ratio, etc.
- 3) Size and location of the pressure relief device.
- 4) Manner and the condition in which the relief is to be uncovered.
- 5) Level of turbulence or agitation.
- 6) Ignition strength and number of sources.
- 7) Confining and exhausting the explosion discharge.

### 5.2.1 Effect of Mixture Strength and Fuel

The effect of mixture strength between the lower and upper explosive limits on the burning velocity and the rate of increase in pressure as well

as the maximum explosion pressure in the case of closed vessel explosions are shown in Figures 2-1, 2-7, and tabulated in NFPA Pamphlet No. 68 (10). Since the burning velocity, the rate of increase of pressure as well as the maximum explosion pressure is greatest for "most explosive" (slightly richer than stoichiometric) mixture, it is necessary to provide the explosion protection for the most explosive mixture. Gloveboxes designed to cope with the most explosive mixture strength will be considered safe for other mixtures.

### 5.2.2 Determination of Vent Area

The vent area requirement for an explosion in a cubical glovebox can be estimated from the general differential equations and boundary conditions presented in Section 2.5 of this report, using  $\chi=3$  for hydrocarbon/air mixture and  $\chi=1.5$  for hydrogen/air mixture.

Experimental data obtained from this study are in agreement with the published data. The explosion pressure (second peak) is a function of the K factor for both cubical and non-cubical gloveboxes under the conditions: 1) the bursting pressure is less than that of the second-peak pressure; 2) L/D ratio is from 1 to 5; and 3) dimension ratio ranges from 1:1:1 to 1:2:3. For the purpose of estimating the vent area requirement on various commonly used glovebox configurations, the numerical solutions of theoretical equations are rearranged into a nomograph as shown in Figure 5-4, and plotted as explosion pressure (second-peak pressure) versus a modified venting parameter for cubical and rectangular glovebox configurations

$$\alpha_G = \frac{CA_v}{S_u A} \left( \frac{P(0)}{\rho_u(0)} \right)^{1/2} \left( \frac{\rho_b(0)}{\rho_u(0)} \right)^{7/6} = \frac{C}{S_u K} \left( \frac{P(0)}{\rho_u(0)} \right)^{1/2} \left( \frac{\rho_b(0)}{\rho_u(0)} \right)^{7/6} \quad (34)$$

for different turbulent indexes ( $\chi$ ). Considerable caution should be exercised in choosing the turbulent index and orifice discharge coefficient (C). In general, low  $\chi$  values conform to high burning velocity mixture and  $\chi$  values increase with the decrease in burning velocity. The suggested value for thin aluminum foil bursting diaphragm is  $\chi=3$  for  $S_u = 40$  cm per sec and  $\chi = 1.5$  for  $S_u = 320$  cm per sec. The value of orifice discharge coefficient, C, usually varies from 0.6 for a sharp-edged small opening on a large wall to 0.98 for a well rounded nozzle and 1.0 for the case of  $K = 1$ . For gloveboxes of much larger than the sizes used in this program or bursting pressure much smaller than that observed in this program, vent areas estimated from Figure 5-3 should be considered as slightly on the conservative side. Under the conditions described above, the vent opening can be positioned at any one of the six walls as long as the same K factor is used.

For gloveboxes of large L/D ratio ( $L/D > 3$ ) the vent opening should be positioned as close to the source of ignition as possible. If the source of ignition is not known, one must usually allow for the worst case.

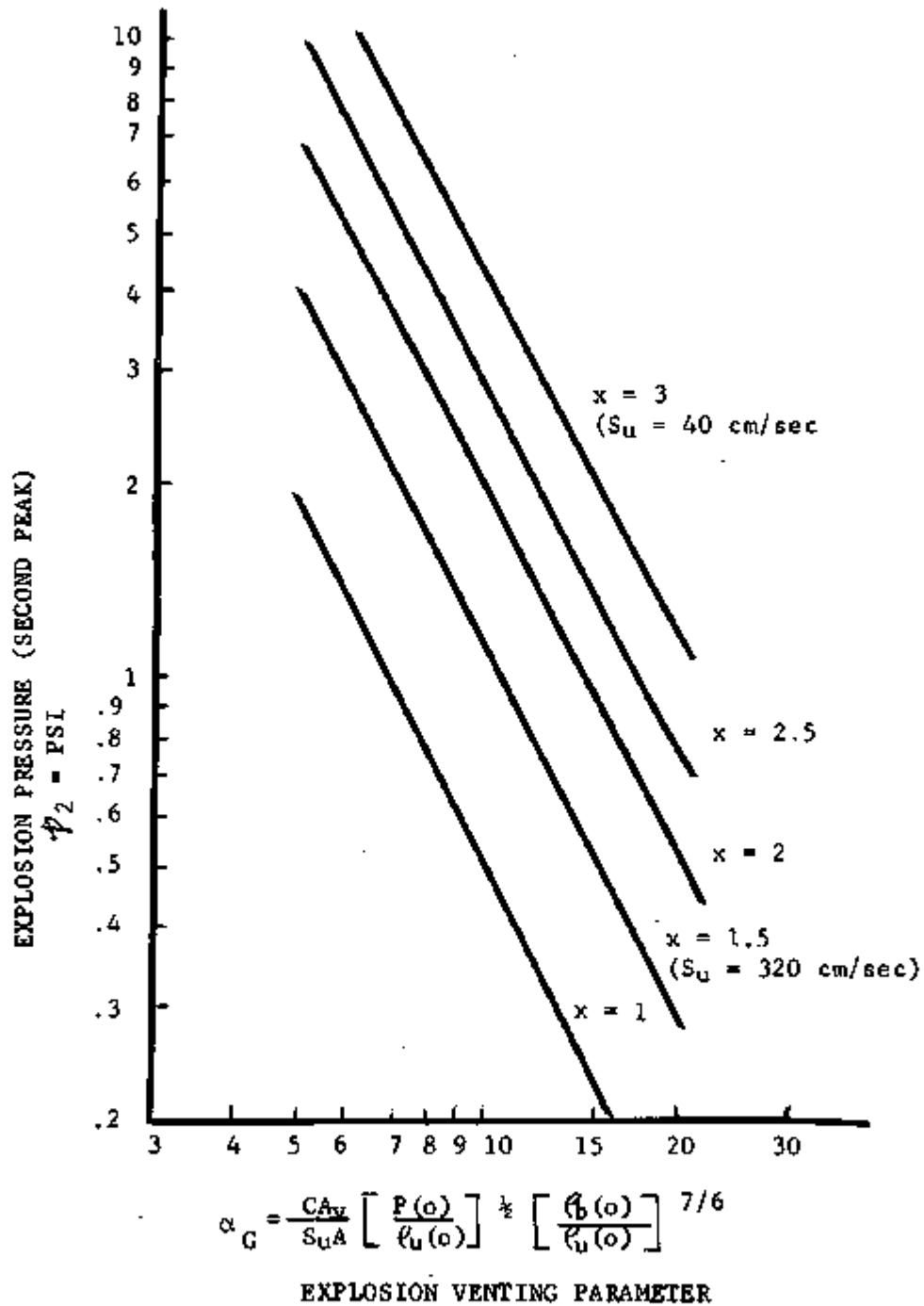


FIG. 5-4 NOMOGRAPH FOR BURSTING DIAPHRAGM EXPLOSION RELIEF DESIGN (THIN METAL DIAPHRAGM WITH BURSTING PRESSURE NOT MUCH DIFFERENT FROM THAT SHOWN IN FIGURE 3-18)

Explosion venting in the long duct work type of gloveboxes,  $L/D > 3$ , has not been investigated in this study. Some of the available empirical data are summarized in Section 2.5.2. For the low pressure explosion venting application where K factor is very close to 1, the explosion pressure (second peak) is nearly invariant with  $L/D$  for  $L/D > 3$  and increases with  $L/D$  for larger values. Under certain conditions in duct of  $L/D > 40$  an ordinary deflagration of acetylene/air mixture may be developed into a detonation.<sup>(27)</sup>

### 5.2.3 Selection of Vent Relief Device

A most useful collection of data on types of low pressure relief vent is given in the NFPA Explosion Venting Code No. 68 (10). Burgoyne and Wilson (21) demonstrated that a smoothly opening vent relief such as plate valve or a lightweight hinged plate tend to produce lower explosion pressure (second peak) than bursting types of vent relief. The lower second-peak pressure with smoothly opening vent relief was thought to be due to a lower level of turbulence effect (low  $\chi$ ). As described in Appendix B, butterfly dampers or valves of various sizes activated by a pressure switch are being used by several AEC operations. In view of the special requirements of 1) large vent area (more than half of cross-sectional area of the glovebox); 2) air seal under normal operating conditions and 3) rapid relief in case of explosion, the bursting diaphragm seems to be a good choice.

Because of the absence of knowledge of dynamic bursting characteristics of diaphragms, the diaphragm material and thickness can be selected on the basis of static bursting data as long as the static bursting pressure of the diaphragm selected is lower than the static rupture pressure of the weakest glovebox component. Although the actual dynamic bursting pressure will be somewhat higher than the static bursting pressure, such will also be the case for the glovebox components. General guidelines in selecting bursting diaphragms for glovebox application are as follows:

1) The bursting pressure of the diaphragm should be considerably less than the rupture pressure of the weakest component of the glovebox.

2) The effect of the bursting pressure of the diaphragm on the maximum explosion pressure for a particular vent area or K factor is described in detail in Section 4.2.2 of this report. In general, it seems indicated that the bursting pressure of the diaphragm should be kept as low as possible.

3) For a particular vent area, the static bursting pressure of various materials can be determined from equations (31), (32) and (33) or from Figure 5-5. The bursting pressure of a given material increases with thickness of the diaphragm and decreases with the increase in area.

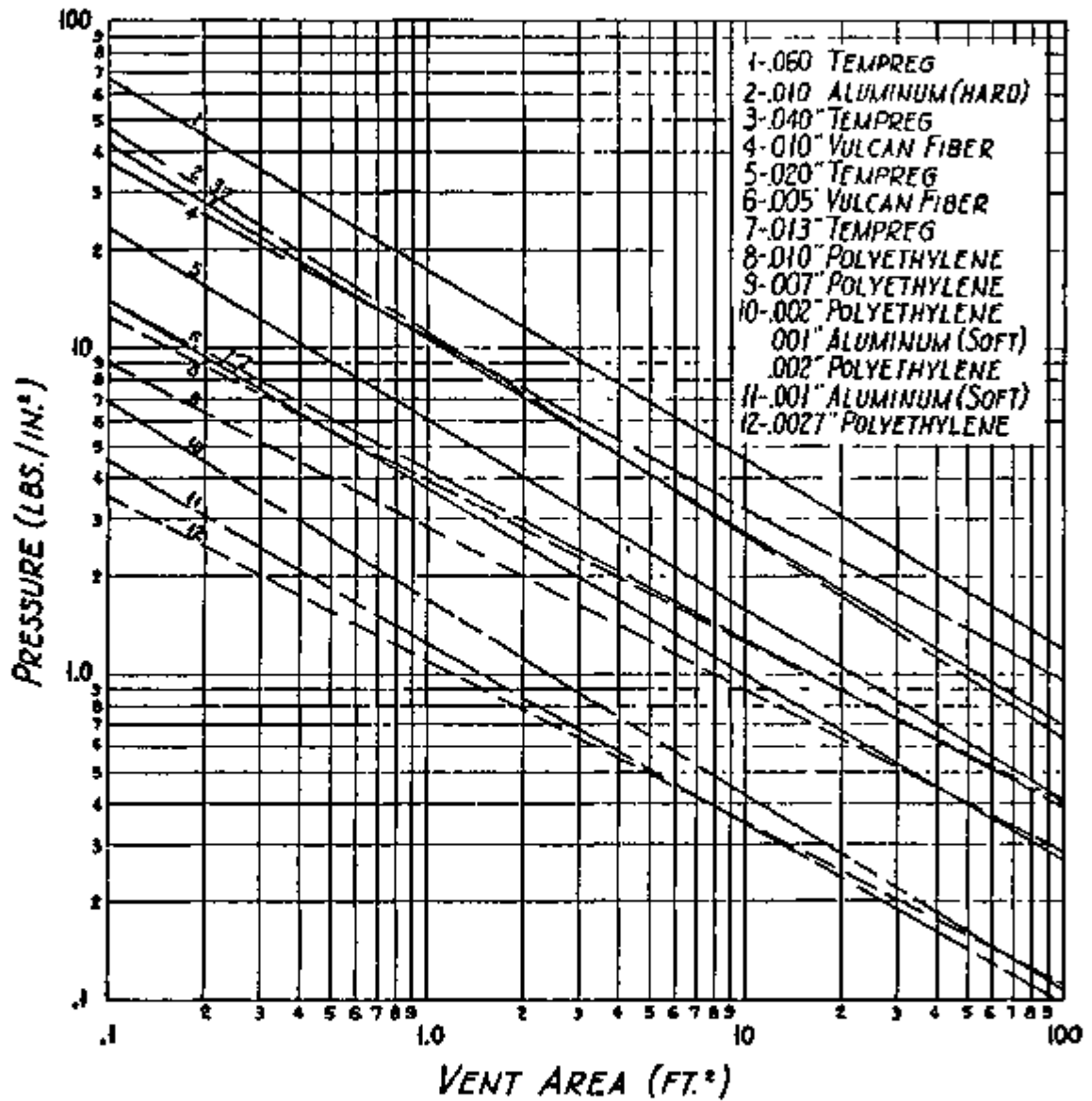


Figure 5-5 Rupture pressure vs. vent area of various venting materials. (The graph shows that the bursting pressure of venting materials is a function of the vent area.)

Reference (10)

4) The dynamic bursting pressure under actual explosion conditions increases with the increase of the maximum rate of pressure rise or burning velocity (see Figure 3-18).

5) For a given vent area, the bursting pressure of a circular geometry is lower than the square geometry. Rectangular geometry is conducive to highest bursting pressure.

6) For a given vent area, the actual dynamic bursting pressure decreases with increase in glovebox size. For a hydrocarbon explosion in a cubical glovebox configuration of larger than 1000 cu ft, the dynamic bursting pressure would be very close to the static bursting pressure.

#### 5.2.4 Air Ventilation Obstacles and Multiple Sources of Ignition

The effect of turbulence, obstacles and multiple source of ignition is to increase the rate of pressure rise.

As described earlier, under turbulence conditions of burning, the radial propagating flame speed,  $S_b$ , increases by a factor of  $X$  and, therefore, the rate of pressure rise as well as the maximum explosion pressure (second peak) will increase considerably as indicated by Equation (11) and Figure 4-2. Under turbulent conditions, the unburned fuel is thrown more rapidly into contact with the flame than is the case when the explosion flame expands spherically in a laminar fashion. The increase in the rate of pressure rise and maximum pressure under turbulent conditions is a consequence of the increased rate of combustion  $d\xi/dt$ .

Published work on the effect of turbulence can be summarized as follows:

1) Turbulence can be created by fan, high ventilation rate, obstacles, sudden bursting of the diaphragm, etc.

2) Increase in turbulence level will result in a slight increase in the first pressure peak and in the bursting pressure of the diaphragm. However, the effect of turbulence on the bursting pressure of the diaphragm poses no threat to the integrity of the glovebox. If the bursting diaphragm can withstand a higher pressure under turbulence conditions, so can the other components.

3) Increase in turbulence level will result in a significant increase in the second-peak pressure. Results obtained from this study indicate that the turbulence induced by the sudden bursting of the diaphragm seems to be much higher than the effect that may be created by normal obstacles and air ventilation rate up to one air change per min. Under the test conditions carried out in this program, no significant increase in second peak due to obstacles and ventilation has been observed.

4) The effect of air ventilation has been studied in this program only for cubical configurations. In case of a large L/D ratio or long duct-shape glovebox, no significant increase in explosion pressure is expected if the air inside the glovebox is moving not too much higher than the burning speed of the mixture. For gases moving in a long L/D glovebox or duct work, the intensity of turbulence is related directly to the gas velocity and the scale of the cross-sectional area in the direction of the flow, or Reynolds number of the moving gas.

#### 5.2.5 Confining and Exhausting the Explosion Discharge

Discussion so far has been directed toward the development and relief of the explosion pressure from the glovebox. For AEC operations the explosion hazard cannot be said to be controlled until some means of confining and cleaning the exhaust gases released from the glovebox is provided.

Several possible methods can be considered for this purpose. The most convenient method is to exhaust the gases through the present or separate emergency ventilation systems, provided that the ventilation duct work is large enough to handle the large quantity of exhaust hot gas over a short period of time (less than one second) without overpressuring the ventilation duct works. The reason for this is that any pressure increase in the duct work will slow down the pressure relief performance and, therefore, an even higher explosion pressure will result inside the glovebox. For instance, the maximum volumetric expansion resulting from a combustion explosion inside a glovebox of  $V$  in volume, filled with hydrocarbon and air, is about  $8.2 V$ . For a 100 cu ft glovebox, about 50 percent of the expansion occurred during the latter period, indicated by a second pressure peak of less than 20 milliseconds. Therefore, the duct work should be sized at least large enough to handle about 20,000 cu ft per second of hot gas without appreciable increase in pressure. It seems indicated that exhaust of maximum explosion hazard from a glovebox through a long duct work is almost impossible.

One of the methods which may prove to be feasible, is to connect several individual gloveboxes to a large chamber through a minimum length of large duct work (larger than the cross-section of the diaphragm). In order to confine the maximum credible explosion discharge, this chamber has to be constructed to withstand the same pressure as the glovebox. To confine the explosion discharge from a glovebox of volume  $V$ , and not to cause serious increase in explosion pressure inside the glovebox, the volume ratio between the glovebox and the confining chamber  $V_c$  has to be larger than that indicated in Figure 4-1. For example, in order to confine the explosion discharge resulting from a bursting diaphragm which is designed to give a second-peak pressure of 3 psi one may consider the glovebox as a balloon of  $V_u(0) = V_1$ , exploded in a chamber of  $V = V_c + V_1$ .

For a maximum explosion pressure of 3 psi, Figure 4-1 shows that

$$\frac{V_u(0)}{V} = \frac{V_1}{V_c + V_1} = 0.0197 \quad (35)$$

$$\text{Therefore, } V_c = V_1 \left( \frac{1}{0.0197} \right)^{-1} = 49.1V_1 \quad (36)$$

The confining chamber has to be about 49 times larger than the volume of the glovebox.

However, as indicated in the theoretical calculations, over the period of the explosion approximately less than 1/3 of the mixture was actually burned; the remaining 2/3 was exhausted through the opening in the unburned state. If a suitable flame arrestor can be installed at the inside of the bursting diaphragm or sufficient dilution of the unburned gas occurs inside the confining chamber to prevent the continuous burning of the exhausted unburned gas inside the chamber, a chamber of  $49V_1/3 = 16.3V_1$ , 16.3 times larger than the glovebox volume, would be sufficient.

Obviously the volume requirement can be reduced considerably if sufficient filter area is provided for the chamber. As indicated in Figure 3-14, this confining chamber, 16.3 times larger than the glovebox volume, may prove to be adequate to confine the explosion discharge resulting from a bursting diaphragm which is designed to give a second-peak pressure of 1 psi, if a filter area of  $K = A/A_f = 20$  is provided on the wall of the confining chamber.

The confining chamber can be taken to be the form of an expandable space. The expandable space could be fabricated of 0.001-in. thick aluminum foil to which is bonded a thin, high-strength plastic such as Mylar. In case of explosion, the expandable confining chamber will expand from zero volume to a final volume  $V_c$ . For the explosion of hydrocarbon and air mixture, the final volume  $V_c$  should be 8.2 times larger than the glovebox volume. This expandable space could be installed directly on the glovebox and allowed to expand into the working area if sufficient space is available. If there is inadequate space in the work area, the device could be installed so that expansion would occur external to the structure.

Additional experimental and theoretical work in these areas is needed to verify the validity of the approaches proposed above.

#### 5.2.6 Design and Construction of Bursting Diaphragm Explosion Pressure Relief

In order to illustrate the use of the guidelines, described previously, a sample design computation for a 9 ft x 6 ft x 3 ft glovebox is presented. Assume the weakest component in this glovebox is the glove which has a static bursting pressure of 1 psi and dynamic bursting pressure of 2 psi. This glovebox is ventilated through two small 8-in. x 8-in. x 6-in. high-efficiency filter units at the rate of 1/2 air change per minute. The possible source of fuel is assumed to be leakage of propane gas inside the glovebox at



several most unfavorable locations. Since we cannot predetermine the location of the leaks, it is not possible to apply the protection procedure described in Section 5.1. The design procedure for bursting diaphragm explosion pressure relief is illustrated as follows:

Calculation:

Assume the explosion reaction is a homogeneous mixing of propane and air with ideal gas behavior under stoichiometric and adiabatic conditions. In the reaction



the average molecular weight of the unburned mixture is

$$M_u = \frac{1}{24.81} \times 44 + \frac{5}{24.81} \times 32 + \frac{18.81}{24.81} \times 28 = 29.4$$

the average molecular weight of the burned mixture is

$$M_b = \frac{3}{25.81} \times 44 + \frac{4}{25.81} \times 18 + \frac{18.81}{25.81} \times 28 = 28.3$$

1) Mass Density of Burned and Unburned Mixtures

Based on the ideal gas law, one lb-mole of this gas mixture occupies 359 ft<sup>3</sup> in volume. Therefore, the mass density of the unburned mixture at the standard atmospheric condition (14.7 psi and 293°K) is

$$\rho_u(0) = \left( \frac{29.42}{359} \right) \left( \frac{1}{32.3} \right) \left( \frac{273}{293} \right) = 0.00246 \frac{\text{lb sec}^2}{\text{ft}^4}$$

and the mass density of the burned mixture at the theoretical adiabatic flame temperature of 2265°K (11) is

$$\rho_b(0) = \left( \frac{28.3}{359} \right) \left( \frac{1}{32.2} \right) \left( \frac{273}{2265} \right) = 0.000295 \frac{\text{lb sec}^2}{\text{ft}^4}$$

2) Venting Parameter

From Equation (34)

$$\alpha_G = \frac{C}{S_{uK}} \left( \frac{P(0)}{\rho_u(0)} \right)^{1/2} \left( \frac{\rho_b(0)}{\rho_u(0)} \right)^{7/6}$$

Where

$$C = 0.6$$

$$S_u = 48 \text{ cm/sec} = 1.57 \text{ ft/sec}$$

$$P(0) = 14.7 \text{ psi} = 2119 \text{ lb/ft}^2$$

$$\rho_u(0) = 0.00246 \text{ lb sec}^2/\text{ft}^4$$

$$\rho_u(0) = 0.000295 \text{ lb sec}^2/\text{ft}^4$$

$$K = \frac{A}{A_v}$$

Therefore,

$$\alpha_G = \frac{0.6}{1.574K} \left( \frac{2119}{0.00246} \right)^{1/2} \left( \frac{0.000295}{0.00246} \right)^{7/6} = \frac{30}{K}$$

At maximum pressure of 2 psi we find from Figure 5-4 for  $x=3$ ,  $\alpha_G = 15.5$

Therefore,

$$K = \frac{30}{15.5} = 1.94$$

In case the K factor approaches 1, then, a cut-and-try method of computation with a larger C value should be used.

### 3) Vent Area and Vent Location

Vent opening should be located on the wall which has smaller cross-sectional area and not facing the working area. It is, therefore, desirable to position the opening on one of the 6 ft x 3 ft walls. For a vent area factor of  $K = 1.94$ , the vent area

$$A_v = \frac{A}{K} = \frac{6 \times 3}{1.94} = 9.3 \text{ ft}^2$$

Diameter of the diaphragm

$$d = 41.3 \text{ in.}$$

### 4) Bursting Pressure of the Diaphragm

The static bursting pressure of a 0.001-in. thick soft aluminum diaphragm can be estimated by substituting the following values into Equations (31), (32) and (33).

$$\sigma_d = 13.3 \times 10^3 \text{ lb/in}^2 \quad \epsilon = 0.3$$

$$E = 9 \times 10^6 \text{ lb/in}^2 \quad \delta = 0.001 \text{ inch}$$

$$d = 41.3 \text{ inches}$$

$$y = \frac{13.3 \times 10^3 \times (41.3)^2}{4 \times 0.976 \times 9 \times 10^6} = 0.762 \text{ inches}$$

$$\sigma_b = \frac{4 \times 9 \times 10^6 \times (0.001)^2}{(41.3)^2} \left[ \frac{2}{1-0.3} \left( \frac{0.762}{0.001} \right) + \frac{1}{2} \left( \frac{0.762}{0.001} \right)^2 \right] = 6,500 \text{ lb/in}^2$$

$$p_b = \frac{4 \times 0.001 \times 6,500}{41.3} = 0.63 \text{ lb/in}^2$$

The static bursting pressure (first pressure peak) can be estimated also from Figure 5-4 as 0.37 and 0.45 psi. The estimated values for the static bursting pressure are much lower than the static bursting limit of 1 psi; the estimated vent area of  $A_v = 9.3$  sq ft is considered as acceptable.

#### 5) Confining and Exhausting the Explosion Discharge

The volume of the explosion discharge confining chamber can be estimated from Equation (8) (or Figure 4-1) as

$$\frac{V_u(0)}{V} = \left( \frac{1}{1.4} \right)^{\frac{1-1.4}{1.4}} \left/ \left( \frac{28.3}{29.4} \frac{2265}{293} \left( \frac{14.7+2}{14.7} \right)^{\frac{1-1.4}{1.4}} - 1 \right) \right. = 0.0144$$

Using Equations (35) and (36) and letting  $V_1 = V_u(0) = 162 \text{ ft}^3$ , we obtain the volume of the confining chamber.

$$V_c = V_1 \left( \frac{1}{0.0144} - 1 \right) = 68.5 \times 162 = 11,100 \text{ ft}^3$$

As described in Section 5.2.5, about 2/3 of the unburned gas mixture which was exhausted from the glovebox before the flame front approached the opening, may be diluted to a state that cannot be burned. It is anticipated that the confining chamber would be designed at about 3000  $\text{ft}^3$ , if sufficient filter units are provided on the confining chamber. Further experimental investigation in this area is recommended.

6) Construction

A proposed method of bursting diaphragm construction is to hold the thin diaphragm on the outside wall of the glovebox by metal flange and gaskets. The inside of the diaphragm can be firmly supported by a fiber glass mat and metal grill of not more than 10 percent in metal area. In order to protect the diaphragm from outside puncture, a lightweight hinged door is recommended.

In case a thicker or stronger diaphragm is necessary, the opening of the vent can be expedited or bursting pressure of the diaphragm can be reduced by installing a diaphragm cutter at the outside of the diaphragm.

## VI

RECOMMENDATIONS FOR FURTHER STUDY

To extend application of the results obtained in this phase of the study program, the following work areas are recommended for further investigation and experimentation.

- 1) Experimental study of explosion venting with filter wall.
- 2) Investigation of other venting methods, such as blowout panels and hinged doors.
- 3) Investigation of methods of containing and exhausting the explosion discharge.
- 4) Detail engineering design and full-scale demonstration under various practical operating conditions.
- 5) Dynamic response of gloves, windows and other components.
- 6) Fundamental study of the explosion venting mechanism to determine the exact cause of the x factor and the prolonged burning time in comparison with the theoretical value.

## VII

NOMENCLATURE

a	Equivalent radius of the vessel or glovebox.
A	Cross-section area of side containing the vent.
$A_v$	Vent Area.
$A_F$	Cross-Sectional area of the filter unit.
B	Constant.
C	Orifice discharge coefficient.
$C_1C_2$	Filter constants.
D	Diameter or characteristic length dimension of the short surface of a chamber.
d	Diameter of the diaphragm.
$d_f$	Diameter of the filter fibers.
E	Young's Modulus.
F	Correction factor for equivalent area of filter in relation to free opening.
$f_1f_2$	Functions.
K	Vent area factor $K = A/A_v$ .
k	Constant.
L	Characteristic length, dimension of the long surface of a chamber.
$M_u$	Effective unburned gas molecular weight.
$M_b$	Effective burned gas molecular weight.
$m_0$	Initial mass of the gas mixture.
$m_{rb}$	Mass of the burned gas mixture remaining in the chamber.
$m_{ru}$	Mass of the unburned gas mixture remaining in the chamber.
$m_{lb}$	Mass of the burned gas mixture which has left the chamber.
$m_{lu}$	Mass of the unburned gas mixture which has left the chamber.
$N_{Re}$	Reynolds number.

$n_b$	Number of moles of the unburned gas.
$n_u$	Number of moles of the burned gas.
$P$	Pressure, absolute.
$P(o)$	Initial pressure, absolute.
$P(t)$	Pressure at time $t$ , absolute.
$P(e)$	Pressure at the end of the combustion process, absolute.
$P(m)$	Maximum explosion pressure in a closed vessel, absolute.
$P_b$	Bursting pressure of the diaphragm, psi.
$p$	Pressure, psi or psf.
$P_1$	First pressure peak, psi.
$P_2$	Second pressure peak, psi.
$R$	Universal gas constant.
$r_b$	Radius of the spherically propagated combustion wave.
$S_u$	Burning velocity.
$S'_u$	Burning velocity at standard condition.
$S_b$	Flame speed.
$T_u, T_b$	Absolute temperature; $T_u$ for unburned gas; $T_b$ for burned gas.
$t$	Time.
$V$	Volume of a chamber or glovebox.
$V_u(o)$	Volume of the unburned gas mixture at initial or balloon volume.
$V_b(e)$	Volume of the burned gas at the end of the combustion process.
$v'$	Actual face velocity across the filter media surface.
$v_s$	Superficial velocity based on the cross-sectional area of the filter unit.
$X$	Turbulence correction factor.
$Y$	Maximum deflection at the center of the diaphragm.
$z$	Void Fraction.

- $\alpha_F$  Filter explosion venting parameter, see Equation (30).
- $\alpha$  Explosion venting parameter for spherical vessel, see Equation (16).
- $\alpha_G$  Explosion venting parameter modified for cubical and non-cubical gloveboxes, see Equation (34).
- $\beta$  Exponent indicating dependence of burning velocity on pressure.
- $\gamma$  Adiabatic index, = 1.4 for air.
- $\delta$  Thickness of the diaphragm.
- $\epsilon$  Poisson ratio.
- $\zeta$  Dimensionless pressure ratio,  $P(t)/P(o)$ .
- $\lambda$  Dimensionless unburned gas remaining,  $m_{ru}/m_o$ , see Equation (18)
- $\mu$  Viscosity
- $\xi$  Dimensionless burned gas remaining,  $m_{rb}/m_o$ , see Equation (17)
- $\rho_u$  Density of the unburned gas,  $\text{lb sec}^2/\text{ft}^4$ ,  $\text{slug}/\text{ft}^3$ ,  $\rho_u(o)$  is that at the initial condition.
- $\rho_b$  Density of the burned gas,  $\text{lb sec}^2/\text{ft}^4$ ,  $\text{slug}/\text{ft}^3$ .
- $\sigma$  Expansion ratio,  $\sigma = P(m)/P(o)$ .
- $\sigma_b$  Bursting strength of the diaphragm.
- $\sigma_d$  Ultimate strength of the diaphragm material.
- $\psi_u$  Fraction of the total exit area,  $A_v$ , through which unburned gas flows.
- $\psi_b$  Fraction of the total exit area,  $A_v$ , through which burned gas flows.
- $\omega$  Mass burning speed,  $\omega = \rho_u(o)gS_u$
- $\tau$  Dimensionless time, see Equation (15).
- $v$  Dimensionless density, see Equation (19)
- (o), (t), (e), (m) Represent the time element; initial, anytime t, and end of the combustion process.
- Suffix u, b Represent the unburned and burned gases.



## VIII

REFERENCES

1. "Glovebox Fire Safety, A Guide for Safe Practices in Design, Protection and Operation" Prepared by Factory Mutual Research Corporation for United States Atomic Energy Commission, 1967.
2. Gibbs, G.J., and Calcote, H.F., "Effect of Molecular Structure on Burning Velocity" J. Chem. Eng. Data, V.5, pp. 226-237, 1959.
3. Linnett, J.W. "Methods of Measuring Burning Velocities" 4th Symp. (International) on Combustion. Williams & Wilkins Co., Baltimore, Md., pp. 20-35, 1953.
4. Zabetakis, M.G., "Flammability Characteristics of Combustible Gases and Vapors" Bulletin 627, Bureau of Mines, U.S. Department of the Interior, 1965.
5. Lewis, B., and von Elbe, G. "Combustion Flames and Explosion of Gases" 2nd Edition, Academic Press Inc., 1961.
6. Nagy, J., Conn, J.W., and Verakis, H.C. "Explosion Development in a Spherical Vessel" U.S. Department of the Interior, Bureau of Mines, 1969, Report of Investigations 7279
7. Maisey, H.R. "Gaseous and Dust Explosion Venting" Part 1. Chemical and Process Engineering, October 1965.
8. Cousins, E.W. and Cotton, P.E. "The Protection of Closed Vessels Against Internal Explosion" Trans. ASME Paper s-1-PRI 2, 1951.
9. Harris, G.F.P. "The Effect of Vessel Size and Degree of Turbulence on Gas Phase Explosion Pressure in Closed Vessels" Combustion and Flame, 11, 17, 1967.
10. "Explosion Venting" NFPA No. 68, National Fire Protection Association, 1954.
11. Steffensen, R.J., Agnew, J.T. and Olson, R.A. "Tables for Adiabatic Gas Temperature and Equilibrium Composition of Six Hydrocarbons" Engineering Extension Series No. 122, Engineering Bulletin of Purdue University, Vol. 2 No. 3, May 1966.
12. Benson, R.S.F., Burgoyne, J.H. "Crankcase Explosions in Marine Engines" The British Shipbuilding Research Association, Report No. 76, R.B. 629, 1951.
13. Jones, H. "Coal Dust Explosion in Completely Closed Rooms" Ministry of Supply Advisory Council of Scientific Research & Technical Development, Explosion Research Committee, Jan. 12, 1943.

14. Palmer, K.N. and Rogowski "The Use of Flame Arresters for Protection of Enclosed Equipment in Propane-Air Atmospheres" I Chem. E. Symposium Series No. 25, Instn. Chem. Engrs. London, 1968.
15. Bird, R.B. et al "Transport Phenomena" John Wiley & Sons Inc., pp. 196, 1960.
16. Chen, C.Y. "Filtration of Aerosol by Fibrous Media" Chemical Reviews, Vol. 55, No. 3 pp. 595, June 1955.
17. Simmonds, W.A. & Cabbage, P.A. "The Design of Explosion Reliefs for Industrial Drying Ovens" Symposium on Chemical Process Hazards, Instn. Chem. Engrs. 1960.
18. Bonyun, M.E. "Protecting Pressure Vessels With Rupture Disks" Chemical & Metallurgical Engineer, Vol. 42. No. J, pp. 260, May 1935.
19. Juvinali, R.C. "Engineering Considerations of Stress, Strain and Strength" pp. 169-174, McGraw Hill, 1967.
20. Roark, R.J. "Formulas for Stress and Strain" Third Edition, McGraw Hill, 1954.
21. Burgoyne, J.H. and Wilson, M.J.G. "The Relief of Pentane Vapor-Air Explosions in Vessels", Symposium on Chemical Process Hazards, Instn. Chem. Engrs. p. 25, 1960.
22. Harris, G.F.P. and Briscoe, P.G. "The Venting of Pentane Vapor-Air Explosions in a Large Vessel", Combustion and Flame, Vol. 11, 1967.
23. Rasbash, D.J. and Rogowski, Z.W. "Relief of Explosions in Duct Systems", Symposium on Chemical Process Hazards, Instn. Chem Engrs., 1960.
24. Rogowski, Z.W. and Rasbash, D.J. "Relief of Explosions in Propane-Air Mixtures Moving in a Straight Unobstructed Duct", Second Symposium on Chemical Process Hazards, Instn. Chem. Engrs., 1963.
25. Markstein, G.H., "Instability Phenomena in Combustion Waves", Fourth Symposium (International) on Combustion, p. 49, September 1952.
26. Rasbash, D.J. "Discussion of Papers Presented at The Third Session of Symposium on Chemical Process Hazards", Instn. Chem. Engrs., 1960.
27. Smith, J.B. "Explosion Pressures in Industrial Piping Systems" Proc. International Acetylene Assoc., New York, pp. 279-293, 1949.
28. Anderson, W.L. and Anderson, T. "Effect of Shock Overpressures on High Efficiency Filter Units", 9th Air Cleaning Conference, Boston, September 1966.

APPENDIX AMATHEMATICAL MODELING OF EXPLOSION VENTING  
INCLUDING FREE VENTING

A general mathematical model is developed describing explosions in glove boxes which are vented in a variety of different ways. The model is solved numerically on a computer for a wide class of venting conditions to predict the way in which venting conditions influence the explosions.

A-1 THE EXPLOSION PROCESS

Figure (A-1) shows a simplified diagram of the explosion process resulting from a central ignition of a homogeneous gas mixture. The explosion is treated as an outward propagating spherical flame front, even though there is some distortion due to gas efflux leaving the enclosure.

Conservation of mass for the entire enclosure provides

$$m_o = m_{rb}(t) + m_{ru}(t) + m_{lb}(t) + m_{lu}(t) \quad (A-1)$$

where

$m_o$  is the initial gas mass.

$m_{rb}(t)$  is the burnt gas remaining in enclosure.

$m_{ru}(t)$  is the unburnt gas remaining in enclosure.

$m_{lb}(t)$  is the burnt gas which has left enclosure.

$m_{lu}(t)$  is the unburnt gas which has left enclosure.

The relationship among the various mass flows is obtained by differentiating the above expression with respect to time.

Thus:

$$\frac{dm_{rb}}{dt} = - \left( \frac{dm_{ru}(t)}{dt} + \frac{dm_{lu}(t)}{dt} + \frac{dm_{lb}(t)}{dt} \right) \quad (A-2)$$

It is well known that the propagation speed  $S_u$  of a deflagration wave into an unburnt mixture depends only on the gas mixture, almost independent of pressure.

Thus, for a spherical wave of radius  $r_b$ , the rate of unburnt mass consumption within enclosure is

$$\frac{d(m_{ru} + m_{lu})}{dt} = - 4\pi r_b^2 S_u \rho_u(t) \quad (A-3)$$

where  $4\pi r_b^2$  is the sphere surface area and  $\rho_u(t)$  is the density of the unburnt gas in the enclosure. In the above equation all combustion taking place outside the enclosure is ignored.

16215.1

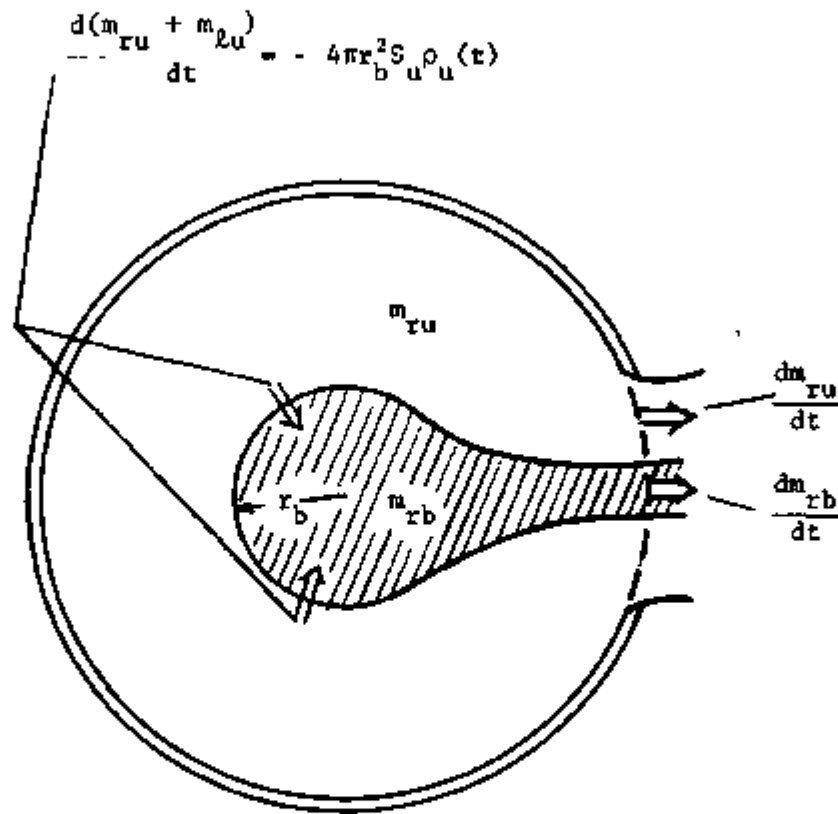


FIG. A-1 CONCEPTUAL MODEL OF THE EXPLOSION VENTING

The burnt sphere radius can be related to the burnt gas remaining in the enclosure,  $m_{rb}$ , by

$$m_{rb} = \frac{4\pi}{3} r_b^3 \rho_b(t) \quad (A-4)$$

or

$$r_b(t) = \left( \frac{3}{4\pi} \frac{m_{rb}(t)}{\rho_b(t)} \right)^{1/3} \quad (A-5)$$

where  $\rho_b(t)$  is the spacial average of the burnt gas density.

Combining equations (A-2) (A-3) (A-4) and (A-5), we find:

$$\frac{dm_{rb}}{dt} = 4\pi\chi S_u \rho_u(t) \left( \frac{3}{4\pi} \frac{m_{rb}(t)}{\rho_b(t)} \right)^{2/3} - \frac{dm_{lb}}{dt} \quad (A-6)$$

and

$$\frac{dm_{ru}}{dt} = -4\pi\chi S_u \rho_u(t) \left( \frac{3}{4\pi} \frac{m_{rb}(t)}{\rho_b(t)} \right)^{2/3} - \frac{dm_{lu}}{dt} \quad (A-7)$$

The constant  $\chi$  multiplying  $S_u$  above is a factor which describes the effect of: increased burning rate due to gas turbulence; and of increased flame area due to a non spherical flame. The effect of this factor on explosion intensity is explored in all solutions.

The above two equations can be solved, once one knows the pressure, as well as the rate that burnt and unburnt gases leave the enclosure. Section 2 provides a differential equation for the pressure response.

## A-2 PRESSURE RESPONSE AND ADIABATIC COMPRESSION

It is necessary to determine how the combustion increases the pressure in the chamber, since it is this increased pressure which drives the gas out of

## FACTORY MUTUAL RESEARCH CORPORATION

the enclosure.

In this model, the pressure is regarded as uniform throughout the enclosure. This assumption is valid if the gas velocities within the enclosure are much less than the speed of sound.

Initially the enclosure contains only unburnt gas at ambient temperature  $T_u(0)$  and pressure  $P(0)$ . The equation of state provides

$$P(0)V = \frac{m_o}{M_u} RT_u(0),$$

where  $V$  is the enclosure volume;  $M_u$ , the effective unburnt gas molecular weight; and  $R$ , the universal gas constant.

At a later time,  $t$ , the burnt gas must also be considered; thus,

$$P(t)V = \frac{m_{rb}(t)}{M_b} RT_b(t) + \frac{m_{ru}(t)}{M_u} RT_u(t)$$

where  $T_b(t)$  is the space averaged burnt gas temperature.

The ratio of these two equations provides

$$\frac{P(t)}{P(0)} \frac{T_u(0)}{T_u(t)} = \frac{m_{rb}(t)M_u T_b(t)}{m_o M_b T_u(t)} + \frac{m_{ru}(t)}{m_o}$$

or in terms of density

$$\frac{P(t)}{P(0)} \frac{T_u(0)}{T_u(t)} = \frac{m_{rb}(t)}{m_o} \frac{\rho_u(t)}{\rho_b(t)} + \frac{m_{ru}(t)}{m_o}$$

For adiabatic compression of the unburnt gas

$$\frac{P(t)}{P(0)} = \left( \frac{\rho_u(t)}{\rho_u(0)} \right)^{\gamma_u}$$

or

$$\frac{P(t)}{P(0)} \cdot \frac{T_u(0)}{T_u(t)} = \frac{P(t)}{P(0)} \cdot \left[ \frac{P(0)}{P(t)} \cdot \frac{\rho_u(t)}{\rho_u(0)} \right] = \left( \frac{P(t)}{P(0)} \right)^{1/\gamma_u}$$

which combines with state equation as

$$\left(\frac{P(t)}{P(0)}\right)^{1/\gamma_u} = \frac{m_{rb}(t)}{m_o} \frac{\rho_u(t)}{\rho_b(t)} + \frac{m_{ru}(t)}{m_o} \quad (A-8)$$

At this point we shall assume that the burnt gas also behaves as a simple adiabatic compressed gas. That is, we shall assume that

$$\frac{P(t)}{P(0)} = \left(\frac{\rho_b(t)}{\rho_b(0)}\right)^{1/\gamma_b} \quad (A-9)$$

with  $\gamma_b = \gamma_u = \gamma$ . This assumption is not strictly valid, because, as the gas is compressed, the temperature of the burnt gas behind the combustion wave is not uniform in space, since the combustion is taking place at different pressures<sup>(5)</sup>. However, this assumption is approximately valid for small pressure variations and avoids the necessity of considering partial differential equations. Thus with

$$\frac{\rho_u(t)}{\rho_b(t)} = \left(\frac{P(t)}{P(0)}\right)^{1/\gamma - 1/\gamma} \frac{\rho_u(0)}{\rho_b(0)} = \frac{\rho_u(0)}{\rho_b(0)}$$

The pressure equation (A-8) becomes

$$\left(\frac{P(t)}{P(0)}\right)^{1/\gamma} = \frac{m_{rb}(t)}{m_o} \frac{\rho_u(0)}{\rho_b(0)} + \frac{m_{ru}(t)}{m_o} \quad (A-10)$$

or differentiating with respect to time

$$\frac{d}{dt} \left(\frac{P(t)}{P(0)}\right) = \gamma \left(\frac{P(t)}{P(0)}\right)^{1-1/\gamma} \left\{ \frac{\rho_u(0)}{\rho_b(0)} \frac{d}{dt} \left(\frac{m_{rb}(t)}{m_o}\right) + \frac{d}{dt} \left(\frac{m_{ru}(t)}{m_o}\right) \right\}$$

Combining this equation with equations (A-6) and (A-7) one obtains (with

$$\rho_u(t)/\rho_b^{2/3}(t) = \rho_u(0)/\rho_b^{2/3}(0) (P(t)/P(0))^{1/3},$$



## FACTORY MUTUAL RESEARCH CORPORATION

$$\frac{d}{dt} \left( \frac{P(t)}{P(0)} \right) = \gamma \left( \frac{P(t)}{P(0)} \right)^{1-1/\gamma} \left\{ \left( \frac{\rho_u(0)}{\rho_b(0)} - 1 \right) \frac{4\pi\chi S_u \rho_u(0)}{\rho_b^{2/3}(0)} \left( \frac{P(t)}{P(0)} \right)^{1/3\gamma} \left( \frac{3m_{rb}}{4\pi} \right)^{2/3} - \frac{\rho_u(0)}{\rho_b(0)} \frac{d}{dt} \left( \frac{m_{lb}}{m_o} \right) - \frac{d}{dt} \left( \frac{m_{lu}}{dt} \right) \right\} \quad (A-11)$$

The above equation relates the pressure response in terms of the mass flows. It remains now to formulate the venting mass flow equations.

A-3. VENTING CONDITIONS

Section 3.1 calculates the mass flow of burnt and unburnt gas leaving the enclosure through an orifice that bursts open after the pressure rises to its bursting pressure  $P_b$ . This formulation also applies to the free venting case by setting  $P_b = P(0)$ , that is, the burst occurs at or before ignition. The second part of this section calculates the mass flow through a filter which is assumed to be always open.

## A-3.1 FREE-VENT

For isentropic flow of a compressible gas one has

$$\frac{v^2}{2} + \frac{\gamma}{\gamma-1} \frac{P}{\rho} = \frac{\gamma}{\gamma-1} \frac{P_{res}}{\rho_{res}}$$

where  $P_{res}$  and  $\rho_{res}$  are the gas pressure and gas density in the reservoir where the gas is regarded as stagnant.

If  $V_1$  is the velocity of the gas at the orifice of area  $A_1$ , then

$$\frac{dm}{dt} = CA_1 \rho_1 V_1 = CA_1 \rho_1 \sqrt{\frac{2\gamma}{\gamma-1} \frac{P_{res}}{\rho_{res}} \left( 1 - \frac{P_1 \rho_{res}}{P_{res} \rho_1} \right)}$$

The 'Vena Contracts' constant  $C = 0.6$  corrects for the fact that the gas efflux jet contracts to 0.6 of the sharp-edged orifice some distance downstream of the orifice.

Using the adiabatic expression

$$\rho_1 = \rho_{\text{res}} \left( \frac{P_1}{P_{\text{res}}} \right)^{1/\gamma}$$

we find

$$\frac{dm}{dt} = CA_1 \rho_{\text{res}} \left( \frac{P_1}{P_{\text{res}}} \right)^{1/\gamma} \sqrt{\frac{2\gamma}{(\gamma-1)} \frac{P_{\text{res}}}{\rho_{\text{res}}} \left[ 1 - \left( \frac{P_1}{P_{\text{res}}} \right)^{1-1/\gamma} \right]}$$

or rearranging

$$\frac{dm}{dt} = CA_1 \sqrt{\frac{2\gamma}{(\gamma-1)} \rho_{\text{res}} P_{\text{res}}} \left( \frac{P_1}{P_{\text{res}}} \right)^{1+1/\gamma} \sqrt{\left( \frac{P_{\text{res}}}{P_1} \right)^{\frac{\gamma-1}{\gamma}} - 1}$$

This equation is applied to both the burnt and unburnt gases.

For the burnt gas  $P_{\text{res}} = P(t)$ ,  $P_1 = P(0)$ , and

$$\rho_{\text{res}} = \rho_b(t) = \rho_b(0) \left( \frac{P(t)}{P(0)} \right)^{1/\gamma}$$

which yields

$$\frac{dm_{\text{lb}}}{dt} = CA_v \psi_b \sqrt{\frac{2\gamma}{\gamma-1} \rho_b(0) P(0)} \sqrt{\left( \frac{P(t)}{P(0)} \right)^{\frac{\gamma-1}{\gamma}} - 1} \quad (\text{A-12})$$

where  $\psi_b$  is the fraction of the total exit area,  $A_1 = A_v$ , through which burnt gases flow.

Similarly for the unburnt gases  $P_{\text{res}} = P(t)$ ,  $P_1 = P(0)$ , and

$$\rho_{\text{res}} = \rho_u(t) = \rho_u(0) \left( \frac{P(t)}{P(0)} \right)^{1/\gamma}$$

which yields

$$\frac{dm_{\ell u}}{dt} = C_A \psi_u \sqrt{\frac{2\gamma}{\gamma-1} \rho_u(0) P(0)} \sqrt{\frac{P(t)}{P(0)} \frac{\gamma-1}{\gamma} - 1} \quad (\text{A-13})$$

where  $\psi_u = 1 - \psi_b$  is the unburnt exit area fraction.

### A-3.2 FILTER VENTING

As shown in Section 2.3 of this report, a laminar gas flowing through a filter can be described by Poiseuille flow, that is,

$$\frac{dm}{dt} = C_1 A_F D \frac{(P(t) - P(0))}{\mu}$$

where  $C_1$  is the filter constant having units of (1/length),  $A_F$  is the filter area, and  $\rho$  is the gas density. The dynamic gas viscosity,  $\mu$ , is independent of pressure; however, it is approximately proportional to temperature.

For unburnt gas, we find, therefore,

$$\frac{dm_{\ell u}}{dt} = C_1 \psi_u A_F \frac{\rho_u(t) T_u(0)}{\mu(0) T_u(t)} (P(t) - P(0))$$

or

$$\frac{dm_{\ell u}}{dt} = C_1 \psi_u A_F \frac{\rho_u(0)}{\mu(0)} P(0) \left( \frac{P(t)}{P(0)} \right)^{\frac{2-\gamma}{\gamma}} \left( \frac{P(t)}{P(0)} - 1 \right), \quad (\text{A-14})$$

assuming that the temperature of the unburnt gas flowing through the filter is identical to the unburnt gas in the enclosure. Here again  $\psi_u$  is the fraction of the filter exit area through which unburnt gas flows.

Similarly for burnt gas, we find

$$\frac{dm_{\ell b}}{dt} = C_1 \psi_b A_F \frac{\rho_b(t) T_b(0)}{\mu(0) T_b(t)} (P(t) - P(0))$$

assuming that  $\mu$  does not depend on the type of gas, and only on its temperature.

Now, assuming  $M_u = M_b$ , we find

$$\frac{dm_{rb}}{dt} = C_1 \psi_b A_F \frac{\rho_u(0)P(0)}{\mu(0)} \left( \frac{\rho_b(0)}{\rho_u(0)} \right)^2 \left( \frac{P(t)}{P(0)} \right)^{\frac{2-\gamma}{\gamma}} \left( \frac{P(t)}{P(0)} - 1 \right) \quad (A-15)$$

#### A-4. GOVERNING EQUATIONS

This section summarizes the equations and transforms them into dimensionless form, so that they can be conveniently solved mathematically.

##### A-4.1 FREE-VENT AND BURSTING DIAPHRAGM

The differential equation (A-11) for the pressure response can be combined with the venting equations (A-12) and (A-13) and the adiabatic relation (A-9)

$$\frac{d}{dt} \left( \frac{P(t)}{P(0)} \right) = \gamma \left( \frac{P(t)}{P(0)} \right)^{1-1/\gamma} \left\{ \left[ \frac{\rho_u(0)}{\rho_b(0)} - 1 \right] \frac{4\pi\chi S_u \rho_u(0)}{\rho_b^{2/3}(0)} \left( \frac{P(t)}{P(0)} \right)^{1/3\gamma} \left( \frac{3m_{rb}(t)}{4\pi} \right)^{2/3} - \left[ \left( \frac{\rho_u(0)}{\rho_b(0)} \right)^{1/2} \psi_b + \psi_u \frac{CA_v}{m_o} \sqrt{\frac{\nu\gamma\rho_u(0)P(0)}{\gamma-1}} \sqrt{\left( \frac{P(t)}{P(0)} \right)^{\frac{\gamma-1}{\gamma}} - 1} \right] \right\} \quad (A-16)$$

This equation provides the change in pressure as a function of pressure and burnt gas remaining  $m_{rb}(t)$ . To solve this equation, we also need an equation for  $m_{rb}(t)$  which can be obtained by combining equation (A-6) and (A-12),

$$\frac{d}{dt} \left( \frac{m_{rb}}{m_o} \right) = \frac{4\pi\chi S_u \rho_u(0)}{\rho_b^{2/3}(0) m_o} \left( \frac{P(t)}{P(0)} \right)^{1/3\gamma} \left( \frac{3m_{rb}}{4\pi} \right)^{2/3} - \frac{CA_v \psi_b}{m_o} \sqrt{\frac{\nu\gamma}{\gamma-1}} \rho_b(0) P(0) \sqrt{\left( \frac{P(t)}{P(0)} \right)^{\frac{\gamma-1}{\gamma}} - 1} \quad (A-17)$$

These two equations are sufficient to describe the burning process. Before they are solved it is highly desirable to express them in dimensionless form so that the governing parameters or scaling factors can be displayed.

Define 1) A Dimensionless time  $\tau$  as

$$\tau = \frac{t S_u}{a} \left( \frac{\rho_u(0)}{\rho_b(0)} \right)^{2/3},$$

2) A Dimensionless orifice coefficient,  $\alpha$ , as

$$\alpha = \frac{2 C A v_a}{S_u m_o} \left( \frac{\rho_b(0)}{\rho_u(0)} \right)^{7/6} (\rho_u(0) P(0))^{1/2},$$

3) A Dimensionless burnt gas remaining,  $\xi$ , as

$$\xi = \frac{m_{rb}}{m_o},$$

4) A Dimensionless pressure as

$$\zeta = \frac{P(t)}{P(0)},$$

finally, 5) A Dimensionless density ratio,  $\nu$ , as

$$\nu = \frac{\rho_u(0)}{\rho_b(0)}.$$

In terms of these parameters and variables, the pressure equation (A-16) becomes

$$\frac{d\zeta}{d\tau} = 3\gamma(\nu-1)\chi\zeta^{\frac{3\gamma-2}{3\gamma}} \xi^{2/3} - (\nu\psi_b + \nu^2\psi_u)\gamma\zeta^{\frac{\gamma-1}{\gamma}} \alpha \sqrt{\frac{\gamma}{\gamma-1} (\zeta^{\frac{\gamma-1}{\gamma}} - 1)} \quad (A-18)$$

and the dimensionless burnt gas remaining equation (A-17) becomes

$$\frac{d\xi}{d\tau} = 3\chi\zeta^{1/3\gamma} \xi^{2/3} - \psi_b \alpha \sqrt{\frac{\gamma}{\gamma-1} (\zeta^{\frac{\gamma-1}{\gamma}} - 1)} \quad (A-19)$$

The equations for the other mass flows are similar.

The initial conditions for the explosion are quite simple:  $\zeta = \frac{P}{P(0)} = 1$ ; and  $\xi = \frac{m_{rb}}{m_o}$ , some very small number ( $\ll 1$ ) which simulates the ignition source.

For the case of bursting diaphragm venting, the venting parameter  $\alpha$  is set

to zero until the pressure reaches the diaphragm burst pressure, since no gas is permitted to escape from the enclosure; after the burst of the diaphragm, gas escapes according to the above formulas.

Experimentally, it is quite difficult to determine the exact proportion of burnt and unburnt gases escaping. Therefore, several different values of  $\psi_u$  and  $\psi_b = 1 - \psi_u$  have been used. These theoretical results give reasonable agreement for experiment for  $\psi_u = 1$ ,  $\psi_b = 0$ . The results for these various cases are discussed in section 4.2.1 of this report.

#### A-4.2 FILTER VENTING EQUATIONS

The differential equation (A-11) for pressure response can be combined with the venting equations (A-14) and (A-15) to obtain,

$$\frac{d}{dt} \left( \frac{P(t)}{P(0)} \right) = \gamma \left( \frac{P(t)}{P(0)} \right)^{1-1/\gamma} \left\{ \left( \frac{\rho_u(0)}{\rho_b(0)} - 1 \right) \frac{4\pi\chi S_u \rho_u(0)}{\rho_b^{2/3}} \left( \frac{P(t)}{P(0)} \right)^{1/3\gamma} \left( \frac{3m_{rb}(t)}{4\pi} \right)^{2/3} - \left( \psi_b \frac{\rho_b(0)}{\rho_u(0)} + \psi_u \right) \frac{C_1 A_F \rho_u(0) P(0)}{\mu(0) m_o} \left( \frac{P(t)}{P(0)} \right)^{\frac{2-\gamma}{\gamma}} \left( \frac{P(t)}{P(0)} - 1 \right) \right\}$$

This equation can be converted to its dimensionless form by defining a dimensionless filter coefficient,  $\alpha_F$ , as

$$\alpha_F = \frac{C_1 A_F \rho_u(0) P(0)}{S_u \mu(0) m_o} \left( \frac{\rho_b(0)}{\rho_u(0)} \right)^{5/3}$$

The above pressure response equation becomes

$$\frac{d\zeta}{d\tau} = 3\gamma(\nu-1)\chi\zeta^{\frac{3\gamma-2}{3\gamma}}\xi^{2/3} - (\psi_b + \nu\psi_u)\gamma\alpha_F\zeta^{1/\gamma}(\zeta-1) \quad (A-20)$$

Similarly, the equation (A-6) for burnt gas remaining combines with the filter equation (A-15)

$$\frac{d\xi}{d\tau} = 3\gamma(\nu-1)\chi\zeta^{1/3\gamma}\xi^{2/3} - \frac{\psi_b\alpha_F}{\nu}\zeta^{\frac{2-\gamma}{\gamma}}(\zeta-1) \quad (A-21)$$

These last two equations are sufficient to determine the pressure response.

#### A-5 NUMERICAL SOLUTION TECHNIQUE

The fourth order Runge-Kutta technique was employed in solving the simultaneous non-linear ordinary differential equations. A computer program was developed which is stable for all cases of engineering interest. The accuracy of the program is attested by the fact that all four forms of mass ( $m_{rb}$ ,  $m_{ru}$ ,  $m_{lb}$  and  $m_{lu}$ ) add up to  $m_o$ , even though they are computed from separate differential equations.

The program is set up in a general form so that a wide variety of engineering questions can be explored with a minimum of time and expense. Although any finding should be verified by experiment, this program has been and will be instrumental in suggesting which experiments are of particular practical importance.

APPENDIX BSUMMARY OF CURRENT SAFETY PRACTICES  
AT AEC GLOVEBOX FACILITIES

To avoid duplication of studies and considerations previously made by AEC and its contractors, the AEC, Chicago Operations Office, Safety and Technical Services Division, solicited information on the glovebox venting problem from all AEC glovebox facilities. The information received further substantiated the need to conduct tests and studies on glovebox explosion venting.

The following summary presents the information received from most of AEC's glovebox facilities on overpressurization control for gloveboxes:

1. To avoid an overpressure failure of glovebox containment in the direction of operating personnel, the operating side of the glovebox could be designed with a greater safety factor. Glove ports and other penetrations could be equipped with metal covers when not in use. A frangible or releasing panel could be installed on an unattended side of the glovebox. Most facilities depend on the following policies.
2. Gloveboxes are usually designed and tested to limit leakage, and to withstand specified positive and negative pressures up to 4 in. water gauge. Currently, there is no design criteria available which takes into consideration the containment of explosive forces in gloveboxes. Therefore, prevention of overpressure failures in gloveboxes has depended upon administrative controls. Most facilities have established operating limits and procedures which prohibit placing potentially explosive materials or unsafe quantities of flammable liquids in gloveboxes. Also, ignition sources can be eliminated, inert systems can be used, or increased ventilation can be provided. In addition, gloveboxes can be monitored for combustible gas mixtures, or for oxygen in the case of inert systems. Alarm instrumentation can be provided that will signal abnormal pressure conditions.
3. There are several methods used to handle overpressures that may develop:
  - 1) Mercoid switches are used to sense ordinary working overpressures on inert gas systems, to trip an exhaust valve, and to dump the inert gas. Dwyer switches are used on air systems to sense overpressures and to interrupt the electrical circuit which stops the air supply blower. On most systems, a liquid-filled bubbler is used through which overpressure can relieve itself to a duct system or to the atmosphere, whichever is applicable.
  - 2) The inlet and exhaust system filters on air systems are used to provide release for pressure. An automatic pressure-controlled emergency exhaust duct that has a capacity greater than the capacity of the pipe that supplies the gas is used on dry air and inert systems. Exhaust system blowers are installed with standbys and connected to an emergency power supply system.



- 3) A pressure relief device consisting of a large vinyl ball seated by gravity inside a vertically mounted plastic reducing coupling is installed to permit gases to bypass the scrubbing system and to go directly to the final large-size absolute filter.
  - 4) Open-leg manometers are used to relieve overpressures or underpressures on inert systems that could be caused by a malfunction of the system. Consideration is being given to a spring loaded panel which would open to relieve an overpressure condition.
  - 5) Solenoid valves on all services that might pressurize a box are activated by pressure switches. Ample-sized exhaust system capacity is provided to accommodate any additional gas volume generated by an explosion. Automatic valving (e.g., Maxitrol Series 210) is installed in parallel with the normal exhaust path to relieve excessive overpressure and/or vacuum that may develop.
  - 6) A separate purge ventilation system connected to each glovebox and equipped with a 10-inch butterfly damper (Keystone valve) is automatically controlled by a pressure switch. Pressurized equipment within gloveboxes is vented through pressure relief valves to the process air exhaust system.
4. From experience, implosions develop at a much slower rate than oxidation and decomposition explosions in gloveboxes. Therefore, conventional safeguards for underpressures are much easier to incorporate into gloveboxes. Since methods described above are considered satisfactory, further studies in the control of implosions in gloveboxes are not deemed essential at this time.

APPENDIX C

TABLES

SUMMARY OF TEST DATA

TABLE 1 - BALLOON EXPLOSION IN THE 27 FT<sup>3</sup> ALUMINUM CHAMBER

Test No.	$V_u(a)$	$V_u(a)/V$	Gas	Conc.	$P_1$	No. of Filters	No. of Gloves	Air Circ.
	$\times 10^{-2}, \text{ft}^3$	%						Rate
				Vol. %	Psi			CFM
A-1	3.54	0.131	C <sub>2</sub> H <sub>6</sub>	4	0.136	-	-	-
A-2	3.54	0.131	"	"	0.158	-	-	-
A-3	7.08	0.263	"	"	0.407	-	-	-
A-4	7.08	0.263	"	"	0.324	-	-	-
A-5	7.08	0.263	"	"	0.324	-	-	-
A-6	10.62	0.343	"	"	0.468	-	-	-
A-7	10.62	0.343	"	"	0.446	-	-	-
A-8	10.62	0.343	"	"	0.532	-	-	-
A-9	21.24	0.784	"	"	1.2	-	-	-
A-10	21.24	0.784	"	"	1.17	-	-	-
A-11	35.40	1.31	"	"	1.75	-	-	-
A-12	35.40	1.31	"	"	2.0	-	-	-
AA-120	53.1	1.97	"	"	3.43	-	-	-
AA-121	53.1	1.97	"	"	3.43	-	-	-

TABLE 2 - BALLOON EXPLOSION IN 24 FT<sup>3</sup> WOODEN GLOVEBOX

Test No.	$V_u(a)$	$V_u(a)/V$	Gas	Conc.	$P_1$	No. of Filters	No. of Gloves	Air Circ.
	$\times 10^{-2}, \text{ft}^3$	%						Rate
				Vol. %	Psi			CFM
W-1	3.54	0.127	C <sub>2</sub> H <sub>6</sub>	4	0.0376	1	-	-
W-2	7.08	0.295	"	"	0.101	1	-	-
W-3	10.62	0.442	"	"	0.137	1	-	-
W-4	21.24	0.884	"	"	0.36	1	-	-
W-5	31.86	1.775	"	"	0.576	1	-	-
W-6	42.5	2.36	"	"	1	1	-	-
W-7	3.54	0.148	"	"	0.056	2	-	-
W-8	7.08	0.295	"	"	0.056	2	-	-
W-9	10.62	0.442	"	"	0.101	2	-	-
W-10	21.24	0.884	"	"	0.32	2	-	-
W-11	42.5	1.775	"	"	0.525	2	-	-
W-21	21.24	0.884	"	"	0.245	2	2	48
W-22	31.86	1.325	"	"	0.294	2	2	"
W-23	42.5	1.775	"	"	0.613	2	2	"
W-24	53.1	2.21	"	"	0.784	2	2	"
W-25	63.75	2.65	"	"	0.710	2	2	"
W-26	74.34	3.1	"	"	0.784	2	2	"
W-27	85	3.53	"	"	1.35	2	2	"
W-28	99	3.98	"	"	1.715	2	2	"
W-21	21.24	0.884	"	"	0.294	2	-	24
W-42	31.86	1.325	"	"	0.416	2	-	"
W-43	42.5	1.775	"	"	0.66	2	-	"
W-44	53.1	2.21	"	"	1.08	2	-	"
W-45	63.75	2.65	"	"	1.225	2	-	"
W-46	63.75	2.65	"	"	1.08	2	-	"
W-47	74.34	3.1	"	"	1.45	2	-	"
W-48	74.34	3.1	"	"	1.59	2	-	"
W-49	85	3.53	"	"	1.45	2	-	"
W-50	85	3.53	"	"	1.96	2	-	"
W-57	53.1	2.21	"	"	0.905	2	2	0
W-58	53.1	"	"	"	0.605	2	1	0
W-59	53.1	"	"	"	0.735	2	2	0
W-60	53.1	"	"	"	0.785	2	2	0
W-61	53.1	"	"	"	0.77	2	2	24
W-62	53.1	"	"	"	0.66	2	2	24
W-63	53.1	"	"	"	0.66	2	2	36
W-64	53.1	"	"	"	0.92	2	2	36
W-65	53.1	"	"	"	0.905	2	2	36
W-66	53.1	"	"	"	0.81	2	2	48

TABLE 2 - CONTINUED

Test No.	$V_0(Q)$ $\times 10^{-2}, \text{ ft}^3$	$V_0(Q)/V$ $\Sigma$	Gas	Conc.	$P_1$ Feet	No. of Filters	No. of Discs	AEC Cate- gories
W-67	53.1	2.21	"	4	0.835	2	2	48
W-68	53.1	"	"	"	0.835	2	2	60
W-69	53.1	"	"	"	1.005	2	2	60
W-70	53.1	"	"	"	1.175	2	2	60
W-71	53.1	"	"	"	0.633	2	2	72
W-72	53.1	"	"	"	1.175	2	2	72
W-73	53.1	"	"	"	0.775	2	2	72
W-13	10.62	0.442	"	"	0.1842	2	2	70
W-14	21.24	0.890	"	"	0.2945	2	2	70
W-15	31.86	1.285	"	"	0.577	2	2	70
W-16	42.57	1.715	"	"	0.86	2	2	70
W-17	53.1	2.21	"	"	1.225	2	2	48
W-18	10.62	0.442	"	"	0.4906	2	2	48
W-19	21.24	0.894	"	"	0.269	2	2	48
W-20	31.86	1.335	"	"	0.491	2	2	48
W-21	42.57	1.775	"	"	0.803	2	2	48
W-22	53.1	2.21	"	"	0.906	2	2	48
W-23	63.75	2.65	"	"	1.17	2	2	48
W-24	21.24	0.894	"	"	0.417	2	2	34
W-25	31.86	1.325	"	"	1.15	2	2	24
W-26	42.5	1.715	"	"	1.10	2	2	24
W-27	53.1	2.21	"	"	1.385	2	2	24
W-28	31.86	1.325	"	"	0.858	2	2	24
W-29	63.75	2.65	"	"	1.187	2	2	24
W-75	21.24	0.894	"	"	0.392	2	2	24
W-76	21.24	0.894	"	"	0.416	2	2	24
W-77	31.86	1.335	"	"	0.493	2	2	24
W-78	31.86	1.325	"	"	0.612	2	2	24
W-79	31.86	1.325	"	"	0.62	2	2	24
W-80	33.1	2.21	"	"	0.892	2	2	24
W-81	53.1	2.21	"	"	0.906	2	2	24
W-82	21.24	0.894	"	"	0.392	2	2	24
W-83	53.1	2.21	"	"	0.506	2	2	24
W-84	62.5	1.775	"	"	0.715	2	2	24
W-85	42.5	1.775	"	"	0.71	2	2	24
W-86	21.24	0.894	"	"	0.367	2	2	24
W-87	21.24	0.894	"	"	0.392	2	2	48
W-88	21.24	0.894	"	"	0.441	2	2	48
W-89	21.24	0.894	"	"	0.441	2	2	48
W-90	31.86	1.325	"	"	0.488	2	2	48
W-91	31.86	1.325	"	"	0.637	2	2	48
W-92	21.24	0.894	"	"	0.808	2	2	48
W-93	21.24	0.894	"	"	0.392	2	2	48
W-94	31.86	1.325	"	"	0.612	2	2	48
W-95	42.5	1.775	"	"	1.01	2	2	48
W-96	42.5	1.775	"	"	0.96	2	2	48
W-97	42.5	1.775	"	"	0.784	2	2	48
W-98	53.1	2.21	"	"	0.908	2	2	48
W-99	53.1	2.21	"	"	0.710	2	2	48
W-100	53.1	2.21	"	"	1.02	2	2	48
W-101	53.1	2.21	"	"	1.12	2	2	48
W-102	53.1	2.21	"	"	1.05	2	2	48
W-103	21.24	0.894	"	"	0.394	2	2	60
W-104	31.86	1.325	"	"	0.579	2	2	60
W-105	42.5	1.775	"	"	0.637	2	2	60
W-106	53.1	2.21	"	"	1.02	2	2	60
W-107	42.5	1.775	"	"	0.612	2	2	60
W-108	35.4	1.475	"	"	0.588	2	2	60
W-109	31.86	1.325	"	"	0.583	2	2	72
W-110	21.24	0.894	"	"	0.882	2	2	72
W-111	21.24	0.894	"	"	0.295	2	2	0
W-112	21.24	0.894	"	"	0.245	2	2	0

Test No.	$V_0(\alpha)$	$V_0(\alpha)/V$	Gas	Conc.	$P_1$	No. of Filters	No. of Gloves	Air Circ.
	$\times 10^{-3}, \text{ft}^3$	Z						Rate
				Vol. X	Psi			CFM
M-113	21.24	0.884	$C_3H_8$	4	1.02	2	2	0
M-114	21.24	0.884	"	"	0.343	2	2	0
M-115	21.24	0.884	"	"	0.808	2	2	0
M-116	53.1	2.21	"	"	0.446	2	2	0
M-117	53.1	2.21	"	"	0.6125	2	2	0
M-118	63.75	2.65	"	"	1.15	2	2	0
M-119	74.34	3.1	"	"	0.955	2	2	0
M-120	74.34	3.1	"	"	1.445	2	2	0
M-121	85	3.55	"	"	1.2	2	2	0
M-122	85	3.55	"	"	1.4	2	2	0
M-123	99	4.15	"	"	1.52	2	2	0
M-124	99	4.15	"	"	1.62	2	2	0
M-125	99	4.15	"	"	1.6	2	2	0

TABLE 3 - FRASE-VENT VERSUS FILTER IN BALLOON EXPLOSION

Test No.	$V_0(\alpha)/V$	Gas	Gas Conc.	$P_1$	$T_1$	Frag-Vent Size	K Factor	No. of Filters	Comments
	Z								
AA-96	1.97	$C_3H_8$	4	1.08	76	65"x64"	30.675	-	-
AA-97	"	"	"	"	90	"	"	-	-
AA-98	"	"	"	1.20	76	"	"	-	-
AA-100	"	"	"	0.91	70	"	"	-	-
AA-101	"	"	"	1.13	76	"	"	-	-
AA-102	"	"	"	1.3	68	"	"	-	-
AA-105	"	"	"	2.26	85	5" dia.	66	-	-
AA-106	"	"	"	1.70	88	"	"	-	-
AA-107	"	"	"	1.70	80	"	"	-	-
AA-108	"	"	"	2.4	88	4" dia.	103.2	-	-
AA-109	"	"	"	1.87	-	"	"	-	-
AA-110	"	"	"	1.87	-	"	"	-	-
AA-111	"	"	"	2.23	-	"	"	-	-
AA-112	"	"	"	1.8	-	"	"	-	-
AA-113	"	"	"	2.31	-	3" dia.	183.45	-	-
AA-114	"	"	"	2.505	-	"	"	-	-
AA-128	"	"	"	2.31	-	"	"	-	-
AA-115	"	"	"	2.6	-	2" dia.	412.74	-	-
AA-116	"	"	"	3.12	-	"	"	-	-
AA-117	"	"	"	3.0	-	"	"	-	-
AA-118	"	"	"	3.4	-	1" dia.	165.1	-	-
AA-119	"	"	"	3.2	-	"	"	-	-
AA-167	"	"	"	0.71	-	2-64"x64" openings	15.1	-	Equivalence of one filter area
AA-168	"	"	"	0.71	-	"	"	-	"
AA-169	"	"	"	0.835	-	"	"	-	"
AA-165	"	"	"	0.64	-	3-64"x64" openings	10.23	-	Equivalence of three filter area
AA-166	"	"	"	0.64	-	"	"	-	"
AA-164	"	"	"	0.30	-	4-64"x64" openings	7.7	-	Equivalence of four filter area
AA-167	"	"	"	0	-	"	"	-	"
AA-146	"	"	"	2.31	-	"	30.675	1	-
AA-148	"	"	"	2.31	-	"	"	"	-
AA-150	"	"	"	2.38	-	"	"	"	-
AA-153	"	"	"	2.20	-	"	"	"	-
AA-154	"	"	"	2.46	-	"	"	"	-
AA-155	"	"	"	1.9	-	"	15.1	2	-
AA-156	"	"	"	2.1	-	"	"	"	-
AA-157	"	"	"	1.62	-	"	20.83	3	-
AA-158	"	"	"	1.33	-	"	"	"	-
AA-159	"	"	"	1.33	-	"	7.7	6	-
AA-160	"	"	"	1.35	-	"	"	"	-
AA-161	"	"	"	1.15	-	"	"	"	-
AA-162	"	"	"	1.15	-	"	"	"	-
AA-171	"	"	"	0.784	-	"	6.135	5	-
AA-172	"	"	"	1.12	-	"	"	"	-
AA-173	"	"	"	1.07	-	"	"	"	-
AA-174	"	"	"	1.17	-	"	5.11	6	-
AA-175	"	"	"	0.784	-	"	"	"	-
AA-176	"	"	"	0.78	-	"	"	"	-

TABLE 4 - BURSTING DIAPHRAGM PRESSURE RELIEF OF THE 27 CU. FT.  
CUBICAL CHAMBER (FILLED COMPLETELY WITH NON-HOMOGENEOUS PROPANE AND AIR MIXTURE)

Table 4-1 Bursting diaphragms of different sizes

Test No.	K Factor	Vane dia. in.	Gas	Conc. %	$P_1$	$T_1$	$P_2$	$T_2$	Comments
					Psi	mscc	Psi	mscc	
AA-179	5.1	18	C <sub>3</sub> H <sub>8</sub>	4	1.86	55	2.7	160	-
AA-190	"	"	"	"	1.89	57	2.57	150	-
AA-181	"	"	"	"	1.71	60	2.65	190	-
AA-219	"	"	"	"	1.62	34	2.5	90	-
AA-220	"	"	"	"	1.62	25	2.84	110	-
AA-221	"	"	"	"	1.79	36	2.84	125	-
AA-222	"	"	"	"	1.62	36	2.84	175	-
AA-230	"	"	"	"	1.565	25	2.5	175	-
AA-232	"	"	"	"	1.52	15	2.84	175	-
AA-233	"	"	"	"	1.79	30	2.80	200	-
AA-234	"	"	"	"	1.86	30	2.92	170	-
AA-235	"	"	"	"	1.57	30	3.30	150	-
AA-284	4.13	20	"	4	1.91	27	1.27	130	-
AA-285	"	"	"	"	1.52	30	0.59	225	-
AA-286	"	"	"	"	1.52	31.25	0.343	177.5	-
AA-288	"	"	"	"	1.98	27.6	2.16	160	-
AA-290	"	"	"	"	2.0	36	2.1	172	-
AA-291	"	"	"	"	1.91	31.2	3.14	150	-
AA-292	"	"	"	"	1.57	28.5	0.685	195	-
AA-293	"	"	"	"	2.81	32.5	0.352	180	-
AA-294	"	"	"	4	1.4	44.6	4.5	180	-
AA-295	"	"	"	"	2.1	30	1.65	150	-
AA-296	"	"	"	"	2.06	28.5	2.06	140	-
AA-297	"	"	"	"	2.0	32.5	2.25	167.5	-
AA-298	"	"	"	"	1.41	32.5	4.95	190	All diaphragm heavily creased.
AA-299	"	"	"	"	0.785	25	2.08	165	"
AA-300	"	"	"	"	0.785	27.5	0.44	175	"
AA-301	"	"	"	"	1.91	25	3.08	110	-
AA-302	"	"	"	"	1.76	32.5	0.59	172.5	-
AA-303	"	"	"	"	1.71	30	1.175	140	-
AA-304	"	"	"	"	1.665	27.5	0.93	125	-
AA-305	"	"	"	"	1.42	30	0.294	160	-
AA-306	"	"	"	"	1.76	40	2.98	182.5	-
AA-307	"	"	"	"	1.91	30	0.421	225	-
AA-308	"	"	"	"	1.81	30	3.38	180	-
AA-312	"	"	"	"	1.91	37.4	2.45	150	Ignition with Fan running.
AA-313	"	"	"	"	1.94	27.5	2.45	120	-
AA-314	"	"	"	"	1.81	25.0	0.294	167.5	-
AA-272	2.86	24	"	4	1.81	36	1.81	178	-
AA-276	"	"	"	"	1.82	"	0.245	"	-
AA-277	"	"	"	"	1.66	36	2.2	164	-
AA-278	"	"	"	"	1.37	36	0.245	178	-
AA-280	"	"	"	"	1.32	44	1.77	220	-
AA-281	"	"	"	"	1.57	36	0.345	170	-
AA-282	"	"	"	"	1.65	34	0.347	180	-
AA-283	"	"	"	"	1.57	36	0.294	178	-
AA-259	1.615	32	"	4	0.98	40	0.3	205	-
AA-260	"	"	"	"	0.98	37.6	0.3	175	-
AA-261	"	"	"	"	0.28	25	0.122	160	-
AA-262	"	"	"	"	0.27	45	0.147	165	-

Table 4-A continued

Test No.	K Factor	Vent dia. in.	Gas	Conc., %	P <sub>1</sub> Psi	T <sub>1</sub> msec	P <sub>2</sub> Psi	T <sub>2</sub> msec	Comments
AA-315	4.13	20	C <sub>3</sub> H <sub>8</sub>	4	2.0	30	1.078	172.5	-
AA-316	"	"	"	"	1.7	32.5	0.764	195	-
AA-317	"	"	"	"	1.7	27.5	0.843	145	-
AA-318	"	"	"	"	1.32	44.5	0.245	200	-
AA-246	2.86	24	"	4	1.52	25	1.12	1.25	-
AA-247	"	"	"	"	1.30	20	0.27	175	-
AA-248	"	"	"	"	1.03	25	0.147	175	-
AA-249	"	"	"	"	1.47	35.4	0.76	170	-
AA-250	"	"	"	"	1.15	32.0	0.51	192	-
AA-266	"	"	"	"	1.47	60	-	-	-
AA-267	"	"	"	8	1.08	275	-	-	-
AA-268	"	"	"	"	1.175	255	-	-	Test chamber was noted to be considerably hot after explosion.
AA-269	"	"	"	9.5	0.0705	-	-	-	The explosion did not rupture the diaphragm.
AA-270	"	"	"	"	0.0705	-	-	-	-
AA-271	"	"	"	4	1.42	22	0.44	-	-

Table 4-B Effect of filter partitions and air circulation on the bursting diaphragm explosion relief

Test No.	K Factor	Vent dia. in.	Gas	Conc., %	P <sub>1</sub> , psi	T <sub>1</sub> , msec	P <sub>2</sub> , psi	T <sub>2</sub> , msec	Air Cir. Rate CFM	No. of Filters	Comments
AA-236	15.42	12	C <sub>3</sub> H <sub>8</sub>	4%	3	4	0	2	0	2	-
AA-236	5.12	18	"	"	1.35	20	0.27	200	0	2	-
AA-237	"	"	"	"	1.25	25	0.25	190	0	2	-
AA-238	"	"	"	"	1.35	25	0.318	175	0	2	-
AA-239	"	"	"	"	0.98	120	-	-	27	2	-
AA-240	"	"	"	"	0.975	100	-	-	27	2	-
AA-332	"	"	"	"	2.2	35	1.1	177	0	2	-
AA-333	"	"	"	"	2.4	30	2.96	197.5	0	2	-
AA-334	"	"	"	"	2.9	32.5	0.784	145.0	0	2	-
AA-251	2.86	24	"	"	1.05	20	0.2	175	0	2	-
AA-252	"	"	"	"	1.15	20	0.27	160	0	2	-
AA-253	"	"	"	"	0.955	30	0.167	175	0	2	-
AA-254	"	"	"	"	1.35	30	0.22	190	0	2	-
AA-255	"	"	"	"	1.078	44	-	-	27	2	-
AA-256	"	"	"	"	0.71	60	-	-	27	2	-
AA-320	2.10	20	"	"	1.96	25	0.882	110	0	2	-
AA-321	"	"	"	"	1.96	22.5	0.6	120	0	2	-
AA-322	"	"	"	"	2.0	35	0.44	177.5	0	2	-
AA-323	"	"	"	"	1.81	32.5	0.44	149	0	2	-
AA-324	"	"	"	"	1.81	37.6	0.88	200	0	2	-
AA-325	"	"	"	"	1.52	40	0.88	208	0	2	-
AA-326	"	"	"	"	2.0	30	0.735	110	0	2	-
AA-327	"	"	"	"	2.0	27.5	1.94	110	0	2	-

Table 4-B continued

Vent Diameter 18" with Screen Partition and Two Filters

Test No.	K Factor	Vent Dia. in.	Gas	Conc., %	P <sub>1</sub> , psi	T <sub>1</sub> , msec	P <sub>2</sub> , psi	T <sub>2</sub> , msec	Air Cir. Rate CFM	No. of Filters	Partition	Comments
AA-241	5.12	18	C <sub>3</sub> H <sub>8</sub>	4%	1.32	68	-	-	27	2	-	-
AA-242	"	"	"	"	1.69	45	-	-	27	2	-	-
AA-243	"	"	"	"	1.42	40	-	-	27	2	-	-
AA-257	2.86	24	"	"	1.35	45	0.122	190	27	2	1	-
AA-258	"	"	"	"	1.30	50	0.194	190	27	2	1	-
AA-223	5.12	18	"	"	1.62	32	2.84	160	-	-	1	-
AA-224	"	"	"	"	1.59	25	2.84	150	-	-	1	-
AA-225	"	"	"	"	1.62	26	2.84	170	-	-	1	-
AA-226	"	"	"	"	1.62	40	2.94	180	-	-	1	-

TABLE 3-BURSTING DIAPHRAGM ON THE 27 CU. FT. CUBICAL CHAMBER (HOMOGENEOUS MIXTURE, COMPLETELY FILLED)

Table 3-A Bursting diaphragm of different sizes

Test No.	K Factor	Vent dia. in.	Gas	Conc. %	$P_1$	$T_1$	$P_2$	$T_2$	Comments
					Psi	msec	Psi	msec	
AA-336	5.1	18	$C_2H_2$	4	1.54	37.5	2.64	185	using the set-up shown in Fig. 3-3 but with 20 min. mixing with fan.
AA-337	"	"	"	"	1.54	37.5	7.7*	217	
AA-338	"	"	"	"	1.96	43	2.64	160	
AA-339	"	"	"	"	2.4	45	7.7*	160	
AA-340	"	"	"	"	2.4	45	10*	160	
AB-23	2.86	24	"	4	0.95	30	-	-	using the set-up shown in Fig. 3-6
AB-24	"	"	"	4.3	0.9	30	2.4	240	
AB-25	"	"	"	5.08	1.16	35	1.45	180	
AB-26	"	"	"	4.6	0.9	30	-	-	
AB-28	"	"	"	5.08	1.3	40	-	-	
AB-29	"	"	"	5.08	1.1	30	0.5	224	
AA-341	1.61	32	"	4	1.170	50	1.69	230	using the set-up shown in Fig. 3-3 but with 20 min. mixing with fan
AA-342	"	"	"	"	1.176	47.5	0.67	208	
AA-343	"	"	"	"	1.12	43.5	0.167	215	
AA-344	"	"	"	"	0.931	40.0	0.167	217	
AA-345	"	"	"	"	0.98	57.5	0.135	230	

\* represents the estimated value because the second peak pressure appeared higher than the calibrated range.

using the set-up shown in Fig. 3-4

AB-3	1.61	32	$C_2H_2$	4.42	0.98	62.5	-	-	-
AB-5	"	"	"	4.1	1.02	35	1.3	210	-
AB-6	"	"	"	4.14	1.05	45	1.15	210	-
AB-9	"	"	"	4.14	1.0	40	0.5	230	-
AB-10	"	"	"	4.14	0.70	52.5	1.1	245	Continuous purge while ignition.
AB-11	"	"	"	4.3	1.05	32.4	-	-	" " " "
AB-12	"	"	"	4.35	0.7	45	-	-	" " " "
AB-13	"	"	"	4.35	0.82	35	0.45	205	-
AB-14	"	"	"	4.35	0.85	25	-	-	-
AB-15	"	"	"	4.35	0.81	35	-	-	-
AB-16	"	"	"	4.35	0.85	35	-	-	-
AB-17	"	"	"	4.35	0.85	37.5	-	-	-
AB-18	"	"	"	4.9	1.0	35	0.75	-	-
AB-19	"	"	"	4.92	1.05	37.5	0.70	257.5	-
AB-20	"	"	"	5.0	1.07	52.5	1.05	240	-
AB-21	"	"	"	6.36	0.95	102.3	-	-	-

Table 3-B Effect of filters partitions and air circulation on the bursting diaphragm explosion relief

Test No.	K Factor	Vent dia. in.	Gas	Conc. %	$P_1$	$T_1$	$P_2$	$T_2$	No. of Filters	No. of Partitions	Cont. purg (CFM)
					Psi	msec	Psi	msec			
<u>Vent Diameter 24" with A) Diaphragm and 2 Filters</u>											
AB-31	2	24	$C_2H_2$	5.08	1.2	40	1.55	180	2	-	485
AB-32	"	"	"	"	1.26	45	0.8	275	2	-	485
AB-33	"	"	"	"	1.20	45	-	-	2	-	-
AB-34	"	"	"	4	1.5	35	1.05	270	2	-	485
<u>Vent Diameter 24" with A) Diaphragm with Screen Partitions</u>											
AB-27	2	24	$C_2H_2$	5.08	1.35	35	0.67	174	-	-	1
AB-28	"	"	"	4.26	1.30	40	-	-	-	-	1



TABLE 6

C-7

BURSTING DIAPHRAGM PRESSURE RELIEF ON THE 27 CU. FT. CUBICAL CHAMBER FILLED COMPLETELY WITH HYDROGEN/AIR MIXTURE

Test No.	K Factor	Vent Dia.	Gas	Hydrogen Conc. %	P <sub>1</sub> PSI	T <sub>1</sub> msec	P <sub>2</sub> PSI	T <sub>2</sub> msec	Comments
AA-187	1.615	32	H <sub>2</sub>	40	3.01	15	9.4	22	-
AA-188	"	"	"	"	2.38	17	8.6	19	-
AA-189	"	"	"	"	2.38	-	8.3	-	-
AA-191	1	30x36	"	"	1.56	8	2.72	16	-
AA-193	"	"	"	"	1.74	9	2.72	16	-

TABLE 7- BURSTING DIAPHRAGM PRESSURE RELIEF ON THE 3 FT. DIAMETER CYLINDRICAL TEST CHAMBERS (COMPLETELY FILLED WITH HOMOGENEOUS PROPANE AND AIR MIXTURE)

Table 7-A 26c. Dia. x 3 ft. long cylindrical test chamber (L/D = 1)

Test No.	Vent Dia. in.	No. of Vents	Propane Conc. %	Factor K	P <sub>1</sub> PSI		P <sub>2</sub> PSI		T <sub>1</sub> H sec.	T <sub>2</sub> M sec.
					Rear Transducer	Side Transducer	Rear Transducer	Side Transducer		
AB-38	30	1 Front	5.00	1.44	0.70	0.9	1	1	36	232
AB-39	"	"	"	"	0.75	0.70	1.3	1.8	34	210
AB-40	"	"	4.4	"	1.06	0.80	-	-	36	-
AB-41	"	"	"	"	1.15	1.1	0.8	0.8	36	210
AB-42	"	"	"	"	1.15	1.15	-	-	34	-
AB-43	"	"	"	"	0.80	1.0	-	-	36	-
AB-44	18	1 Top	5.00	-	1.75	1.75	1.15	1.15	36	144
AB-45	"	"	"	-	1.80	1.85	2.25	2.15	36	148
AB-46	"	"	"	-	1.90	-	2.55	-	40	132
AB-47	"	"	"	-	1.55	1.60	3.6	4.1	36	180
AB-48	"	1 Front	"	4	1.93	1.85	-	5.5	40	168
AB-49	"	"	"	"	1.90	1.85	4.6	4.5	36	234
AB-50	"	"	"	"	1.9	1.85	-	6.35	40	172
AB-51	24	"	"	2.25	-	1.34	-	0.85	-	-
AB-52	36	"	"	1	-	0.61	-	0.29	40	260

Table 7-B 36c. Dia. x 9ft. long cylindrical test chamber (L/D = 3)

Test No.	Vent Dia. in.	No. of Vents	Propane Conc. %	Factor K	P <sub>1</sub> PSI		P <sub>2</sub> PSI		T <sub>1</sub> H sec.	T <sub>2</sub> M sec.
					Rear Transducer	Side Transducer	Rear Transducer	Side Transducer		
AB-51	18	1 Front	5.00	4.0	2.45	2.15	3.3	2.65	90	324
AB-52	"	"	"	"	2.65	2.65	-	7.0	136	246
AB-53	"	"	"	"	2.95	2.0	-	6.75	76	312
AB-54	30	1 Front	5.00	4.0	1.15	0.95	0.75	0.55	46	320
AB-57	"	"	"	"	1.4	0.75	0.9	1.15	54	292
AB-58	"	"	"	"	1.25	0.95	0.50	0.70	46	340
AB-59	18	1 Front	5.00	4.0	2.10	1.70	4.1	4.9	60	370
AB-60	"	"	"	"	2.0	1.50	4.7	3.4	112	338
AB-61	18	3 Top	5.00	4.0	1.5	0.9	1.3	0.8	-	-
AB-62	"	"	"	-	1.75	1.6	0.3	0.35	-	-
AB-63	"	"	"	-	1.70	1.6	4.9	5.35	-	-
AB-64	"	"	"	-	1.55	1.55	0.35	0.35	-	-
AB-65	18	1 Front	5.00	4.0	2.1	2.2	4.15	3.4	-	-

TABLE 8- FREE-VENT PRESSURE RELIEF DATA (TEST CHAMBERS WERE COMPLETELY FILLED WITH HOMOGENEOUS MIXTURE OF PROPANE AND AIR)

Test No.	Test Chamber	K Factor	Vent Dia.	Gas	Gas Conc.	P	
						in.	PSI
AB-72	27 cu. ft.	1.61	32	C <sub>3</sub> H <sub>8</sub>	5.00	0.25	-
AB-70	27 cu. ft.	2.86	24	"	"	0.7	-
AB-69	3ft. x 9ft. cyl.	4	18	"	"	1.95	-
AB-68	"	"	"	"	"	2.1	-
AB-69	"	"	"	"	"	2.35	-
AB-72	3ft. x 3ft. cyl.	"	18	"	"	2.1	-
AB-73	"	"	"	"	"	0.8	-
AB-74	"	"	"	"	"	2.7	-
AB-75	"	"	"	"	"	0.9	-

**TABLE 9- FACTORY MUTUAL RESEARCH CORP. TESTS  
ON GLOVE BURSTING PRESSURES (Static)  
(Reference 1)**

GLOVE MATERIAL	CONSTRUCTION	NOMINAL, THICKNESS, IN.		PRESSURE AT BURST, PSI	FAILURE LOCATION
		HAND	SLEEVE		
Neoprene hand joined to neo. sleeve	adhesive joint	0.008	0.015	0.48	Sleeve
Neoprene	one piece	0.015	0.015	0.56	Sleeve
Neoprene	one piece	0.030	0.030	0.98	Sleeve
Neoprene-Leaded	one piece	0.030	0.030	1.09	Sleeve
Neoprene	one piece	0.055	0.055	1.61	Sleeve
Butyl	one piece	0.015	15	0.25	Sleeve
Butyl	one piece	0.030	0.030	0.58	Sleeve
PVC	one piece	0.015	0.015	0.98	Sleeve
PVC	one piece	0.030	0.030	2.09	Sleeve
FRPVC	one piece	0.030	0.030	1.76	Hand/Sleeve
Latex hand joined to neoprene sleeve	mechanical joint	0.009	0.015	0.28	Hand
Latex hand joined to rubber sleeve	adhesive joint	0.009	0.015	0.34	Hand/Sleeve

NOTE: All values are averages of at least two trials. Most results differed by less than 5% from their average; maximum deviation from average, 12%.